



# BRNO UNIVERSITY OF TECHNOLOGY

VYSOKÉ UČENÍ TECHNICKÉ V BRNĚ

## FACULTY OF ELECTRICAL ENGINEERING AND COMMUNICATION

FAKULTA ELEKTROTECHNIKY  
A KOMUNIKAČNÍCH TECHNOLOGIÍ

## DEPARTMENT OF RADIO ELECTRONICS

ÚSTAV RADIOELEKTRONIKY

# MEASUREMENT OF THE SISO/MISO SIGNAL IN THE DVB- T2 SYSTEM

MĚŘENÍ SISO/MISO SIGNÁLU V SYSTÉMU DVB-T2

## BACHELOR'S THESIS

BAKALÁŘSKÁ PRÁCE

### AUTHOR

AUTOR PRÁCE

Šimon Buchta

### SUPERVISOR

VEDOUCÍ PRÁCE

doc. Ing. Ladislav Polák, Ph.D.

BRNO 2024

# Bakalářská práce

bakalářský studijní program **Elektronika a komunikační technologie**

Ústav radioelektroniky

**Student:** Šimon Buchta

**ID:** 228812

**Ročník:** 3

**Akademický rok:** 2023/24

**NÁZEV TÉMATU:**

## Měření SISO/MISO signálu v systému DVB-T2

### POKYNY PRO VYPRACOVÁNÍ:

V teoretické části práce podejte stručný přehled o přenosovém řetězci systému DVB-T2, využívající i diverzitní techniku MISO, a o vysílání ve standardu DVB-T2 v České republice. Navrhněte, realizujte a ověřte měřicí pracoviště pro vysílání a příjem TV signálu ve standardu DVB-T2. Dále diskutujte o chybách, které mohou vzniknout při zpracování signálu v OFDM modulátoru. Navrhněte a ověřte měřicí metodiku pro měření vlivu chyb v OFDM modulátoru na DVB-T2 MISO signál.

V experimentální části práce proveďte měření a analýzu reálného TV signálu DVB-T2. Při měření uvažujte i komerčně dostupné set-top-boxy (STB) a měřicí přístroje. Dále proveďte měření vlivu chyb v OFDM modulátoru na DVB-T2 MISO signál pro různé přenosové scénáře. Výsledky z měření přehledně zpracujte a analyzujte.

### DOPORUČENÁ LITERATURA:

[1] [1] FISCHER, Walter. Digital video and audio broadcasting technology: a practical engineering guide. 3rd ed. New York: Springer, 2010. ISBN 978-3-642-11611-7.

[2] POLAK, Ladislav, Jan KUFA, Roman SOTNER a Tomas KRATOCHVIL. On the Performance of DVB-T2 MISO System: Special Fixed Transmission Scenarios. In: 2021 31st International Conference Radioelektronika (RADIOELEKTRONIKA) [online]. IEEE, 2021, 2021-4-19, s. 1-4 [cit. 2022-05-06]. ISBN 978-1-6654-1474-6. Dostupné z: doi:10.1109/RADIOELEKTRONIKA52220.2021.9420206

**Termín zadání:** 16.2.2024

**Termín odevzdání:** 27.5.2024

**Vedoucí práce:** doc. Ing. Ladislav Polák, Ph.D.

**doc. Ing. Lucie Hudcová, Ph.D.**  
předseda rady studijního programu

### UPOZORNĚNÍ:

Autor bakalářské práce nesmí při vytváření bakalářské práce porušit autorská práva třetích osob, zejména nesmí zasahovat nedovoleným způsobem do cizích autorských práv osobnostních a musí si být plně vědom následků porušení ustanovení § 11 a následujících autorského zákona č. 121/2000 Sb., včetně možných trestněprávních důsledků vyplývajících z ustanovení části druhé, hlavy VI. díl 4 Trestního zákoníku č.40/2009 Sb.

## **ABSTRACT**

This thesis deals with a measurement-based study of the second-generation Digital Terrestrial Video broadcasting system (DVB-T2), examining various transmission techniques and imperfections within the orthogonal frequency division multiplexing (OFDM) modulator. For this study, a universal measurement setup was proposed and implemented. The first part of this work focuses on the measurement and evaluation of a real single-input single-output (SISO) DVB-T2 signal broadcasted in the Czech Republic. The second part examines different DVB-T2 signal configurations, considering multiple-input single-output (MISO) transmission and imperfections in the OFDM modulator with combination of power imbalance between transmitters and in various channels for fixed and mobile reception. The results are evaluated using conventional objective metrics, such as bit and modulation error ratio (BER and MER), as well as from the perspective of the measurement equipment and receivers (set-top boxes – STBs) used.

## **KEYWORDS**

DVB-T2, SISO and MISO transmission, I/Q-errors, BER, MER, QEF

## **ABSTRAKT**

Tato bakalářská práce je zaměřena na měření a analýzu televizního signálu druhé generace digitálního pozemního vysílání (DVB-T2), zahrnující různé přenosové techniky a chyby, jež mohou vzniknout v tzv. OFDM modulátoru. Pro tento účel bylo navrženo a zrealizováno měřicí pracoviště. První část práce je věnována zkoumání a následnému zhodnocení výsledků měření reálného DVB-T2 signálu vysílaného v České republice. Druhá část této práce se zaměřuje na měření signálu DVB-T2 s odlišnou konfigurací, na příklad užití MISO přenosové techniky a přidání vlivu chyb v OFDM modulátoru a výkonového nevyvážení mezi vysílači. Tyto konfigurace jsou zkoumány v různých kanálových modelech pro fixní a mobilní příjem. Získané výsledky jsou zkoumány nejen z pohledu konvenčních objektivních parametrů (MER, BER), ale také z pohledu použitých měřících přístrojů a přijímačů (set-top-boxů).

## **KLÍČOVÁ SLOVA**

DVB-T2, SISO a MISO vysílání, chyby I/Q modulátoru, BER, MER, QEF

## ROZŠÍŘENÝ ABSTRAKT

Tato bakalářská práce je zaměřena na měření a analýzu televizního signálu druhé generace digitálního pozemního vysílání (DVB-T2), zahrnující různé přenosové techniky (SISO a MISO) a chyby, jež mohou vznikat v tzv. OFDM modulátoru. Část práce je věnována měření vysílání reálného TV signálu v módu SISO (single-input single-output), který je užíván v České Republice.

Speciální pozornost v této práci je věnována tzv. vysílací technice MISO (multiple-input single-output), podpořená standardem DVB-T2, a jejím stručnému popisu. Vliv této vysílací techniky na přenos DVB-T2 signálu v různých přenosových podmínkách a při různých chybách, které mohou vzniknout v OFDM modulátoru, jsou jedním z hlavních cílů této práce. Pro měření reálného DVB-T2 signálu a TV signálu vygenerovaného v laboratorních podmínkách bylo navrženo a realizováno laboratorní měřicí pracoviště. Pracoviště vyniká univerzálností, která umožňuje použití různých měřicích přístrojů a přijímačů – set-top-boxů (STB) pro opakované měření.

První část experimentální části práce je věnována měření a analýze reálného DVB-T2 signálu pro čtyři hlavní multiplexy (MUX) v České Republice. Získané výsledky jsou posuzovány z pohledu konvenčních objektivních parametrů, jako například bitová a modulační chyba (BER a MER). Pozornost je také věnována přesnosti měření či rozdílu získaných hodnot z pohledu použitých měřicích přístrojů a STB.

V druhé části experimentální části bakalářské práce jsou prezentovány výsledky z laboratorního měření, zaměřené na vysílací mód MISO. V rámci tohoto měření byla vytvořena signálová konfigurace DVB-T2 vhodná pro MISO. Měření bylo uskutečněno pro různé vysílací scénáře (fixní, mobilní a přenosný). Tyto scénáře byly realizované pomocí různých kanálových modelů dle standardu ETSI. Dále se měřil a analyzoval dopad na kvalitu DVB-T2 MISO vysílání, pokud v OFDM modulátoru vzniknou různé chyby (amplitudová a fázová nevyváženost), a když nastane výkonový imbalance mezi vysílači.

Ze získaných výsledků vyplynulo, že vysílací mód MISO při uvažování různých přenosových scénářů vykazuje různou odolnost proti chybám při přenosu. Zároveň se potvrdilo, že některé měřicí přístroje nejsou vhodné pro dlouhodobé měření a analýzu signálu, především z pohledu vysílacího módu MISO, speciálně pro mobilní vysílací scénáře.



BUCHTA, Šimon. *Measurement of SISO/MISO DVB-T2 signal*. Brno: Brno University of Technology, Fakulta elektrotechniky a komunikačních technologií, Ústav radioelektroniky, 2024, 85 p. Bachelor's Thesis. Advised by doc. Ing. Ladislav Polák, Ph.D.

# Author's Declaration

**Author:** Šimon Buchta  
**Author's ID:** 228812  
**Paper type:** Bachelor's Thesis  
**Academic year:** 2023/24  
**Topic:** Measurement of SISO/MISO DVB-T2 signal

I declare that I have written this paper independently, under the guidance of the advisor and using exclusively the technical references and other sources of information cited in the paper and listed in the comprehensive bibliography at the end of the paper.

As the author, I furthermore declare that, with respect to the creation of this paper, I have not infringed any copyright or violated anyone's personal and/or ownership rights. In this context, I am fully aware of the consequences of breaking Regulation § 11 of the Copyright Act No. 121/2000 Coll. of the Czech Republic, as amended, and of any breach of rights related to intellectual property or introduced within amendments to relevant Acts such as the Intellectual Property Act or the Criminal Code, Act No. 40/2009 Coll. of the Czech Republic, Section 2, Head VI, Part 4.

Brno .....

.....

author's signature\*

---

\*The author signs only in the printed version.

## ACKNOWLEDGEMENT

Rád bych poděkoval vedoucímu semestrální práce panu doc. Ing. Ladislavu Polákovi, Ph.D. za odborné vedení, konzultace, trpělivost a podnětné návrhy k práci.

# Contents

<b>Introduction</b>	<b>15</b>
<b>1 The DVB-T2 Standard</b>	<b>16</b>
1.1 Input processing . . . . .	16
1.2 Bit interleaved coding and modulation (BICM) . . . . .	17
1.3 Frame builder . . . . .	19
1.4 OFDM generation . . . . .	20
<b>2 MISO in DVB-T2 system and Errors in DVB-T2 modulator</b>	<b>22</b>
2.1 MISO in DVB-T2 system . . . . .	22
2.2 Errors in DVB-T2 Modulator . . . . .	24
<b>3 Transmission channel models</b>	<b>25</b>
3.1 AWGN . . . . .	25
3.2 Ricean (RC20) . . . . .	25
3.3 Rayleigh (RL20) . . . . .	25
3.4 Typical Urban (TU6) . . . . .	26
3.5 Rural Area (RA6) . . . . .	26
3.6 Pedestrian Indoor and Outdoor (PI, PO) . . . . .	26
<b>4 Measurement of a Real DVB-T2 SISO</b>	
<b>TV signal</b>	<b>27</b>
4.1 Laboratory workplace for measurement of real DVB-T2 signal . . . . .	27
4.2 Measured objective parameters . . . . .	28
4.2.1 Bit error ratio (BER) before LDPC decoding . . . . .	28
4.2.2 BER after LDPC decoding . . . . .	28
4.2.3 Modulation error ratio (MER) . . . . .	29
4.2.4 Carrier-to-Noise ratio (C/N) . . . . .	29
4.2.5 The number of decoding iterations . . . . .	29
4.3 Digital Terrestrial Video Broadcasting Coverage in the Czech Republic	29
4.4 DVB-T2 system parameters . . . . .	31
4.5 Results . . . . .	32
<b>5 Measurement of the DVB-T2 MISO</b>	
<b>TV signal</b>	<b>38</b>
5.1 Measurement setup . . . . .	38
5.2 DVB-T2 MISO signal configuration . . . . .	39

5.3	Results . . . . .	40
5.3.1	AWGN . . . . .	40
5.3.2	RC20 . . . . .	41
5.3.3	RL20 . . . . .	41
<b>6</b>	<b>Measurement of the DVB-T2 MISO TV signal in portable and mobile channels</b>	<b>54</b>
6.1	DVB-T2 MISO portable and mobile signal configuration . . . . .	54
6.2	Results . . . . .	55
6.2.1	Results for portable scenarios (PI, PO) . . . . .	55
6.2.2	Mobile channel results (TU6, RA6) . . . . .	56
	<b>Conclusion</b>	<b>74</b>
	<b>Bibliography</b>	<b>75</b>
	<b>List of appendices</b>	<b>78</b>
<b>A</b>	<b>Results of MISO measurement</b>	<b>79</b>

# List of Figures

1.1	Block diagram of the DVB-T2 system (based on [2]) . . . . .	16
1.2	Block diagram of input processing system for one PLP input (based on [2]) . . . . .	17
1.3	BICM block diagram (based on [8]) . . . . .	17
1.4	16-QAM constellation diagram: a) without and b) with rotation . . .	18
1.5	T2-frame structure (based on [1]) . . . . .	19
1.6	OFDM module block chain (based on [1]) . . . . .	20
2.1	DVB-T2 MISO network (based on [10]) . . . . .	22
2.2	Modified Alamouti in DVB-T2 (based on [1]) . . . . .	23
2.3	DVB-T2 modulator with IQ errors (based on [1]) . . . . .	24
2.4	Constellation diagram of 16-QAM [from left]: no errors, AI=10%, PI=10° . . . . .	24
4.1	Scheme of measurement workplace for DVB-T2 signal . . . . .	27
4.2	Measurement laboratory workplace for DVB-T2 signal (SISO) . . . .	28
4.3	Example of services included in MUX21 and MUX22 (yellow – TV, blue – Radio, white – other services included) . . . . .	30
4.4	Map of coverage of DVB-T2 signal in Czech Republic for Multiplex (MUX) 21 including location of transmitters [23] . . . . .	31
4.5	Measured results for MUX21 and MUX22 . . . . .	33
4.6	Measured results for MUX23 and MUX24 . . . . .	34
4.7	Measured parameters of signal power (P) and signal quality (Q), marked by solid and dashed lines respectively, for each STB . . . . .	35
5.1	Block diagram of the laboratory workplace for measurement of the DVB-T2 MISO signal . . . . .	38
5.2	Measurement workplace for DVB-T2 signal (MISO) . . . . .	39
5.3	DVB-T2 MISO TV signal: <b>AWGN channel</b> – solid lines: no $I/Q$ -errors, dashed lines: $AI = 10\%$ , dotted lines: $AI = 10\%$ and $PI = 10^\circ$ . . . . .	42
5.4	DVB-T2 MISO TV signal: <b>AWGN channel</b> , power imbalance = 5 dB (SFE: -30 dBm, SFU: -35 dBm) – solid lines: no $I/Q$ -errors, dashed lines: $AI = 10\%$ , dotted lines: $AI = 10\%$ and $PI = 10^\circ$ . . . . .	43
5.5	DVB-T2 MISO TV signal: <b>AWGN channel</b> , power imbalance = 5 dB (SFE: -35 dBm, SFU: -30 dBm) – solid lines: no $I/Q$ -errors, dashed lines: $AI = 10\%$ , dotted lines: $AI = 10\%$ and $PI = 10^\circ$ . . . . .	44
5.6	DVB-T2 MISO TV signal: <b>RC20 channel</b> – solid lines: no $I/Q$ -errors, dashed lines: $AI = 10\%$ , dotted lines: $AI = 10\%$ and $PI = 10^\circ$ . . . . .	45

5.7	DVB-T2 MISO TV signal: <b>RC20 channel</b> , power imbalance = 5 dB (SFE: -30 dBm, SFU: -35 dBm) – solid lines: no $I/Q$ -errors, dashed lines: $AI = 10\%$ , dotted lines: $AI = 10\%$ and $PI = 10^\circ$ . . . . .	46
5.8	DVB-T2 MISO TV signal: <b>RC20 channel</b> , power imbalance = 5 dB (SFE: -35 dBm, SFU: -30 dBm) – solid lines: no $I/Q$ -errors, dashed lines: $AI = 10\%$ , dotted lines: $AI = 10\%$ and $PI = 10^\circ$ . . . . .	47
5.9	DVB-T2 MISO TV signal: <b>RL20 channel</b> – solid lines: no $I/Q$ -errors, dashed lines: $AI = 10\%$ , dotted lines: $AI = 10\%$ and $PI = 10^\circ$ . . . . .	48
5.10	DVB-T2 MISO TV signal: <b>RL20 channel</b> , power imbalance = 5 dB (SFE: -30 dBm, SFU: -35 dBm) – solid lines: no $I/Q$ -errors, dashed lines: $AI = 10\%$ , dotted lines: $AI = 10\%$ and $PI = 10^\circ$ . . . . .	49
5.11	DVB-T2 MISO TV signal: <b>RL20 channel</b> , power imbalance = 5 dB (SFE: -35 dBm, SFU: -30 dBm) – solid lines: no $I/Q$ -errors, dashed lines: $AI = 10\%$ , dotted lines: $AI = 10\%$ and $PI = 10^\circ$ . . . . .	50
6.1	DVB-T2 MISO TV signal: <b>PI</b> – solid lines: no $I/Q$ -errors, dashed lines: $AI = 10\%$ , dotted lines: $AI = 10\%$ and $PI = 10^\circ$ . . . . .	58
6.2	DVB-T2 MISO TV signal: <b>PI</b> , power imbalance = 5 dB (SFE: -30 dBm, SFU: -35 dBm) – solid lines: no $I/Q$ -errors, dashed lines: $AI = 10\%$ , dotted lines: $AI = 10\%$ and $PI = 10^\circ$ . . . . .	59
6.3	DVB-T2 MISO TV signal: <b>PI</b> , power imbalance = 5 dB (SFE: -35 dBm, SFU: -30 dBm) – solid lines: no $I/Q$ -errors, dashed lines: $AI = 10\%$ , dotted lines: $AI = 10\%$ and $PI = 10^\circ$ . . . . .	60
6.4	DVB-T2 MISO TV signal: <b>PO</b> – solid lines: no $I/Q$ -errors, dashed lines: $AI = 10\%$ , dotted lines: $AI = 10\%$ and $PI = 10^\circ$ . . . . .	61
6.5	DVB-T2 MISO TV signal: <b>PO</b> , power imbalance = 5 dB (SFE: -30 dBm, SFU: -35 dBm) – solid lines: no $I/Q$ -errors, dashed lines: $AI = 10\%$ , dotted lines: $AI = 10\%$ and $PI = 10^\circ$ . . . . .	62
6.6	DVB-T2 MISO TV signal: <b>PO</b> , power imbalance = 5 dB (SFE: -35 dBm, SFU: -30 dBm) – solid lines: no $I/Q$ -errors, dashed lines: $AI = 10\%$ , dotted lines: $AI = 10\%$ and $PI = 10^\circ$ . . . . .	63
6.7	DVB-T2 MISO TV signal: <b>TU6</b> – solid lines: no $I/Q$ -errors, dashed lines: $AI = 10\%$ , dotted lines: $AI = 10\%$ and $PI = 10^\circ$ . . . . .	64
6.8	DVB-T2 MISO TV signal: <b>TU6</b> , power imbalance = 5 dB (SFE: -30 dBm, SFU: -35 dBm) – solid lines: no $I/Q$ -errors, dashed lines: $AI = 10\%$ , dotted lines: $AI = 10\%$ and $PI = 10^\circ$ . . . . .	65
6.9	DVB-T2 MISO TV signal: <b>TU6</b> , power imbalance = 5 dB (SFE: -35 dBm, SFU: -30 dBm) – solid lines: no $I/Q$ -errors, dashed lines: $AI = 10\%$ , dotted lines: $AI = 10\%$ and $PI = 10^\circ$ . . . . .	66

6.10	DVB-T2 MISO TV signal: <b>RA6</b> – solid lines: no $I/Q$ -errors, dashed lines: $AI = 10\%$ , dotted lines: $AI = 10\%$ and $PI = 10^\circ$ . . . . .	67
6.11	DVB-T2 MISO TV signal: <b>RA6</b> , power imbalance = 5 dB (SFE: -30 dBm, SFU: -35 dBm) – solid lines: no $I/Q$ -errors, dashed lines: $AI = 10\%$ , dotted lines: $AI = 10\%$ and $PI = 10^\circ$ . . . . .	68
6.12	DVB-T2 MISO TV signal: <b>RA6</b> , power imbalance = 5 dB (SFE: -35 dBm, SFU: -30 dBm) – solid lines: no $I/Q$ -errors, dashed lines: $AI = 10\%$ , dotted lines: $AI = 10\%$ and $PI = 10^\circ$ . . . . .	69
A.1	DVB-T2 MISO TV signal: <b>AWGN</b> , power imbalance = 10 dB (SFE: -25 dBm, SFU: -35 dBm) – solid lines: no $I/Q$ -errors, dashed lines: $AI = 10\%$ , dotted lines: $AI = 10\%$ and $PI = 10^\circ$ . . . . .	80
A.2	DVB-T2 MISO TV signal: <b>AWGN</b> , power imbalance = 10 dB (SFE: -35 dBm, SFU: -25 dBm) – solid lines: no $I/Q$ -errors, dashed lines: $AI = 10\%$ , dotted lines: $AI = 10\%$ and $PI = 10^\circ$ . . . . .	81
A.3	DVB-T2 MISO TV signal: <b>RC20</b> , power imbalance = 10 dB (SFE: -25 dBm, SFU: -35 dBm) – solid lines: no $I/Q$ -errors, dashed lines: $AI = 10\%$ , dotted lines: $AI = 10\%$ and $PI = 10^\circ$ . . . . .	82
A.4	DVB-T2 MISO TV signal: <b>RC20</b> , power imbalance = 10 dB (SFE: -35 dBm, SFU: -25 dBm) – solid lines: no $I/Q$ -errors, dashed lines: $AI = 10\%$ , dotted lines: $AI = 10\%$ and $PI = 10^\circ$ . . . . .	83
A.5	DVB-T2 MISO TV signal: <b>RL20</b> , power imbalance = 10 dB (SFE: -25 dBm, SFU: -35 dBm) – solid lines: no $I/Q$ -errors, dashed lines: $AI = 10\%$ , dotted lines: $AI = 10\%$ and $PI = 10^\circ$ . . . . .	84
A.6	DVB-T2 MISO TV signal: <b>RL20</b> , power imbalance = 10 dB (SFE: -35 dBm, SFU: -25 dBm) – solid lines: no $I/Q$ -errors, dashed lines: $AI = 10\%$ , dotted lines: $AI = 10\%$ and $PI = 10^\circ$ . . . . .	85



# List of Tables

1.1	Scattered Pilot Pattern (PP) to be used for each allowed combination of FFT size and Guard Interval (GI) in SISO mode [2] . . . . .	21
1.2	Scattered Pilot Pattern (PP) to be used for each allowed combination of FFT size and Guard Interval (GI) in MISO mode [2] . . . . .	21
4.1	System parameters of the real DVB-T2 signal for each MUX . . . . .	31
4.2	Table of values of adjustable attenuator while the signal is still demodulated for each measuring device and set-top boxes . . . . .	32
4.3	Data rates of services included in a) MUX 21 and b) MUX 22 (measured on 2023. 11. 13, 1	
4.4	Data rates of services included in a) MUX 23 and b) MUX 24 (measured on 2023. 11. 13, 1	
5.1	System parameters of the DVB-T2 signal MISO . . . . .	40
5.2	Required $C/N$ in unit of dB for QEF reception in <b>AWGN</b> channel without power imbalance . . . . .	51
5.3	Required $C/N$ in unit of dB for QEF reception in <b>AWGN</b> channel with power imbalance of 5 dB (SFU = -35 dBm, SFE = -30 dBm) . . . . .	51
5.4	Required $C/N$ in unit of dB for QEF reception in <b>AWGN</b> channel with power imbalance of 5 dB (SFU = -30 dBm, SFE = -35 dBm) . . . . .	51
5.5	Required $C/N$ in unit of dB for QEF reception in <b>RC20</b> channel without power imbalance . . . . .	52
5.6	Required $C/N$ in unit of dB for QEF reception in <b>RC20</b> channel with power imbalance of 5 dB (SFU = -35 dBm, SFE = -30 dBm) . . . . .	52
5.7	Required $C/N$ in unit of dB for QEF reception in <b>RC20</b> channel with power imbalance of 5 dB (SFU = -30 dBm, SFE = -35 dBm) . . . . .	52
5.8	Required $C/N$ in unit of dB for QEF reception in <b>RL20</b> channel without power imbalance . . . . .	53
5.9	Required $C/N$ in unit of dB for QEF reception in <b>RL20</b> channel with power imbalance of 5 dB (SFU = -35 dBm, SFE = -30 dBm) . . . . .	53
5.10	Required $C/N$ in unit of dB for QEF reception in <b>RL20</b> channel with power imbalance of 5 dB (SFU = -30 dBm, SFE = -35 dBm) . . . . .	53
6.1	DVB-T2 MISO-based signal configuration for portable and mobile reception . . . . .	54
6.2	Required $C/N$ in unit of dB for QEF reception in <b>PI</b> channel without power imbalance . . . . .	70
6.3	Required $C/N$ in unit of dB for QEF reception in <b>PI</b> channel with power imbalance of 5 dB (SFU = -35 dBm, SFE = -30 dBm) . . . . .	70
6.4	Required $C/N$ in unit of dB for QEF reception in <b>PI</b> channel with power imbalance of 5 dB (SFU = -30 dBm, SFE = -35 dBm) . . . . .	70

6.5	Required $C/N$ in unit of dB for QEF reception in <b>PO</b> channel without power imbalance . . . . .	71
6.6	Required $C/N$ in unit of dB for QEF reception in <b>PO</b> channel with power imbalance of 5 dB (SFU = -35 dBm, SFE = -30 dBm) . . . . .	71
6.7	Required $C/N$ in unit of dB for QEF reception in <b>PO</b> channel with power imbalance of 5 dB (SFU = -30 dBm, SFE = -35 dBm) . . . . .	71
6.8	Required $C/N$ in unit of dB for QEF reception in <b>TU6</b> channel without power imbalance . . . . .	72
6.9	Required $C/N$ in unit of dB for QEF reception in <b>TU6</b> channel with power imbalance of 5 dB (SFU = -35 dBm, SFE = -30 dBm) . . . . .	72
6.10	Required $C/N$ in unit of dB for QEF reception in <b>TU6</b> channel with power imbalance of 5 dB (SFU = -30 dBm, SFE = -35 dBm) . . . . .	72
6.11	Required $C/N$ in unit of dB for QEF reception in <b>RA6</b> channel without power imbalance . . . . .	73
6.12	Required $C/N$ in unit of dB for QEF reception in <b>RA6</b> channel with power imbalance of 5 dB (SFU = -35 dBm, SFE = -30 dBm) . . . . .	73
6.13	Required $C/N$ in unit of dB for QEF reception in <b>RA6</b> channel with power imbalance of 5 dB (SFU = -30 dBm, SFE = -35 dBm) . . . . .	73

# Introduction

The second generation of digital terrestrial video broadcasting (DVB-T2) standard, which was firstly published in 2008, is the successor of the DVB-T and can achieve approximately at least 30% to 50% increase of net data rate, as well as better suitability for mobile use compared to older DVB-T standard [1]. Better efficiency of usage of spectrum is enabled due to application better source coding algorithms [2]. The DVB-T2 standard also offers more flexibility such as combinations of different parameters, for example: pilot patterns (PP), code rate (CR), and Guard interval (GI), which can ensure desired robustness in various sectors of digital terrestrial broadcasting [3]. Moreover, two transmission modes are supported, namely: single input single output (SISO) and multiple input single output (MISO) [1].

The aim of this thesis is to provide a measurement-based study of the DVB-T2 system, encompassing the influence of the MISO technique and potential errors, which can occur in the Orthogonal Frequency Division Multiplexing (OFDM) modulator, on the DVB-T2 signal reception. There is introduced an appropriate laboratory workplace for measuring the performance of a real DVB-T2 signal broadcasted in Czech Republic. The main objective is to propose and realize a measurement workplace to generate, transmit, receive and analyze a DVB-T2 MISO signal under different transmission conditions, influenced by different errors that can occur in the OFDM modulator.

This thesis is structured as follows. The first two chapters provide a brief overview of the signal processing chain of the DVB-T2 system, the MISO technique employed in DVB-T2, and errors (amplitude and phase imbalance) in the OFDM modulator. The third chapter introduces a measurement workplace designed to measure and analyze the real DVB-T2 signal broadcasted in the Czech Republic. This chapter also includes an overview of DVB-T2 signal coverage in the Czech Republic, and results of the provided measurements. The fourth chapter presents the modified measurement workplace for measuring and analyzing of the DVB-T2 MISO signal, influenced by different In-phase/Quadrature-phase ( $I/Q$ ) errors, power imbalance and fading channels for fixed reception. The fifth chapter extends this analysis to different mobile and portable fading channels. Finally, the thesis concludes with the seventh chapter.

# 1 The DVB-T2 Standard

The DVB-T2 system currently stands as one of the most widely adopted DVB systems, especially in Europe, with usage extending to more than 140 countries [4]. Compared to its predecessor DVB-T [1], it offers more advanced signal configuration, enables a more efficient utilization of the radio frequency (RF) spectrum. Notably, DVB-T2 achieves a net data rate that is 30% to 50% higher than the DVB-T standard [5]. Consequently, a larger number of programs can be transmitted within the RF spectrum.

The simplified block diagram of the DVB-T2 system is shown in Fig. 1.1. It consists of four main blocks, namely: input processing, bit interleaved coding and modulation (BICM), frame builder and OFDM generation. It is important to note that the block *Input pre-processing* is not part of the main DVB-T2 system. This block contains a demultiplexer or a service splitter for transport streams (TS), which separates the TSs into usable DVB-T2 inputs. The TSs are grouped into Physical Layer Pipes (PLPs). The system inputs can be: one or more MPEG-2 TSs, one or more generic fixed-length streams (GFS) or generic fixed-length packetized (GFPS) and/or Generic continuous streams (GCS). The maximum data rate for any kind of stream at the input is 72 Mbit/s. More details can be found in [2], [6] and [7].

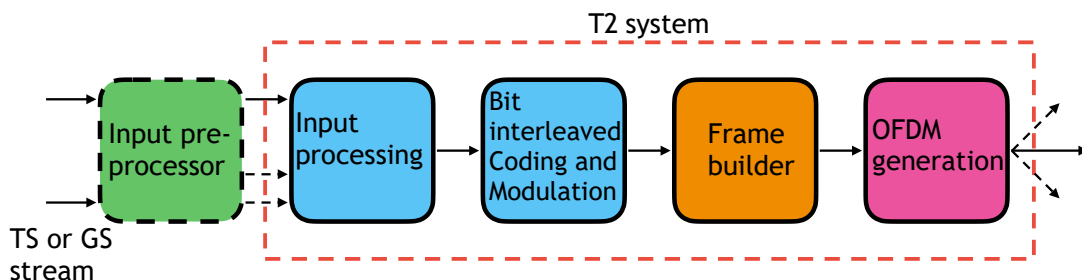


Fig. 1.1: Block diagram of the DVB-T2 system (based on [2])

## 1.1 Input processing

The block diagram of the input processing is illustrated in Fig. 1.2. The input processing block can be divided into two main parts: *Mode* and *Stream adaptation*. The main purpose of the *Mode adaptation module* is to slice input data streams into DATA FIELDS, which are subsequently organized into baseband frames (BBFRAMEs) through the *Stream Adaptation module*. The block diagram of the input processing system is shown in Fig. 1.2.

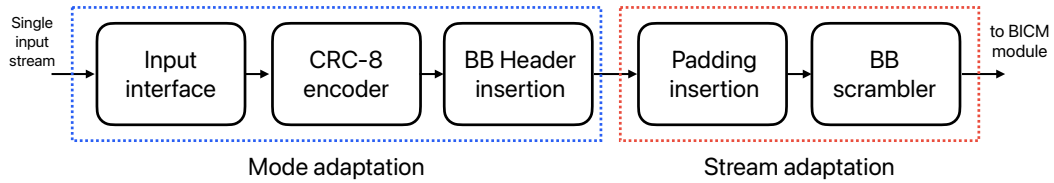


Fig. 1.2: Block diagram of input processing system for one PLP input (based on [2])

The *Mode adaptation module* can be divided into three parts. Initially, in the input interface block, the modulator synchronizes itself. Subsequently, a CRC-8 encoder is applied to the synchronized stream, embedding a checksum that aids in detecting transmission errors. This is followed by the insertion of the BBFRAME header. The header contains information about the data field and its format [1] [2].

In the *Stream adaptation module*, the data output from the *Mode Adaptation module* undergoes padding. This involves filling up the BBFRAMEs to their maximum capacity to align with the required input data length for the Forward Error Correction (FEC) block [2]. It is followed by the BB scrambler, which ensures the randomization of data – long sequences of ones and zeros are broken up to ensure robust and resilient representation of the data for subsequent processing stages [1].

## 1.2 Bit interleaved coding and modulation (BICM)

Sub-system *BICM*, among others, performs outer and inner FEC coding and Bit interleaving [1]. Basic block diagram of the BICM module is plotted in Fig. 1.3.

The input BBFRAMEs from each Physical Layer Pipe (PLP) undergo initial processing in the FEC block. This block ensures the outer and inner FEC coding data, using Bose–Chaudhuri–Hocquenghem (BCH) and low-density parity-check (LDPC) coding [1]. The DVB-T2 standard provides a range of code rate (CR) selections,

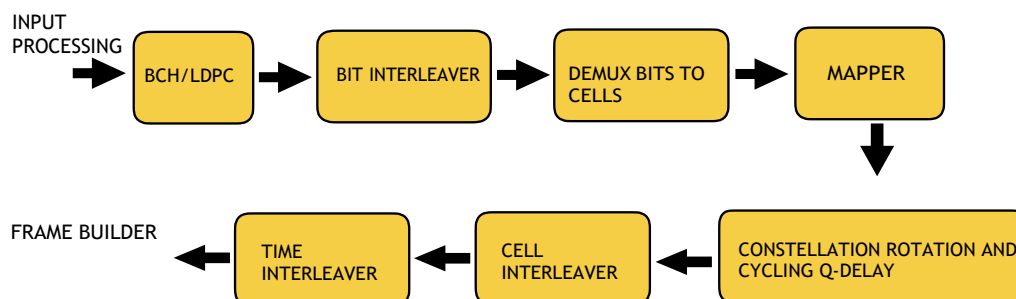


Fig. 1.3: BICM block diagram (based on [8])

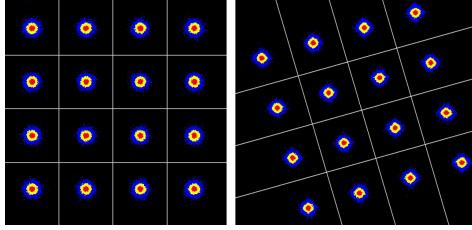


Fig. 1.4: 16-QAM constellation diagram: a) without and b) with rotation

including  $1/2$ ,  $3/5$ ,  $2/3$ ,  $3/4$ ,  $4/5$ , and  $5/6$ . The length of the output FEC frames can be short (16K) or long (32K). The short FEC frame is advantageous for low-rate data streams, whereas the long frame is more suitable for high-rate data streams.

Subsequently, the FEC frames are interleaved on the level of bits (more details can be found in [2] [9]). Following interleaving, the output bit stream undergoes demultiplexing into cells. The FEC frame is partitioned into parallel cell words, a quantity determined by the modulation type in use. The DVB-T2 system provides a choice of four modulation types: QPSK, 16-QAM, 64-QAM, or 256-QAM [8].

In the pursuit of enhanced robustness, the DVB-T2 system also allows to use rotated constellations (see Fig. 1.4) and a process known as  $Q$ -delay. Rotated constellations, also termed Signal Space Diversity (SSD), involve the rotation of initial constellation points by a specific angle contingent upon the employed modulation type. This ensures that each component in the constellation possesses adequate information to independently determine the initially transmitted symbol. However, the advantages of constellation is decreasing when both In-Phase ( $I$ ) and Quadrature ( $Q$ ) components of the symbol experience identical loss in a fading channel. To ensure the right functionality of the constellation rotation, the quadrature components are delayed ( $Q$ -delay). Its purpose is to ensure that the  $I$  and  $Q$  components of the symbol experience independent fading. By transmitting each component in a different carrier and time slot, the system mitigates the risk of both components being affected by identical fading, thereby enhancing robustness [8].

The subsequent steps in the BICM module involve two interleaving blocks, cell and time interleaving. The cells within the FEC codeword are pseudo-randomly interleaved. Subsequently, the cells coming from different FEC blocks are time interleaved originating from different FEC blocks are subjected to time interleaving. This dual interleaving process contributes significantly to system performance, particularly in conjunction with  $Q$ -delay and rotated constellations. The time interleaving involves grouping FEC blocks from the cell interleaver into interleaving frames, which are then mapped onto T2-frames. The primary purpose of time interleaving is to protect data, especially in scenarios involving mobile reception where long burst errors, impulsive noise and low Doppler shift may occur [1], [8].

### 1.3 Frame builder

In the third main block of the DVB-T2 system, namely *Frame builder*, the cells from PLPs are allocated into OFDM symbol carriers, then into T2-frames and finally into T2-super-frames. It can be divided into two main parts: cells mapper and frequency interleaver [8].

The structure of the T2-frame is depicted in Fig. 1.5. Each individual T2-frame consists of several essential components: the P1 symbol, one or more P2 symbols, followed by payload data - PLPs. The P1 symbol serves for three primary purposes: marking the commencement of the DVB-T2 frame, facilitating frequency and time synchronization, and transmitting signaling parameters such as FFT mode and SISO or MISO configurations. The P2 symbol encompasses Layer-1 (L1) signaling information, with the possibility of having 1 to 16 P2 symbols per T2-frame, depending on the utilized FFT mode [1]. Additional details about the frame builder can be found in [2].

Each PLP can be transmitted with different parameters, allowing for variable coding and modulation (VCM). The transmission parameters of PLPs can dynamically change from one T2-frame to another, offering flexibility in terms of data rate and robustness. The maximum number of OFDM symbols is depending on the used guard interval (GI) and FFT type. The T2-frame's maximum duration is limited to 250 ms. At the end of the frame building process, the frequency interleaver is employed to distribute information (data cells from the frame builder) to DVB-T2 OFDM carriers as randomly as possible [1].

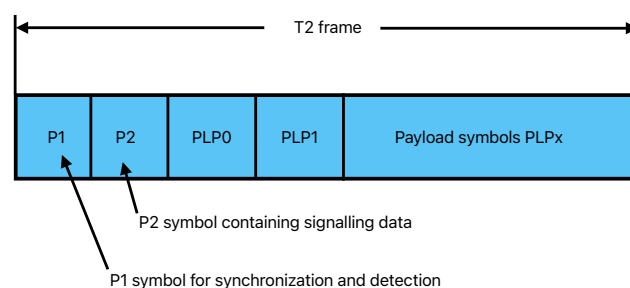


Fig. 1.5: T2-frame structure (based on [1])

## 1.4 OFDM generation

The last main part of the DVB-T2 system, namely *OFDM generation*, takes the cells from the previous *Frame builder* block to insert the relevant reference information, among others pilots and GI. Its block diagram is shown in Fig. 1.6. As it is visible, the MISO-based processing of the DVB-T2 signal employing modified Alamouti encoding is also possible [2].

The initial segment in the OFDM generation block diagram is MISO (Multiple-Input, Single-Output) processing. This processing can be applied to nearly all symbols in DVB-T2 on the cell level. It is reasonable to assume that all DVB-T2 receivers are equipped to receive signals with applied MISO processing. The MISO processing involves taking the input data cells and generating two similar data cell "rows" (low correlation between them) at the output. Each data cell "row" is directed to its respective transmitter. Alamouti encoding is employed to create the two data cell "rows." The encoding is not used to P1 preamble symbol, mentioned in the Frame building part [2].

The subsequent process in the OFDM generation is *Pilot Insertion*. Pilot cells within the OFDM frame serve the purpose of transmitting reference information with known values to the receiver. In the DVB-T2 system, there are five types of pilots: scattered, continual, edge, P2, and frame-closing pilots [2]. Taking scattered pilots as an example, these are employed for channel estimation in the receiver, and there exist eight different patterns, marked as PP (Pilot Patterns) [8]. When a PP with lower density is utilized, more carriers can be allocated to carry payload data. Conversely, PP with higher density excel in compensating for errors (equalization) in the transmission channel [1]. This trade-off allows for adaptability in PP selection based on the specific requirements of the transmission scenario. Combinations of GI and FFT size (OFDM mode) are allowed for both MISO and SISO techniques defining the using of specific PP. Such configurations for SISO and MISO transmission are collected in Table 1.1 and Table 1.2, respectively.

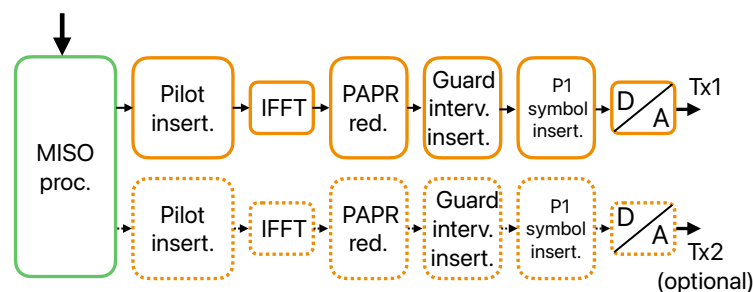


Fig. 1.6: OFDM module block chain (based on [1])



Guard interval							
FFT size	1/128	1/32	1/16	19/256	1/8	19/128	1/4
32K	PP7	PP4	PP2	PP2	PP2	NA	NA
		PP6	PP8	PP8	PP8		
16K	PP7	PP7	PP2	PP2	PP2	PP2	PP1
		PP4	PP8	PP8	PP3	PP3	PP8
		PP6	PP4	PP4	PP8	PP8	
			PP5	PP5			
8K	PP7	PP7	PP8	PP8	PP2	PP2	PP1
		PP4	PP4	PP4	PP3	PP3	
			PP5	PP5	PP8	PP8	
4K, 2K	NA	PP7	PP4	NA	PP2	NA	PP1
		PP4	PP5		PP3		
1K	NA	NA	PP4	NA	PP2	NA	PP1
			PP5		PP3		

Tab. 1.1: Scattered Pilot Pattern (PP) to be used for each allowed combination of FFT size and Guard Interval (GI) in SISO mode [2]

Guard interval							
FFT size	1/128	1/32	1/16	19/256	1/8	19/128	1/4
32K	PP8	PP8	PP2	PP2	NA	NA	NA
	PP4	PP4	PP8	PP8			
	PP6						
16K	PP8	PP8	PP3	PP3	PP1	PP1	NA
	PP4	PP4	PP8	PP8	PP8	PP8	
	PP5	PP5					
8K	PP8	PP8	PP3	PP3	PP1	PP1	NA
	PP4	PP4	PP8	PP8	PP8	PP8	
	PP5	PP5					
4K, 2K	NA	PP4	PP3	NA	PP1	NA	NA
		PP5			PP1		
1K	NA	NA	PP3	NA	PP1	NA	NA

Tab. 1.2: Scattered Pilot Pattern (PP) to be used for each allowed combination of FFT size and Guard Interval (GI) in MISO mode [2]

The major disadvantage of OFDM is its susceptibility to large envelope fluctuations, leading to high Peak-to-Average Power Ratio (PAPR). To address this issue, the DVB-T2 system provides two methods for PAPR reduction: Active Constellation Extension (ACE) and Tone Reservation (TR). The using of these techniques in DVB-T2 is optional and not required [2], [8].

Finally, the GI is inserted. Before this process, the signal must be transformed from the frequency to the time domain (block IFFT). The insertion of GI is crucial for preventing Inter-Symbol Interference (ISI) caused by multipath reception. The GI is inserted at the beginning of each OFDM symbol. Subsequently, a cyclic prefix is employed, involving the replication of the last part of the symbol to the GI.

## 2 MISO in DVB-T2 system and Errors in DVB-T2 modulator

In this chapter, two pivotal topics central to this thesis are discussed. The initial focus is on the MISO transmission technique, examining its applications and implementation within the DVB-T2 system. The latter part of this chapter briefly describe the errors that may arise in the OFDM modulator.

### 2.1 MISO in DVB-T2 system

The DVB-T2 system offers a MISO-based transmission option, not only the conventional SISO transmission. The basic concept of DVB-T2 MISO transmission is captured in Fig. 2.1. Notably, the MISO network differs from the standard Single Frequency Network (SFN) [1] in that it simultaneously transmits two slightly different versions of the desired signals from a multitude of transmitting antennas. In practice, these transmitters are often geographically separated, representing an optimal configuration for MISO network utilization. The deployment of multiple transmitters enables the MISO network to capitalize on transmit diversity, resulting in enhanced SNR, data rate, and network coverage [10].

In the DVB-T2 system, the MISO transmission is based on the modified form of Alamouti scheme [10]. The basic principle of the DVB-T2 MISO system employing the modified Alamouti scheme is depicted in 2.1. As it is visible, the transmitters operate in pairs, simultaneously transmitting payload data in pairs as well.

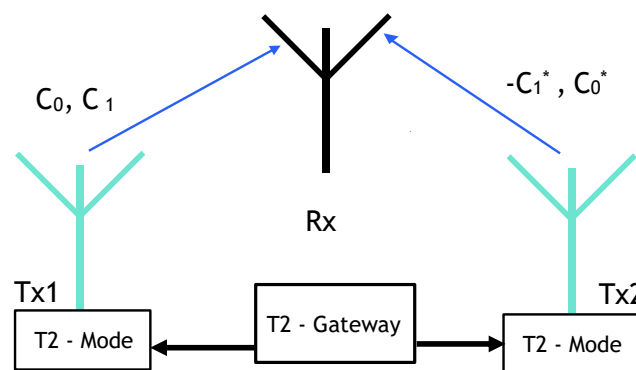


Fig. 2.1: DVB-T2 MISO network (based on [10])

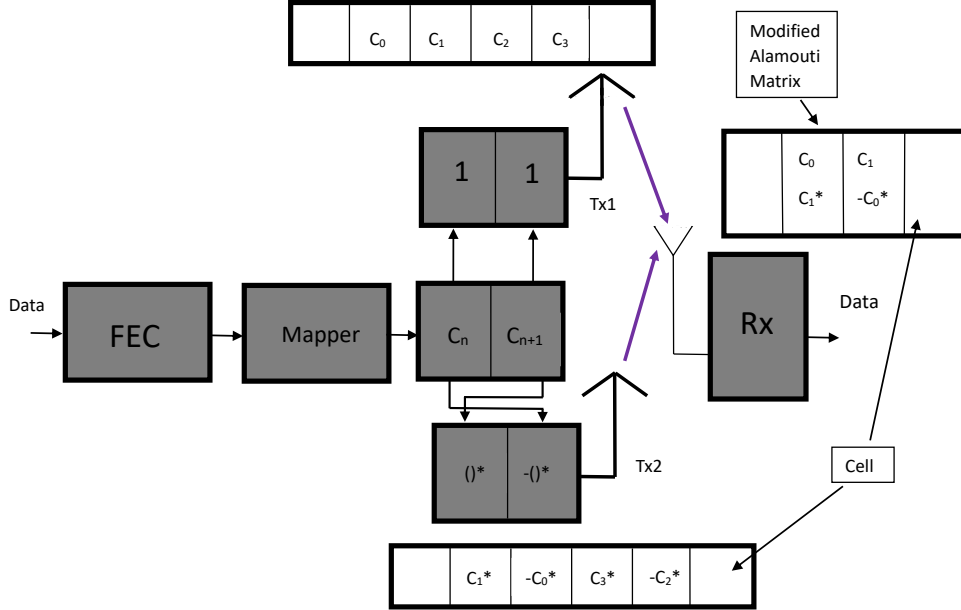


Fig. 2.2: Modified Alamouti in DVB-T2 (based on [1])

The first transmitter (Tx1) in the pair transmits an unmodified version of each constellation pair  $(C_0, C_1, \dots)$ . Conversely, the second transmitter (Tx2) transmits a modulated version of each constellation pair  $(-C_1^*, C_0^*)$  in reversed frequency order. To elaborate, if  $C_0$  is being transmitted on carrier number  $n$  in Tx1, then  $C_1$  is on carrier number  $n + 1$ . In Tx2,  $-C_1^*$  is transmitted on carrier number  $n$ , and  $C_0^*$  is on carrier number  $n + 1$ . Here, the symbol  $*$  signifies the complex conjugation operation. The receiver straightforwardly recovers the individual components from the combined signal using simple mathematical functions. This configuration enhances the diversity of the transmitted signals, contributing to improved reception characteristics in the DVB-T2 MISO network. One of the key advantages of employing the modified Alamouti scheme is its relatively simple implementation on both the transmit and receive sides of the network [1], [10].

As depicted in Fig. 2.1, two essential pieces of equipment are integral to the system. The first is the T2-Gateway, responsible for generating the T2-Modulation Interface (T2-MI) stream encapsulating all the necessary information to describe the content and timing of T2-frames. The second component is the T2-Modulator, which receives the stream from the T2-Gateway and incorporates Alamouti encoding and desired delays into the signal. Crucially, all transmitters in the MISO network must be synchronized to the same clock reference. More information about the DVB-T2 MISO transmission are available in in [10], [11].

## 2.2 Errors in DVB-T2 Modulator

In the DVB-T2 system, the COFDM modulator (it applies FEC to the transmitted signal) is utilized, akin to the OFDM modulator. The basic scheme of the COFDM modulator in the DVB-T2 system, including potential errors [1], is shown in Fig. 2.3.

The OFDM modulator in DVB-T2 begins with an IFFT operation to convert data from frequency to time domain. To address potential inter-symbol interference (ISI), a GI is inserted between OFDM symbols. Prior to transmission, the DVB-T2 signal undergoes RF modulation using an  $I/Q$  modulator. The  $I$  and  $Q$  parts are multiplied by a cosine and sine signal, respectively.

This prepares the signal for transmission within the DVB-T2 system [1].

As seen in Fig. 2.3, precise calibration of both  $I$  and  $Q$  signal branches, along with accurate configuration of the  $90^\circ$  phase shifter, is crucial. Deviations (indicated by red lines) can lead to  $I/Q$ -errors (see Fig. 2.4), comprising Amplitude Imbalance (AI) and Phase Imbalance (PI). AI refers to unequal amplitude levels in the  $I$  and  $Q$  branches, while PI involves a phase difference deviating from  $90^\circ$ . Minimizing these errors is vital for signal integrity and optimal DVB-T2 performance [11].

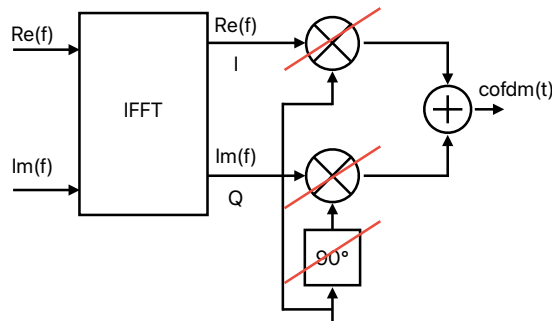


Fig. 2.3: DVB-T2 modulator with IQ errors (based on [1])

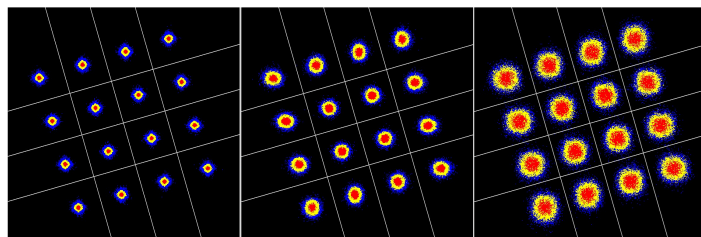


Fig. 2.4: Constellation diagram of 16-QAM [from left]: no errors, AI=10%, PI=10°

## 3 Transmission channel models

### 3.1 AWGN

The Additive White Gaussian Noise (AWGN) channel is defined by a single intended signal between transmitter and receiver, devoid of fading effects, multipath interference, or other signal degradation forms. It solely contains additive white Gaussian noise. This ideal Gaussian channel serves as a reference channel in theoretical analyses and simulations, offering insights into communication system limits. However, it lacks full representation of real-world conditions. Network planning in practical scenarios necessitates more complex and advanced channel models that encompass various impairments and channel characteristics [12].

### 3.2 Ricean (RC20)

The Ricean channel model delineates wireless communication channels featuring both direct and reflected signal paths, comprising a potent direct path alongside weaker multipath components. The RC20 channel model includes 20 significant multipath components. This typically consists of one strong line-of-sight (LOS) path and 19 scattered (echo) paths. Each of the 20 paths has associated delays and power levels. The LOS path generally has the shortest delay and the highest power, while the scattered paths have varying delays (varying from units of  $\mu\text{s}$  to tens of  $\mu\text{s}$ ) and lower power levels. The Ricean factor, denoting the direct path power's ratio to multipath power, is pivotal in fixed rooftop reception planning, factoring in considerations such as signal strength and interference [12], [13].

### 3.3 Rayleigh (RL20)

The RL20 model includes 20 significant multipath components. In contrast to the Ricean channel, the Rayleigh channel lacks a dominant direct path. Instead, it is characterized by multiple reflected signal paths, leading to constructive and destructive interference at the receiver—known as multipath propagation. This phenomenon induces fading, causing rapid variations in signal strength over time and space. Rayleigh fading is non-selective across frequencies, affecting all components of the transmitted signal equally. Each of the 20 paths has associated delays and power levels, following a statistical distribution characteristic of Rayleigh fading. The power of each path is typically exponentially distributed.

Leveraging the Rayleigh channel is crucial for crafting resilient communication systems capable of adapting to fading conditions and sustaining dependable connectivity [12], [13].

### **3.4 Typical Urban (TU6)**

The TU6 channel, featuring 6 paths with wide delay dispersion and relatively strong power, is employed in wireless communication to emulate radio signal propagation in diverse environments, notably densely populated urban areas (e.g., city or town). In such locales, signal propagation is primarily shaped by tall structures like buildings, typically four stories or taller. The TU6 model often encompasses frequency-selective fading, wherein the channel response fluctuates with frequency. Commonly used speed for receiving unit in TU6 channel is 60 km/h [13], [14], [15].

### **3.5 Rural Area (RA6)**

In rural environments, the channel model diverges notably from urban settings due to the scarcity of buildings and other structures, with transmission primarily influenced by vegetation. Again 6 sign paths are included. Communication links in rural areas typically cover longer distances between transmitter and receiver compared to urban counterparts, potentially leading to heightened free-space path loss, where signal strength diminishes with distance. Additionally, the topography of rural regions, including hills, valleys, and vegetation, can introduce further variability in signal propagation. For instance, signals may undergo attenuation when traversing dense vegetation or encounter diffraction effects when crossing hills and valleys. The Doppler effect is calculated based on typical rural speeds, which may vary from stationary to vehicular speeds up to around 100 km/h [13], [15], [16].

### **3.6 Pedestrian Indoor and Outdoor (PI, PO)**

The pedestrian channel model is tailored to replicate realistic conditions for portable reception, assuming a receiver moving at a walking speed of 3 km/h and positioned no less than 1.5 meters above ground level. Distinctions exist between indoor and outdoor scenarios: indoor models factor in obstacles such as walls, furniture, and people, while outdoor models incorporate terrain fluctuations, vegetation, and urban infrastructure [17].

More details about the above mentioned channel models can be find in [18].

## 4 Measurement of a Real DVB-T2 SISO TV signal

This chapter introduces the proposed laboratory workplace allowing to measure and analyze a real DVB-T2 SISO-based TV signal, broadcasted in Czech Republic. In addition, the proposed measurement concept, with minor modifications, is capable to measure and analyze a DVB-T2 MISO signal generated under laboratory conditions. In such a case, influence of different  $I/Q$ -errors on the performance of the DVB-T2 MISO transmission can be measured.

### 4.1 Laboratory workplace for measurement of real DVB-T2 signal

The block diagram of the proposed laboratory workplace appropriate to measure and analyze a SISO-based real DVB-T2 signal is shown in Fig. 5.1. The received DVB-T2 signal from the rooftop antenna goes to an adjustable attenuator, allowing to change the level of the received DVB-T2 signal. Subsequently, the attenuator output branched into two pathways connects to: ETL-TV analyzer together with DVMS1-DTV monitoring system, and a set-top-box (STB). The ETL-TV analyzer precisely measures various DVB-T2 signal parameters (on PHY level) and displays constellation diagrams, and RF spectra. Simultaneously, the DVMS1-DTV monitoring system also measures the dominant part of these parameters, but originally is designed and in this work is used to monitor the TS and bit rates for different TV and radio channels within a selected multiplex (MUX). The continuous results of these measurements are displayed on a PC monitor.

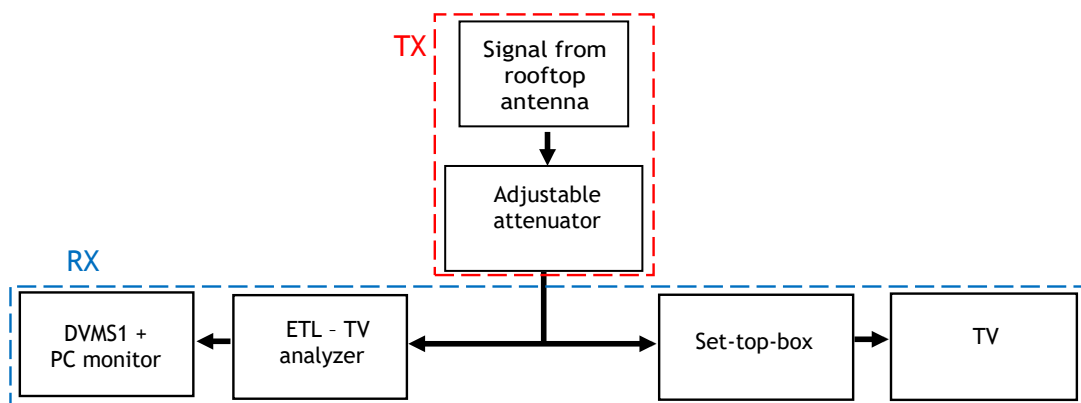


Fig. 4.1: Scheme of measurement workplace for DVB-T2 signal

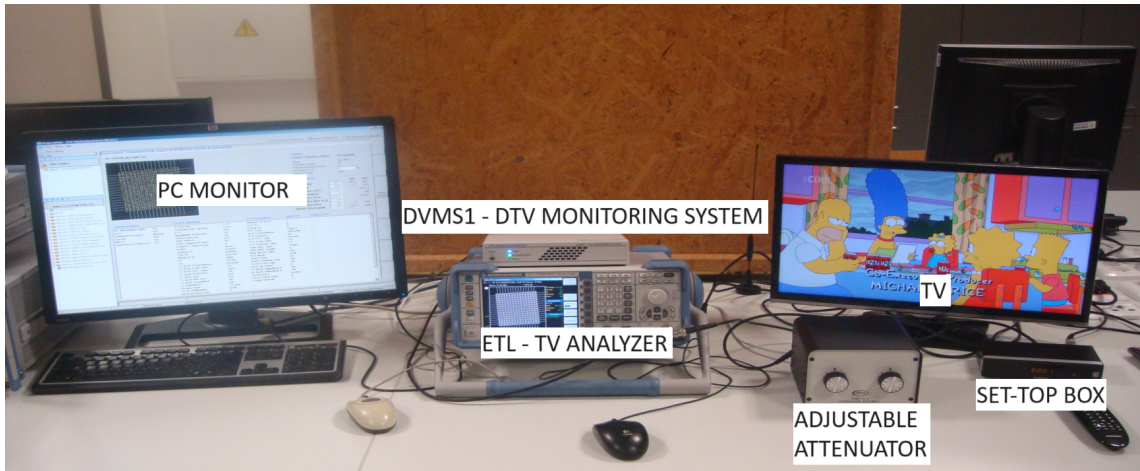


Fig. 4.2: Measurement laboratory workplace for DVB-T2 signal (SISO)

The second path is linked to a STB, specifically the THOMSON THT712. The output of the STB is then connected to a TV. This configuration enables the measurement of both the power and quality of the DVB-T2 signal by a STB. This approach allows for a comprehensive assessment of the signal's characteristics and its impact on the viewing experience. The realized measurement workplace is captured in Fig. 4.2.

## 4.2 Measured objective parameters

In this section, an overview of the objective parameters used to measure the performance of the DVB-T2 signal is briefly described. These parameters serve as quantitative metrics for evaluating various aspects of the DVB-T2 signal quality and transmission characteristics.

### 4.2.1 Bit error ratio (BER) before LDPC decoding

Bit error ratio (BER) before LDPC decoding is a ratio of the incorrectly received bits to the total received bits over a specified time interval. The incorrect reception of bits are dominantly caused by fading or noise occurring in the transmission channel. The LDPC decoding process plays an crucial role in the identification and correction of these erroneous bits. BER is measured independently for each PLP, allowing the detection of occasional bit errors in the received signal at the input of RX [19].

### 4.2.2 BER after LDPC decoding

BER after LDPC decoding, sometimes referred to as before BCH decoding, is defined similarly to the BER before LDPC decoding, However, in this case, it is measured



after the LDPC decoding process but before entering the BCH decoding process, which can repair the remaining erroneous bits [19]. In DVB-T2 specification, the quasi-error-free (QEF) reception is defined as less than one error event per transmission hour, corresponding to a BER after LDPC decoding of  $1.10^{-7}$  or less [2].

### **4.2.3 Modulation error ratio (MER)**

The modulation error ratio (MER) is a parameter that characterizes the impact of all interfering signals on a digitally modulated signal. Each interference is represented as a vector that displaces the constellation point from its ideal center. MER is expressed in decibels (dB). The higher the MER value, the lower the interference during transmission. This parameter provides valuable insights into the overall integrity and robustness of the modulated signal [1].

### **4.2.4 Carrier-to-Noise ratio (C/N)**





The carrier-to-noise ratio (C/N) is the ratio of the received carrier strength to the strength of the received noise. It helps to determine the required signal level for receiving a viable signal amidst background noise and interference. A higher C/N ratio indicates a more favorable signal-to-noise (S/N) of a demodulated signal [10].

### **4.2.5 The number of decoding iterations**





To achieve QEF reception at lower values of C/N the decoding process of LDPC decoder can be repeated. The number of decoding iterations indicates the number of repetitions of the LDPC process. High number of decoding iterations leads to unwanted latency [2].

## **4.3 Digital Terrestrial Video Broadcasting Coverage in the Czech Republic**

The DVB-T2 system has become the predominant DVB standard in the Czech Republic, having replaced its predecessor, DVB-T. The transition process commenced in 2019, during which both broadcasting networks operated concurrently to provide people with the necessary time to adapt to the new standard. The primary objective of transitioning from DVB-T to DVB-T2 was to optimize the RF spectrum usage, specifically narrowing the band from 470 to 790 MHz to a more compact range from 470 to 694 MHz. In 2020, the DVB-T standard was switched off completely and replaced by DVB-T2. [20].

Programme, service	Bit rate [kbit/s]
 ČT1 HD T2	6096
 ČT24 HD T2	4748
 ČT SPORT HD T2	6568
Teletext	225
 ČRo Radiožurnál	128
EPG	1000

(a) MUX21

Programme, service	Bit rate [kbit/s]
 Prima	1984
 Prima COOL	1928
 Prima MAX	1928
 RADIO PROGLAS	48

(b) MUX22

Fig. 4.3: Example of services included in MUX21 and MUX22 (yellow – TV, blue – Radio, white – other services included)

Currently, the broadcasting of the DVB-T2 signal in Czech Republic is organized in four MUXs. Each MUX, marked by the numbers 21, 22, 23, and 24, comprises different TV and radio channels, and is assigned a specific RF within the designated RF band (see Fig. 4.3). Detailed information about the TV and radio channels broadcasted within each MUX can be found in [21].

Presently, the coverage of the Czech Republic by the DVB-T2 signal stands at approximately 99.9% for MUX 21, 22, and 23, while MUX 24 exhibits slightly smaller coverage, around 97.1%. The SFN infrastructure is comprised of 369 TXs geographically and strategically positioned across the entire country to ensure comprehensive coverage for all MUX. The maximum effective radiated power (ERP) of TXs is in the range of 50 dBW to 3 dBW [23]. For a detailed overview of the TXs employed in the Czech Republic, including their locations and names, and comprehensive coverage information for each region, can be found on the websites of Czech Telecommunication Office (CTU) [22]. Further information along with graphical representations of DVB-T2 coverage maps (see Fig. 4.4), can be explored in [23].

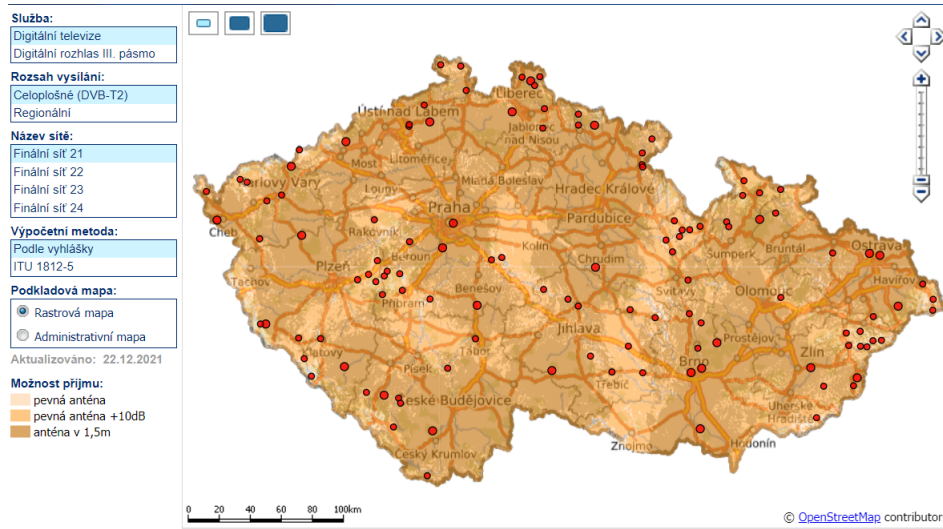


Fig. 4.4: Map of coverage of DVB-T2 signal in Czech Republic for Multiplex (MUX) 21 including location of transmitters [23]

## 4.4 DVB-T2 system parameters

The first measurement, conducted in this work, is focused on the analyze of different MUX-based DVB-T2 signals broadcasted in Czech Republic.

Bandwidth	8 MHz
FFT mode	32K extended
Guard interval	1/8
Code rate	2/3
Pilot pattern	PP2
Transmission technique	SISO
Modulation	256-QAM
Rotation of constellation	ON
Sideband	normal

(a) System parameters

Multiplex (MUX)	Frequency [MHz]
MUX21	514
MUX22	626
MUX23	570
MUX24	674

(b) Transmission frequency of MUXs

Tab. 4.1: System parameters of the real DVB-T2 signal for each MUX

To provide more comprehensive analyses, three different measurement equipment (ETL-TV analyzer, Sefram, DVMS1-DTV monitoring system) and three different STBs (THOMSON TH712, SENCOR SDB5002T, STC6000HD PVR) were used. The overview of the main DVB-T2 system parameters used are summarized in Table 4.1.

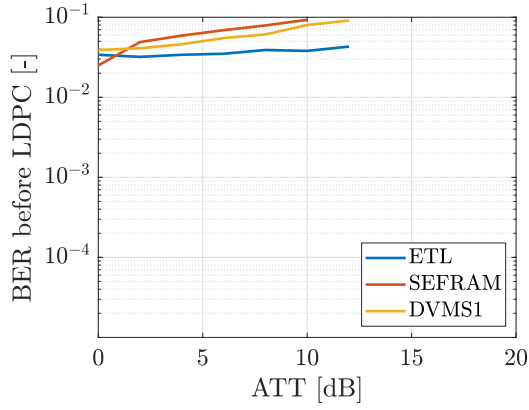
## 4.5 Results

This chapter contains all graphical representations of measured objective parameters, along with table of values of QEF reception according to the attenuation of the level of the received RF signal for each STB and the measuring equipment used (see Table 4.2), and tables showing data rates for each MUX (see Table 4.3 and Table 4.4). The BER before LDPC, MER, and RF level of the signal were measured at various adjusted attenuations. The results for each MUX are shown in Figs. 4.5 and 4.6. In addition there are graphical representations of power and quality of used STBs for each MUX (see Fig. 4.7).

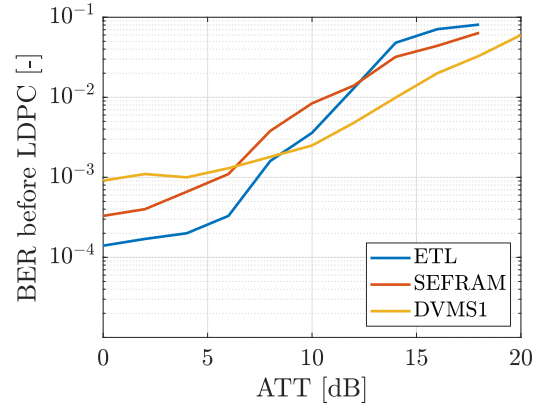
Analyzing the graphical results, it is evident that the RF signal for MUX21 exhibits the highest BER before LDPC, ensuring QEF reception at the lowest attenuation compared to other MUXs (see Table 4.2). Notably, MUX21 has the lowest MER and shows considerable differences between measuring devices (see Fig. 4.5). Figure 4.7 further demonstrates the significant degradation in quality at the lowest attenuation, along with noticeable differences in measured power and quality between STBs. This performance degradation of the DVB-T2 signal for MUX21 could be due to the measurement location or RF spectrum interference visible on the measuring device. On the other hand, notably, MUX22 and MUX23 exhibit the highest quality results for both parameters, BER before LDPC and MER (see Fig. 4.5, Fig. 4.6). Especially mentioning MUX23 results, which can be received even with the attenuation of 20 dB for all measuring devices, for STBs the values are even higher (see Table 4.2). According to expectations, curves obtained for the RF signal level showing a linear decrease with increasing attenuation. In terms of comparing measuring devices, notable differences exist for each measured parameter. However, it can be observed that they exhibit consistency across the board.

Tab. 4.2: Table of values of adjustable attenuator while the signal is still demodulated for each measuring device and set-top boxes

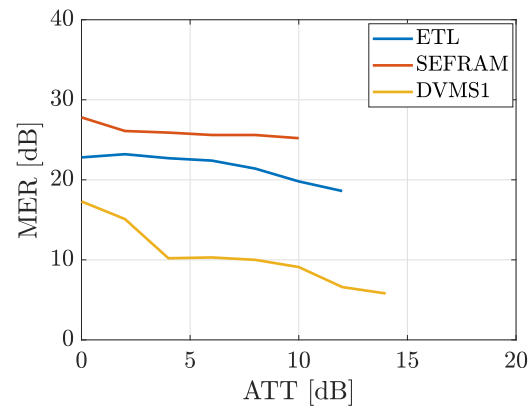
Multiplex	Measuring equipment	ATT [dB]	Set-top-box (STB)	ATT [dB]
MUX21	ETL	12	THOMSON THT712	18
	DVMS1	14	SENCOR SDB 52002T	19
	SEFRAM	10		
MUX22	ETL	18	THOMSON THT712	25
	DVMS1	20	SENCOR SDB 52002T	25
	SEFRAM	18		
MUX23	ETL	20	THOMSON THT712	25
	DVMS1	20	SENCOR SDB 52002T	28
	SEFRAM	20		
MUX24	ETL	16	THOMSON THT712	25
	DVMS1	20	SENCOR SDB 52002T	27
	SEFRAM	14		



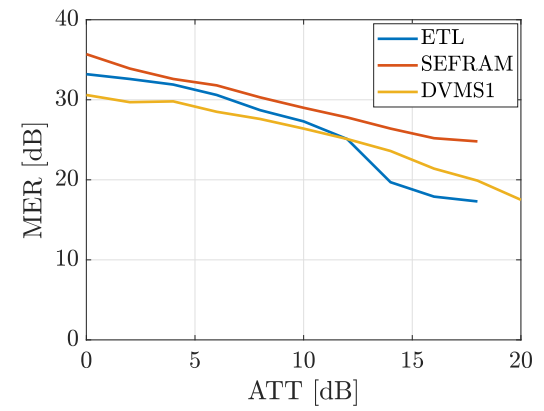
(a) BER before LDPC vs attenuation (MUX21)



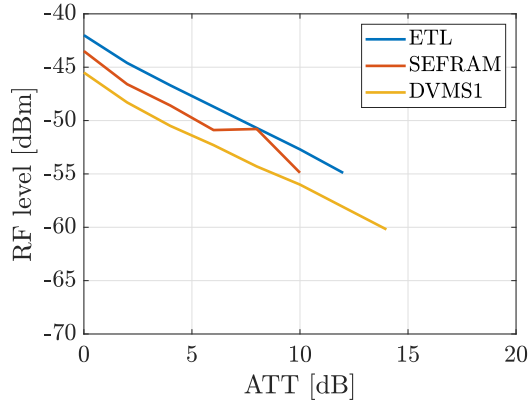
(b) BER before LDPC vs attenuation (MUX22)



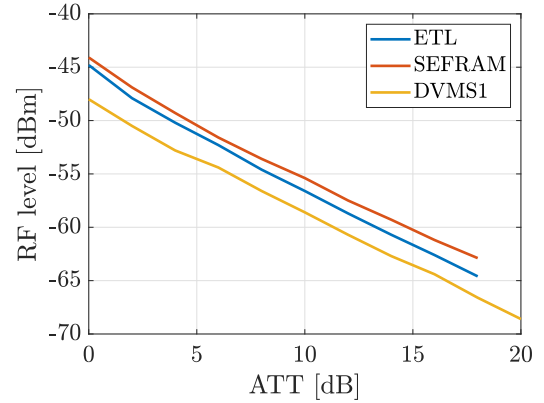
(c) MER vs attenuation (MUX21)



(d) MER vs attenuation (MUX22)

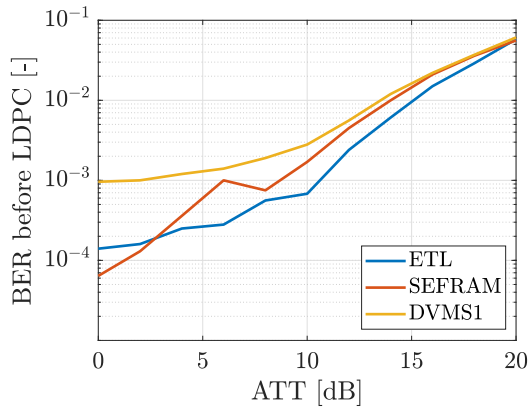


(e) RF level vs attenuation (MUX21)

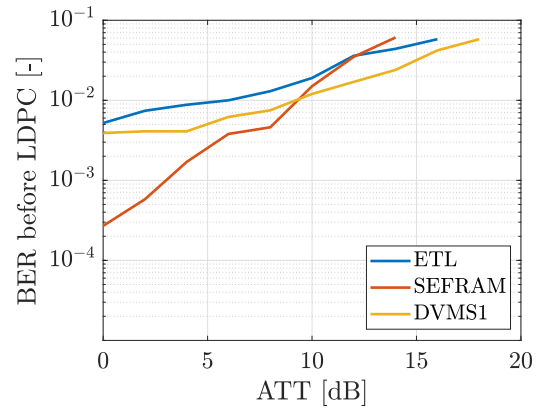


(f) RF level vs attenuation (MUX22)

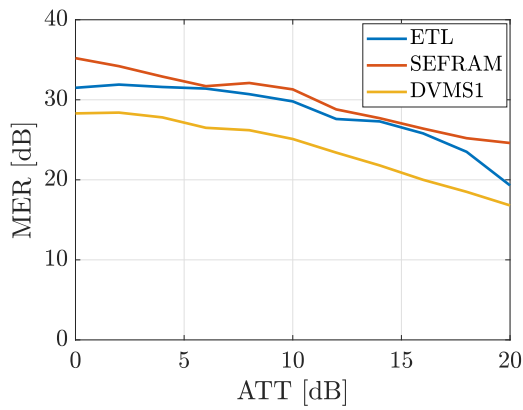
Fig. 4.5: Measured results for MUX21 and MUX22



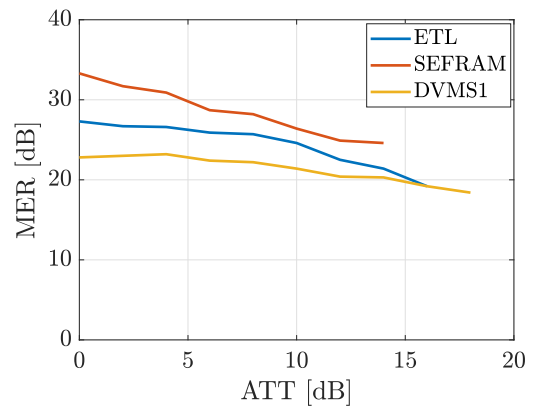
(a) BER before LDPC vs attenuation (MUX23)



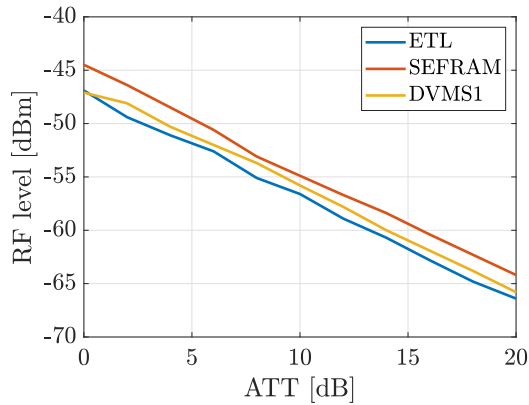
(b) BER before LDPC vs attenuation (MUX24)



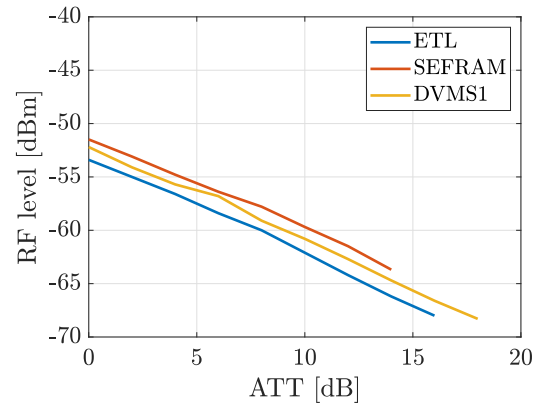
(c) MER vs attenuation (MUX23)



(d) MER vs attenuation (MUX24)

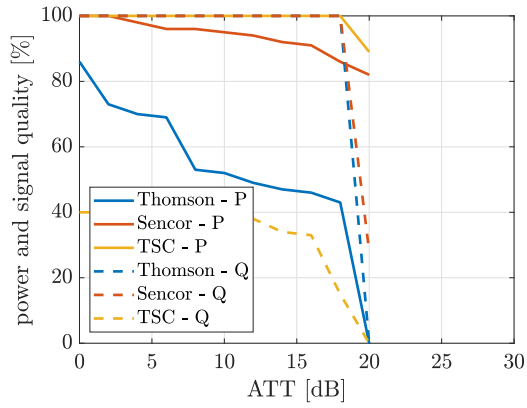


(e) RF level vs attenuation (MUX23)

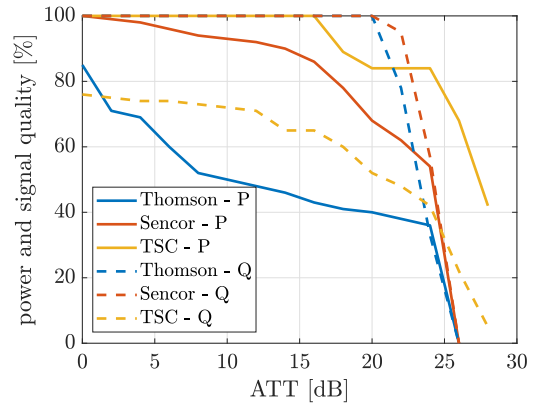


(f) RF level vs attenuation (MUX24)

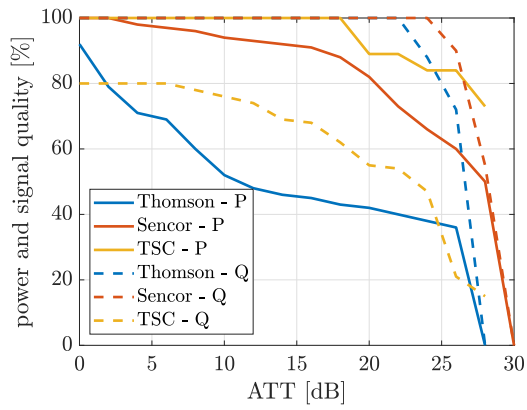
Fig. 4.6: Measured results for MUX23 and MUX24



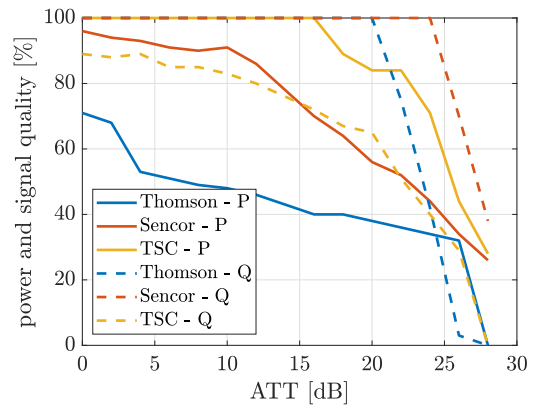
(a) MUX21



(b) MUX22



(c) MUX23



(d) MUX24

Fig. 4.7: Measured parameters of signal power (P) and signal quality (Q), marked by solid and dashed lines respectively, for each STB

Tab. 4.3: Data rates of services included in a) MUX21 and b) MUX22 (measured on 2023. 11. 13, 12:10 PM)

Service	Data rate [Mbit/s]
CT1 HD TV	6.295411
CT2 HD TV	6.342820
CT24 HD TV	6.000671
CT sport HD TV	9.687109
CT:D/art HD TV	3.773251
CT1 SM HD TV	6.295411
CT1 JM HD TV	6.295411
CT1 SVC HD TV	6.295411
CT1 JZC HD TV	6.295411
CRo RADIOZURNAL T2	0.130801
CRo DVOJKA T2	0.099521
CRo VLTAVA T2	0.130715
CRo RADIO WAVE T2	0.131067
CRo D-DUR T2	0.131363
CRo RADIO JUNIOR T2	0.066789
CRo PLUS T2	0.067037
CRo JAZZ T2	0.132363
CRo RZ SPORT T2	0.066517
CRo POHODA T2	1.600279
Null Packets	1.600279
Total data rate	33.301

(a) MUX 21

Service	Data rate [Mbit/s]
Prima COOL	1.374852
Prima ZOOM	2.866281
Prima MAX	1.386708
Ocko STAR	2.163471
Prima	2.597309
Ocko	2.940194
Prima KRIMI	3.491890
RADIO PROGLAS	0.047872
CNN Prima News	1.749521
Prima+1	2.042597
Prima love	1.529134
Prima STAR	1.676680
Prima SHOW	1.892299
Retro Music TV	2.010837
Naladte se na digitalni vysilani CRA	0.770323
Null Packets	1.661944
Total data rate	33.301

(b) MUX 22



Tab. 4.4: Data rates of services included in a) MUX 23 and b) MUX 24 (measured on 2023. 11. 13, 12:10 PM)

<b>Service</b>	<b>Data rate [Mbit/s]</b>
PSI/SI	0.766899
TV Barrandov	1.997020
Nova Cinema	1.196953
BARRANDOV KRIMI	2.2599109
KINO BARRANDOV	1.829698
NOVA	2.502243
Tv NOE	1.880058
Seznam.cz TV	4.457167
Radio Dechovka	0.049688
Cesky Impuls	0.051392
Radio Impuls	0.050400
UKRAJINSKE RADIO	0.055272
Test-1	0.561179
A11	1.373723
SPEKTRUM HOME	1.407636
Test-4	0.562584
Rock Zone 105,9	0.050424
Null Packets	10.615384
Total data rate	33.301

(a) MUX 23

<b>Service</b>	<b>Data rate [Mbit/s]</b>
PSI/SI	0.452469
Nova Action	1.799636
Nova Fun	2.250953
Nova Gold	3.059584
Nova	1.889022
Nova Lady	3.072769
Paramount Network	3.133370
JOJ Family	3.162715
RELAX	2.423990
REBEL	1.087023
Slager original	2.153478
Slager muzika	1.144505
CS Mystery	2.491960
ABC TV	1.608510
TV BRNO 1	1.458986
Radio Cas	0.098266
Radio Cas Rock	0.101410
Televize pres antenu	1.401304
Null Packets	2.158215
Total data rate	37.100

(b) MUX 24

# 5 Measurement of the DVB-T2 MISO TV signal

## TV signal

This chapter describes the proposed workplace, which enables the measurement and analysis of the DVB-T2 MISO-based TV signal under controlled laboratory conditions. The introduced setup allows the exploration of various factors, including the influence of different  $I/Q$ -errors, power imbalance between TXs, and the utilization of different channel models.

### 5.1 Measurement setup

The block diagram of the proposed laboratory workplace eligible to measure and analyze the DVB-T2 MISO-based TV signal under laboratory conditions is shown in Fig. 5.1.

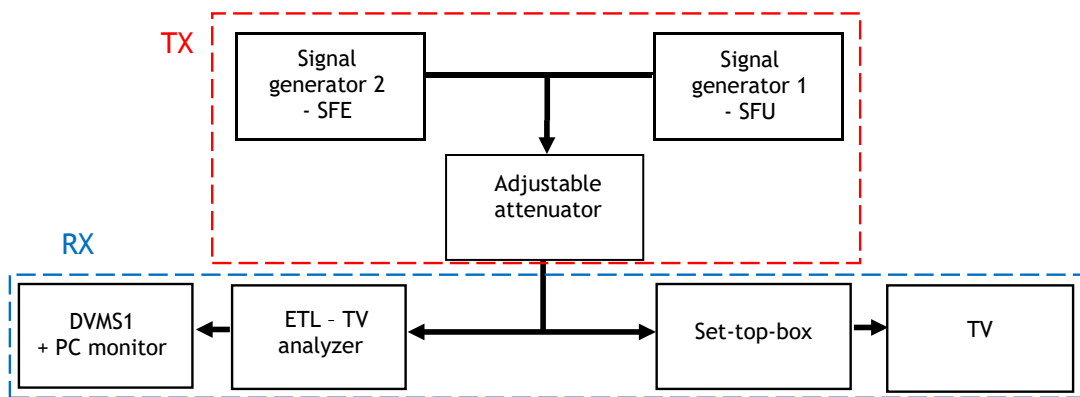


Fig. 5.1: Block diagram of the laboratory workplace for measurement of the DVB-T2 MISO signal

Two generators of the DVB-T2 signal, namely SFU (DVB-T2 RF signal generator no.1) and SFE (DVB-T2 RF signal generator no.2), are employed as TXs. SFU (Generator 1) has the additional capability of providing impairments to emulate different  $I/Q$ -errors. The output RF signals from both generators are combined before passing through an adjustable attenuator. The subsequent components of the laboratory setup are consistent with the previous configuration (see Fig. 4.2): the attenuator output is split into two pathways, connecting to ETL-TV analyzer in conjunction with DVMS1-TS monitoring system, and a STB. The ETL-TV analyzer and DVMS1-TS monitoring system are utilized in the same manner as in the previous measurement, although for this type of measurement, monitoring of TS or bit rates of the testing video is not crucial.

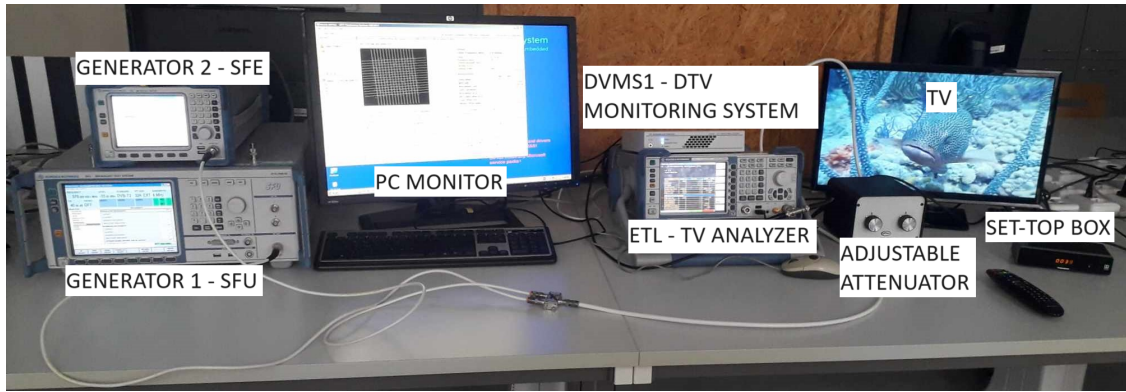


Fig. 5.2: Measurement workplace for DVB-T2 signal (MISO)

The second pathway is connected to the STB, specifically the THOMSON THT712 in this case. The output from the STB is then led to a TV. This setup allows for the measurement of both the power and quality of the DVB-T2 signal, as well as the quality of experience on the side of a viewer. The implemented measurement workplace is shown in Fig. 5.1.

## 5.2 DVB-T2 MISO signal configuration

The second measurement conducted in this study focuses on the analysis of the DVB-T2 MISO-based TV signal, including the study of the DVB-T2 system performance under various transmission conditions such as  $I/Q$ -errors, power imbalance, multipath propagation emulated by different channel models for fixed reception. For a more comprehensive analysis, the same measurement equipment and STBs were employed. The main system parameters of the DVB-T2 used to generate a MISO-based TV signal are summarized in Table 5.1. As it is visible, the main goal was to generate similar DVB-T2 RF signal as in the case of the SISO transmission mode. However, this was not entirely feasible due to the restricted combinations of GI, FFT size, and PPs (see Tab. 1.2). In this measurement, the value of  $C/N$  ratio was varied of the transmitters (TXs) instead of attenuation of the RF signal.

Tab. 5.1: System parameters of the DVB-T2 signal MISO

Frequency	570 MHz
Bandwidth	8 MHz
FFT mode	32K extended
Guard interval	1/16
Code rate	2/3
Pilot pattern	PP2
Transmission technique	MISO
Modulation	256-QAM
Rotation of constellation	ON
channel	AWGN, RL20, RC20

## 5.3 Results

This chapter contains graphical representation of the obtained results, available from Fig. 5.3 to Fig. 5.11, as well as the values of  $C/N$  to achieve QEF reception (Table 5.2 – Table 5.10) for each STB and measuring equipment used.

The performance of the DVB-T2 MISO-based signal was measured in the AWGN, RC20 and RL20 channel models, taking into consideration  $I/Q$ -errors in one TX and power imbalance of 5 dB between TXs (in one TX and subsequently in the other one). BER before LDPC and MER parameters were measured as a dependence on the  $C/N$  ratio of both TXs, as well as for each TX alone while the other TX maintained the maximum defined value of  $C/N$  ratio (in this case:  $C/N = 40$  dB).

Three scenarios were considered in the laboratory measurement. The first (reference) scenario assumes no  $I/Q$ -errors on the side of TX. It is followed by the second and third scenarios, in which  $I/Q$ -errors with AI of 10%, and AI of 10% plus PI of  $10^\circ$  are considered, respectively.

Additionally results of fixed reception scenarios in AWGN, RC20 and RL20 channels are shown in appendix. The obtained results were measured analogously as in this measurement, only difference is considering power imbalance of 10 dB between TXs.

### 5.3.1 AWGN

As it is visible, the impact of  $I/Q$ -errors on the DVB-T2 MISO-based signal is evident. For AI=10%, the performance degradation of the DVB-T2 signal reception, indicated by the measured objective parameters, is significantly less noticeable than for AI=10% and PI= $10^\circ$ . Regarding the measuring equipment used, the obtained

results clearly show that the DVMS1 monitoring system provides distinct results for the MER parameter, unlike the other two measuring devices, which yield more similar results. However, at higher power levels, the MER parameter measured by the DVMS1 device shows more accurate results in comparison to the other equipment. The differences in BER before LDPC among the measuring devices are much more similar with each other.

As seen in Fig. 5.4, there is a significant difference when the interference-free TX (without  $I/Q$ -errors and fading channels) maintains a power 5 dB higher. In this case, the DVB-T2 system performs very well even under  $I/Q$ -errors influence, and the QEF reception is overall better as the  $C/N$  ratio of the other TX decreases. In the opposite scenario, when the higher power level is at the SFU combined with  $I/Q$ -errors, the influence of the  $I/Q$ -errors is intensified.

In Table 5.2 and Table 5.4, some QEF values are missing because were immeasurable with certain measuring equipment or STBs due to the impact of  $I/Q$ -errors.

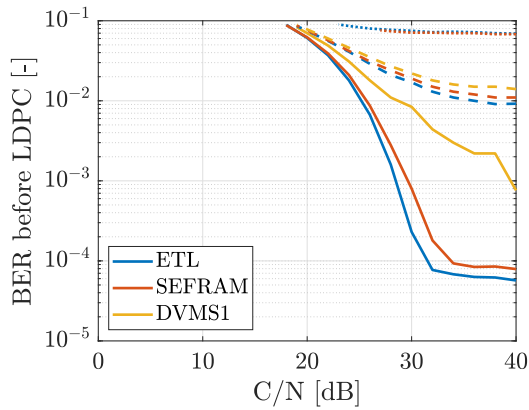
### 5.3.2 RC20

The performance of the DVB-T2 MISO signal affected by  $I/Q$ -errors in the RC20 channel is shown from Fig. 5.6 to Fig. 5.8. The impact on the DVB-T2 MISO system is minimal when only AI = 10% is considered. Overall, the measured BER and MER values are slightly better. This phenomenon can occur when favorable channel conditions are present in the second signal path, reducing the influence of  $I/Q$ -errors compared to the previous measurement. This also positively affects the QEF reception values, as shown in Table 5.5, Table 5.6 and Table 5.4.

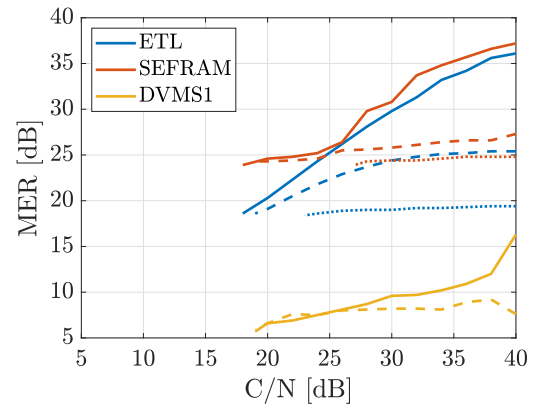
### 5.3.3 RL20

Finally, the same measurements were repeated for the case where RL20 fading channel conditions, emulated by 20 echoes, were applied to the TX1 path. Paradoxically, the obtained results are very similar to the previous case of RC20. The results are depicted from Fig. 5.9 to Fig. 5.10. This similarity can again be caused by favorable channel conditions for one of the TXs. Overall, the MISO-based transmission is not significantly influenced when fading channels for fixed transmission are present at one TX. The QEF values results demonstrates the remarkable resilience of the MISO-based DVB-T2 system to RL20 channel fading (see Table 5.8, Table 5.9 and Table 5.10).

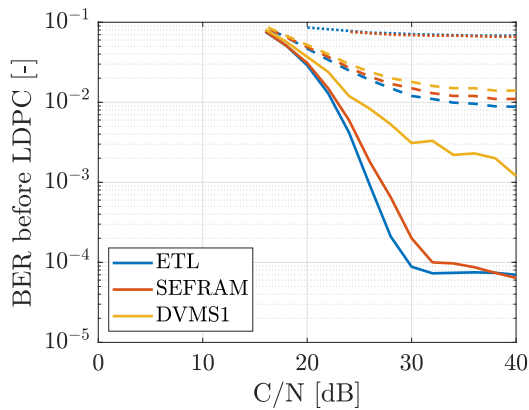
DVMS1 measuring equipment and STC set-top-box exhibit marginally better results of QEF values. However, the BER before LDPC and MER values obtained by DVMS1, especially the MER values, were the most affected by RL20 fading in combination with  $I/Q$ -errors.



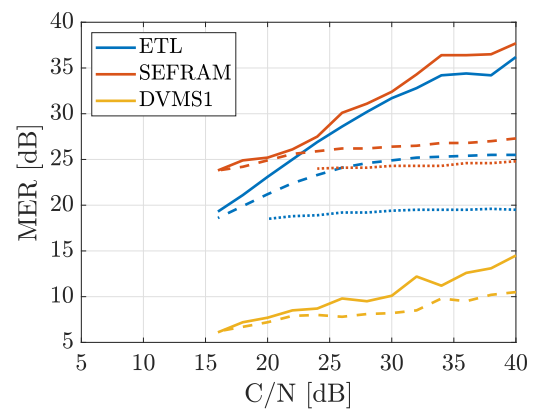
(a) BER vs  $C/N$  ( $C/N$  decreases on both generators)



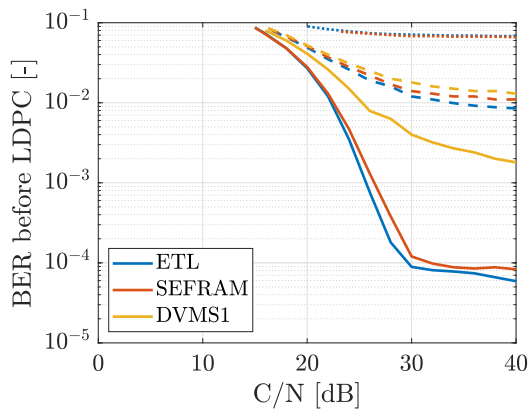
(b) MER vs  $C/N$  ( $C/N$  decreases on both generators)



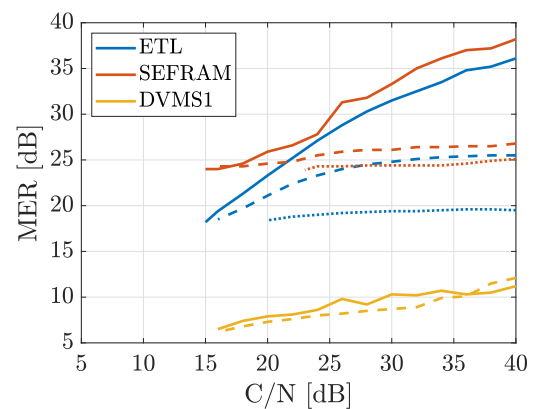
(c) BER vs  $C/N$  ( $C/N$  decreases on SFE)



(d) MER vs  $C/N$  ( $C/N$  decreases on SFE)

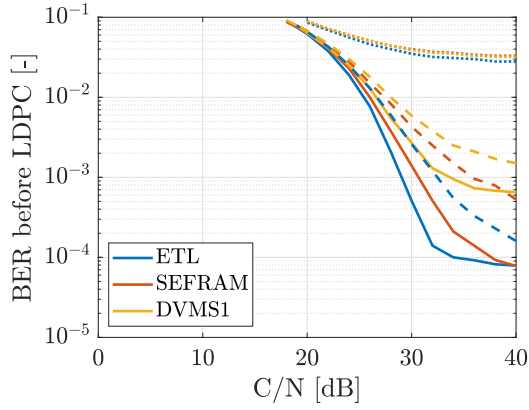


(e) BER vs  $C/N$  ( $C/N$  decreases on SFU)

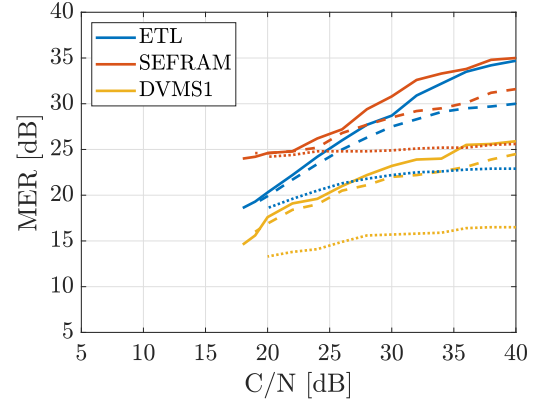


(f) MER vs  $C/N$  ( $C/N$  decreases on SFU)

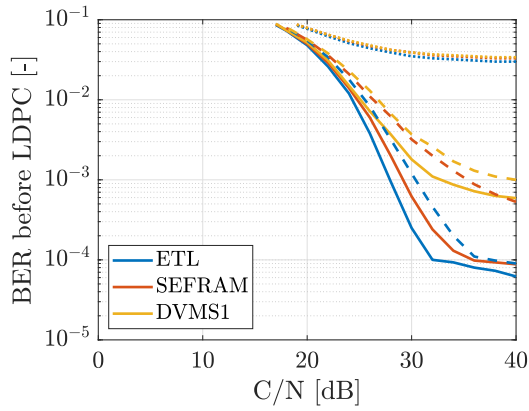
Fig. 5.3: DVB-T2 MISO TV signal: **AWGN channel** – solid lines: no  $I/Q$ -errors, dashed lines:  $AI = 10\%$ , dotted lines:  $AI = 10\%$  and  $PI = 10^\circ$



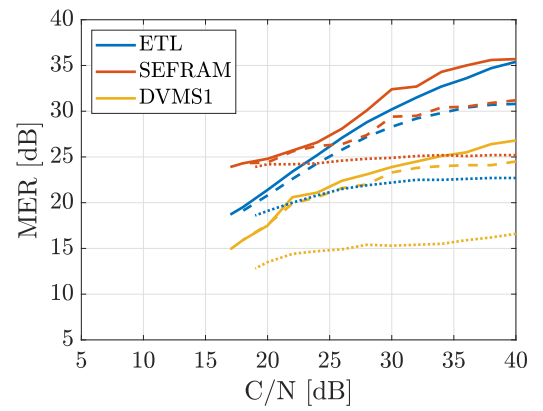
(a) BER vs  $C/N$  ( $C/N$  decreases on both generators)



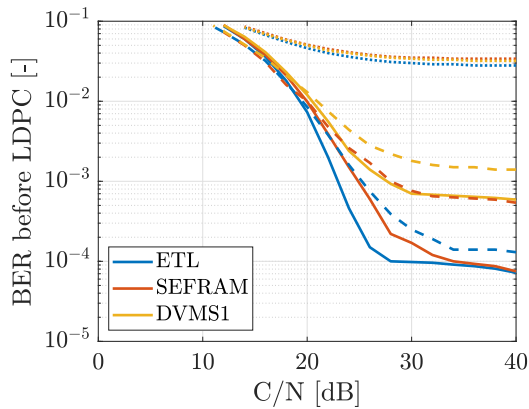
(b) MER vs  $C/N$  ( $C/N$  decreases on both generators)



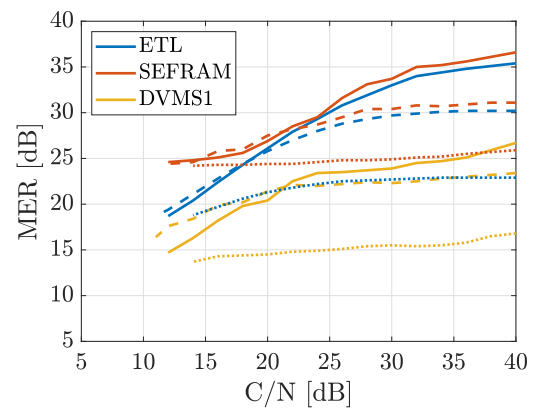
(c) BER vs  $C/N$  ( $C/N$  decreases on SFE)



(d) MER vs  $C/N$  ( $C/N$  decreases on SFE)

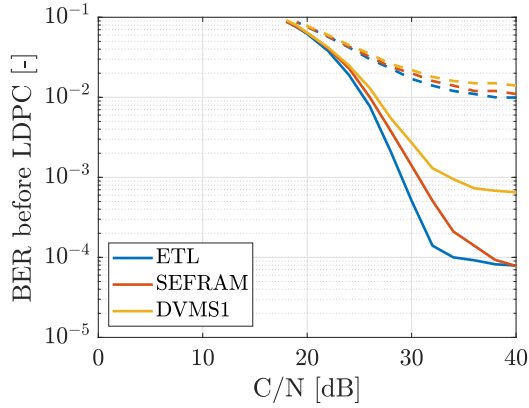


(e) BER vs  $C/N$  ( $C/N$  decreases on SFU)

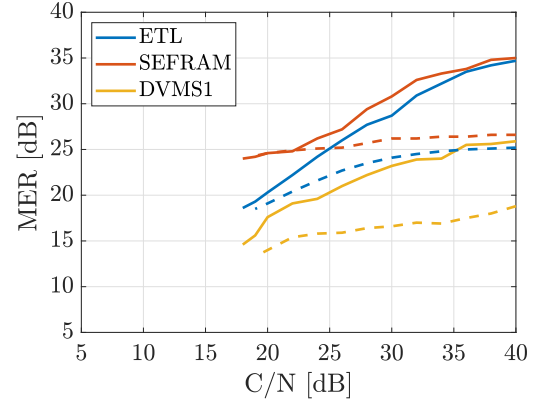


(f) MER vs  $C/N$  ( $C/N$  decreases on SFU)

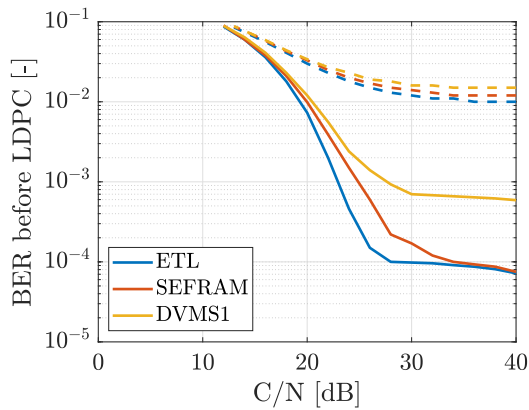
Fig. 5.4: DVB-T2 MISO TV signal: **AWGN channel**, power imbalance = 5 dB (SFE: -30 dBm, SFU: -35 dBm) – solid lines: no  $I/Q$ -errors, dashed lines:  $AI = 10\%$ , dotted lines:  $AI = 10\%$  and  $PI = 10^\circ$



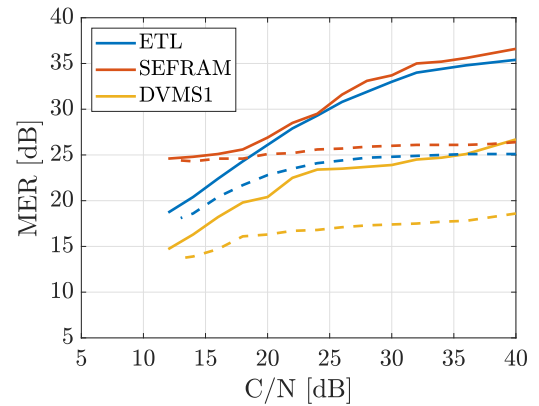
(a) BER vs  $C/N$  ( $C/N$  decreases on both generators)



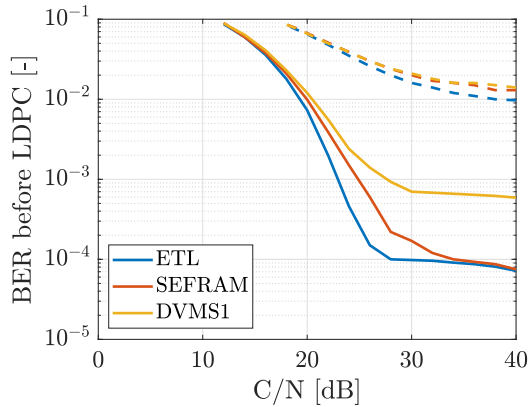
(b) MER vs  $C/N$  ( $C/N$  decreases on both generators)



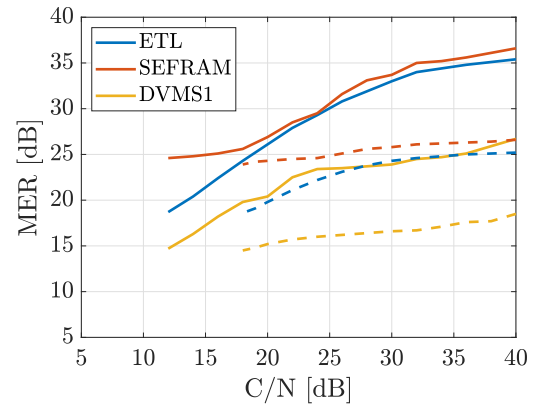
(c) BER vs  $C/N$  ( $C/N$  decreases on SFE)



(d) MER vs  $C/N$  ( $C/N$  decreases on SFE)



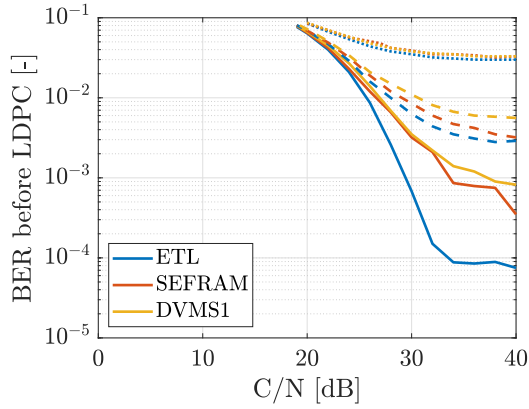
(e) BER vs  $C/N$  ( $C/N$  decreases on SFU)



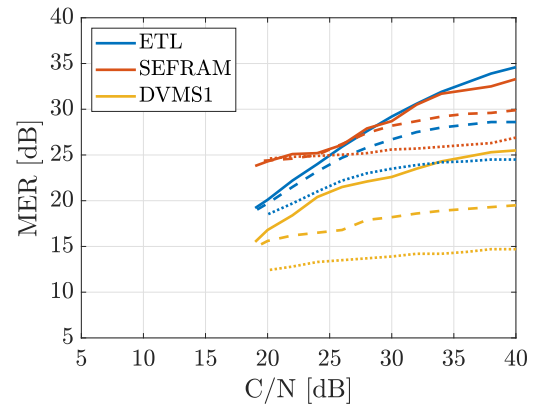
(f) MER vs  $C/N$  ( $C/N$  decreases on SFU)

Fig. 5.5: DVB-T2 MISO TV signal: **AWGN channel**, power imbalance = 5 dB (SFE: -35 dBm, SFU: -30 dBm) – solid lines: no  $I/Q$ -errors, dashed lines:  $AI = 10\%$ , dotted lines:  $AI = 10\%$  and  $PI = 10^\circ$

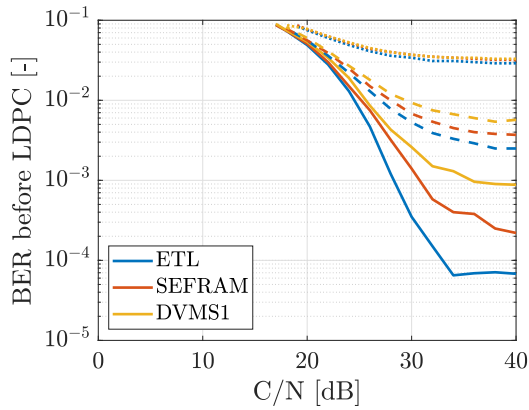




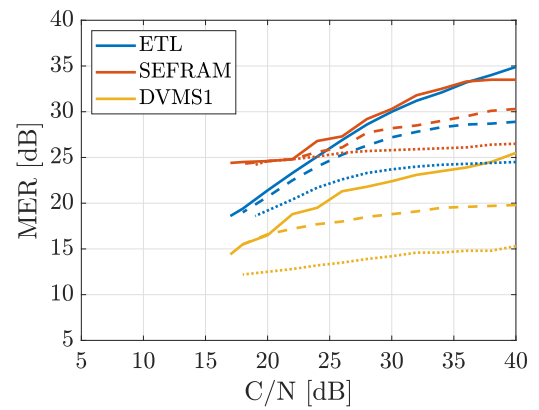
(a) BER vs  $C/N$  ( $C/N$  decreases on both generators)



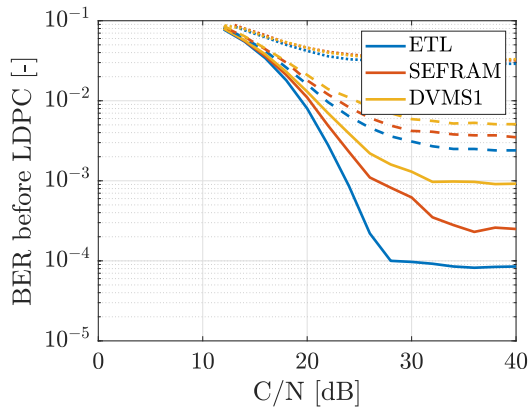
(b) MER vs  $C/N$  ( $C/N$  decreases on both generators)



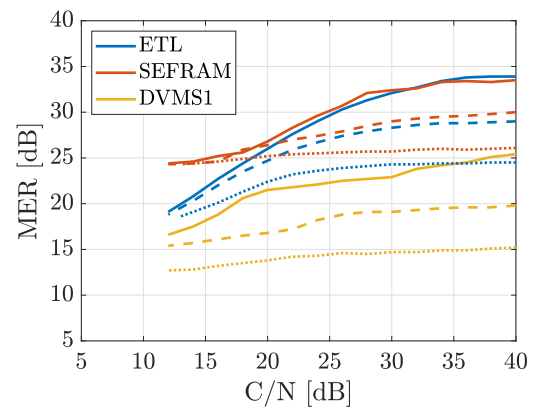
(c) BER vs  $C/N$  ( $C/N$  decreases on SFE)



(d) MER vs  $C/N$  ( $C/N$  decreases on SFE)

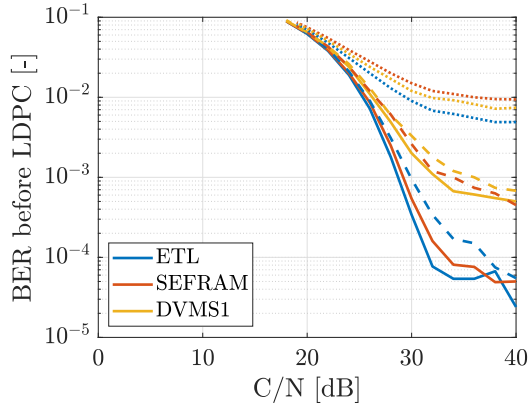


(e) BER vs  $C/N$  ( $C/N$  decreases on SFU)

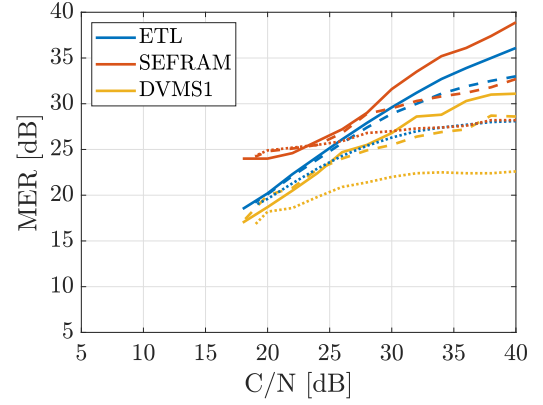


(f) MER vs  $C/N$  ( $C/N$  decreases on SFU)

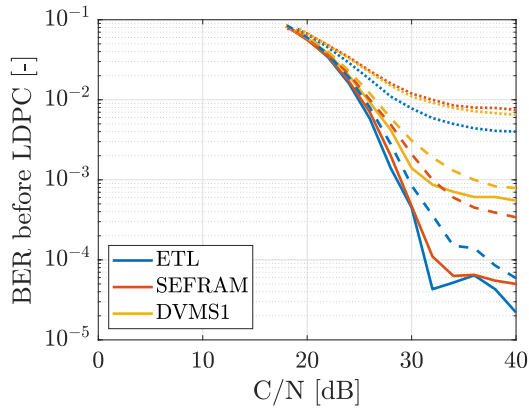
Fig. 5.6: DVB-T2 MISO TV signal: **RC20 channel** – solid lines: no  $I/Q$ -errors, dashed lines:  $AI = 10\%$ , dotted lines:  $AI = 10\%$  and  $PI = 10^\circ$



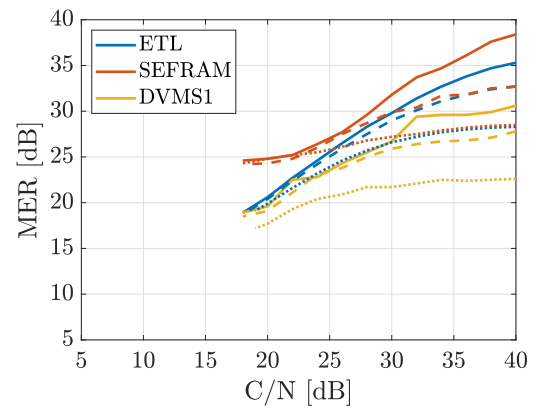
(a) BER vs  $C/N$  ( $C/N$  decreases on both generators)



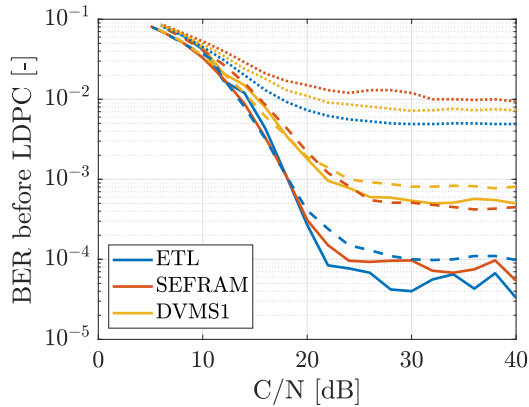
(b) MER vs  $C/N$  ( $C/N$  decreases on both generators)



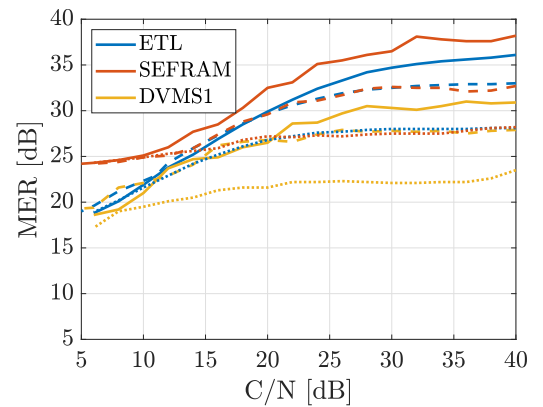
(c) BER vs  $C/N$  ( $C/N$  decreases on SFE)



(d) MER vs  $C/N$  ( $C/N$  decreases on SFE)

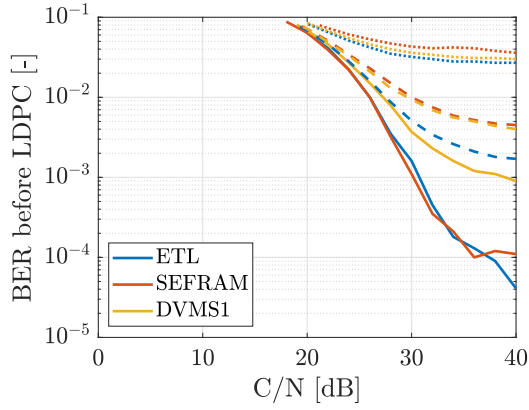


(e) BER vs  $C/N$  ( $C/N$  decreases on SFU)

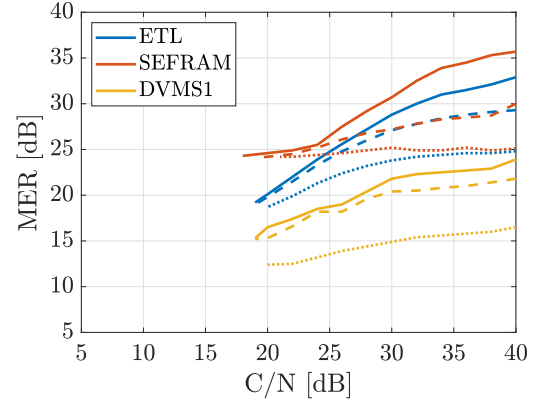


(f) MER vs  $C/N$  ( $C/N$  decreases on SFU)

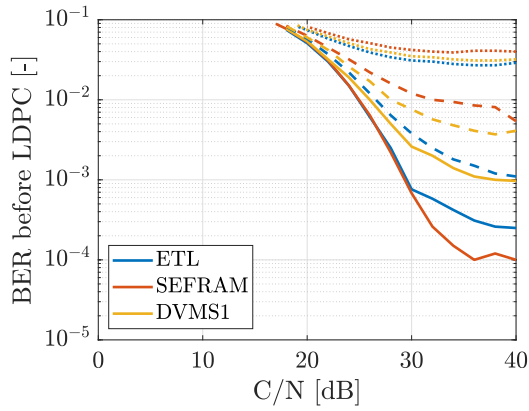
Fig. 5.7: DVB-T2 MISO TV signal: **RC20 channel**, power imbalance = 5 dB (SFE: -30 dBm, SFU: -35 dBm) – solid lines: no  $I/Q$ -errors, dashed lines:  $AI = 10\%$ , dotted lines:  $AI = 10\%$  and  $PI = 10^\circ$



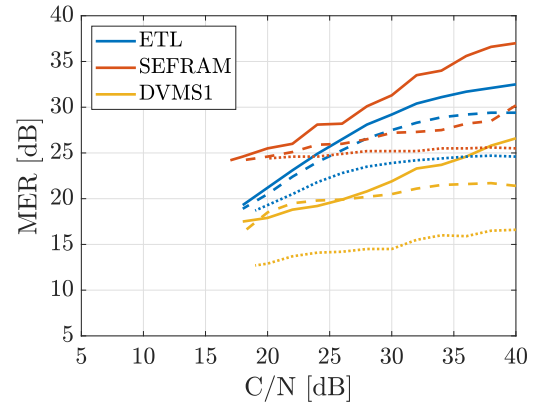
(a) BER vs  $C/N$  ( $C/N$  decreases on both generators)



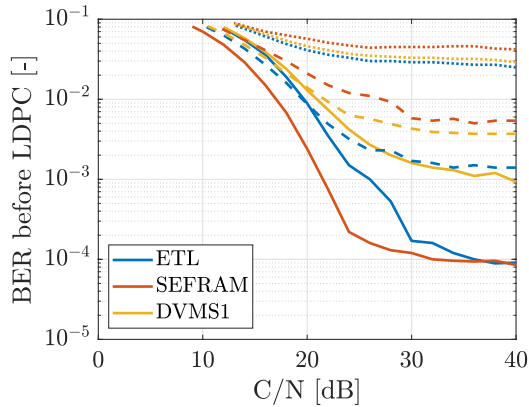
(b) MER vs  $C/N$  ( $C/N$  decreases on both generators)



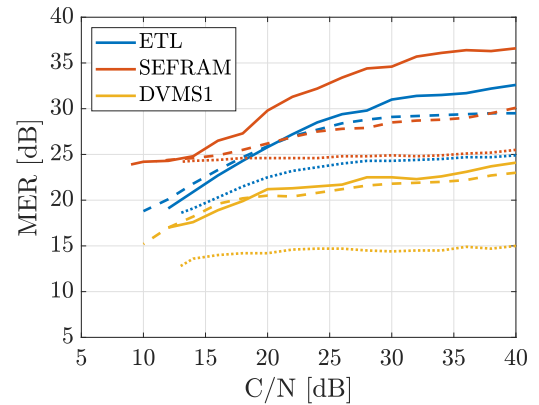
(c) BER vs  $C/N$  ( $C/N$  decreases on SFE)



(d) MER vs  $C/N$  ( $C/N$  decreases on SFE)

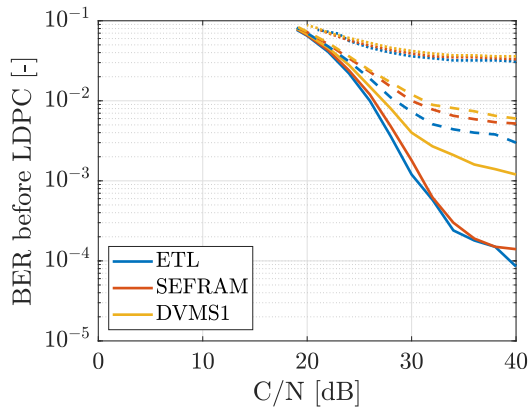


(e) BER vs  $C/N$  ( $C/N$  decreases on SFU)

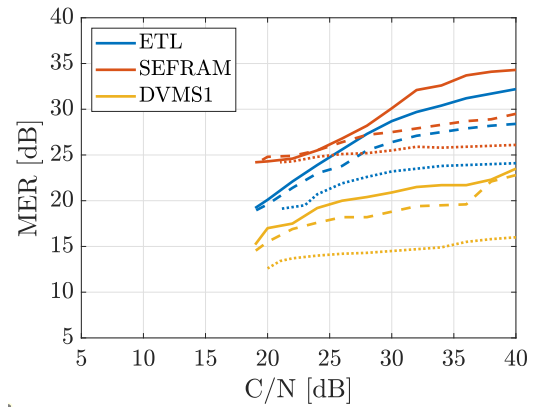


(f) MER vs  $C/N$  ( $C/N$  decreases on SFU)

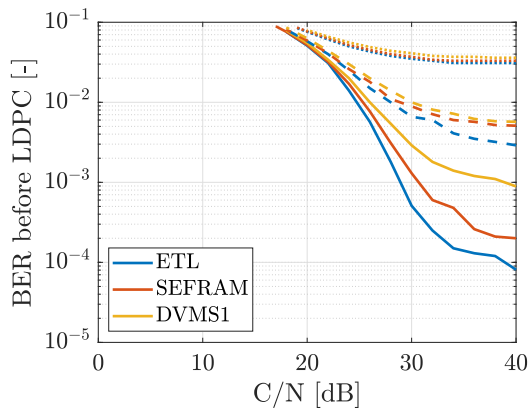
Fig. 5.8: DVB-T2 MISO TV signal: **RC20 channel**, power imbalance = 5 dB (SFE: -35 dBm, SFU: -30 dBm) – solid lines: no  $I/Q$ -errors, dashed lines:  $AI = 10\%$ , dotted lines:  $AI = 10\%$  and  $PI = 10^\circ$



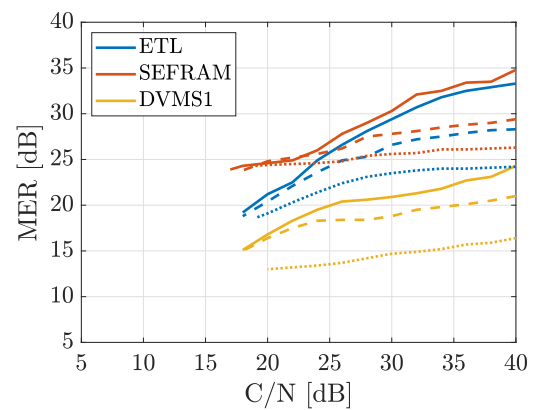
(a) BER vs  $C/N$  ( $C/N$  decreases on both generators)



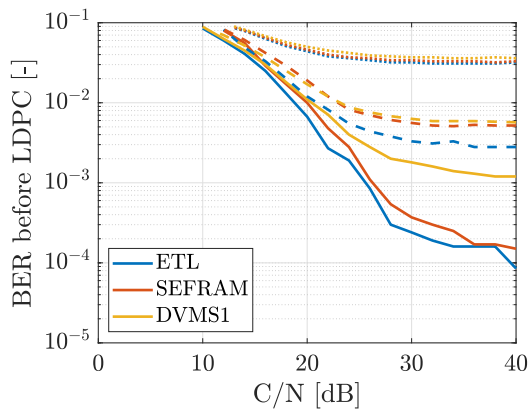
(b) MER vs  $C/N$  ( $C/N$  decreases on both generators)



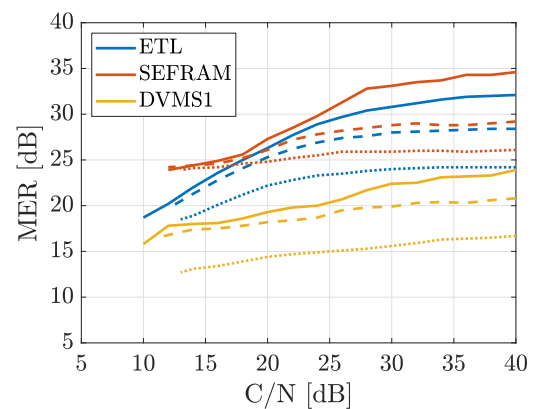
(c) BER vs  $C/N$  ( $C/N$  decreases on SFE)



(d) MER vs  $C/N$  ( $C/N$  decreases on SFE)

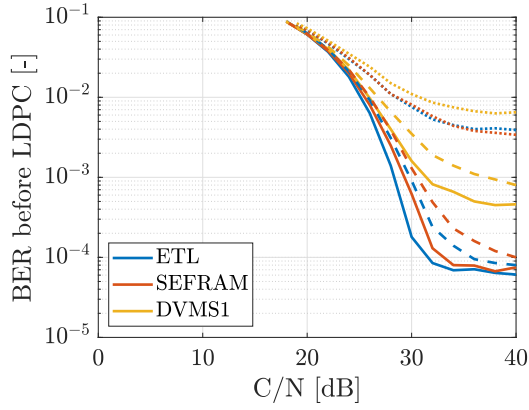


(e) BER vs  $C/N$  ( $C/N$  decreases on SFU)

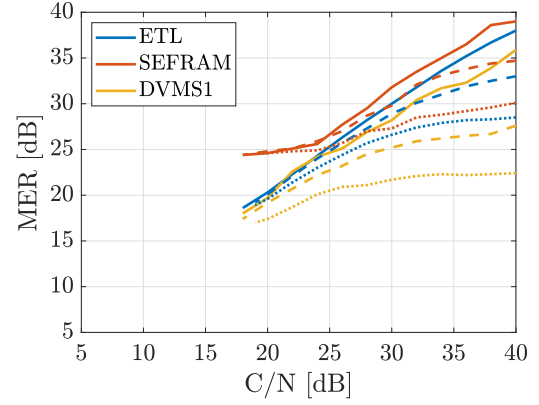


(f) MER vs  $C/N$  ( $C/N$  decreases on SFU)

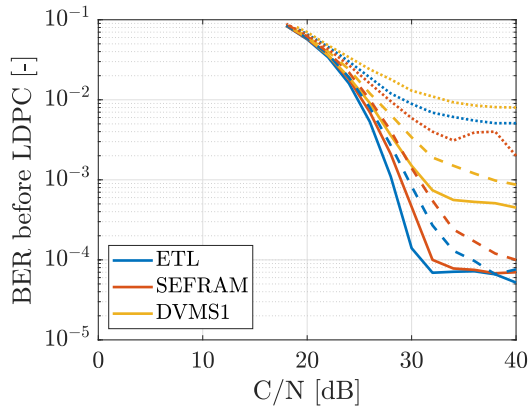
Fig. 5.9: DVB-T2 MISO TV signal: **RL20 channel** – solid lines: no  $I/Q$ -errors, dashed lines:  $AI = 10\%$ , dotted lines:  $AI = 10\%$  and  $PI = 10^\circ$



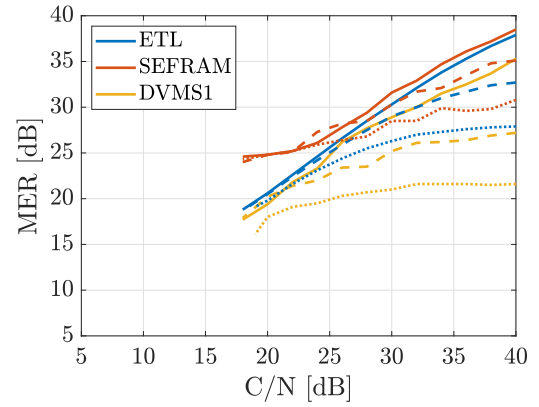
(a) BER vs  $C/N$  ( $C/N$  decreases on both generators)



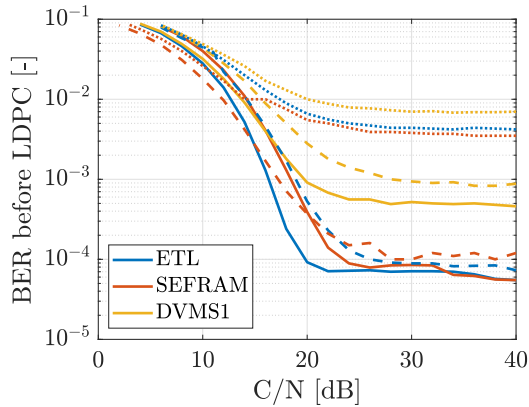
(b) MER vs  $C/N$  ( $C/N$  decreases on both generators)



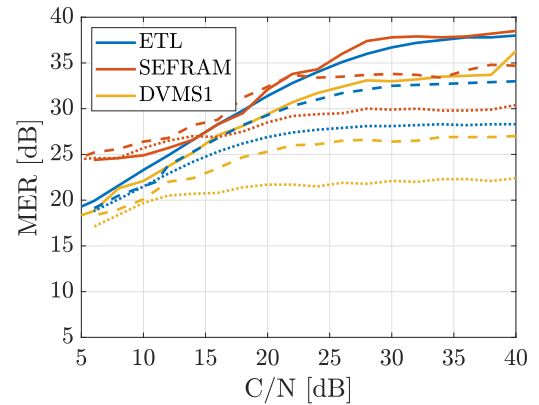
(c) BER vs  $C/N$  ( $C/N$  decreases on SFE)



(d) MER vs  $C/N$  ( $C/N$  decreases on SFE)

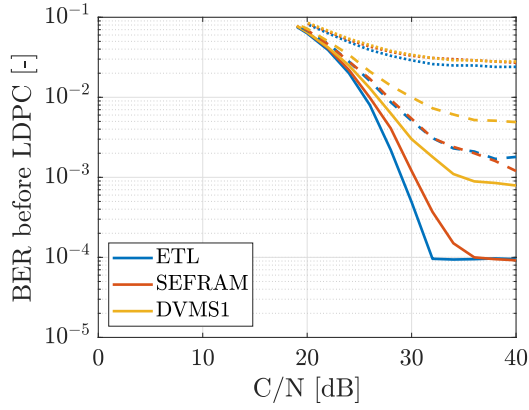


(e) BER vs  $C/N$  ( $C/N$  decreases on SFU)

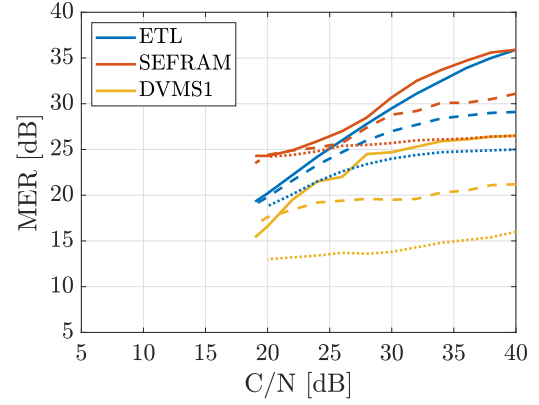


(f) MER vs  $C/N$  ( $C/N$  decreases on SFU)

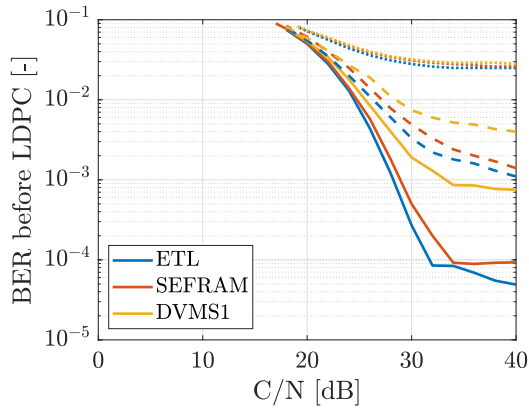
Fig. 5.10: DVB-T2 MISO TV signal: **RL20 channel**, power imbalance = 5 dB (SFE: -30 dBm, SFU: -35 dBm) – solid lines: no  $I/Q$ -errors, dashed lines:  $AI = 10\%$ , dotted lines:  $AI = 10\%$  and  $PI = 10^\circ$



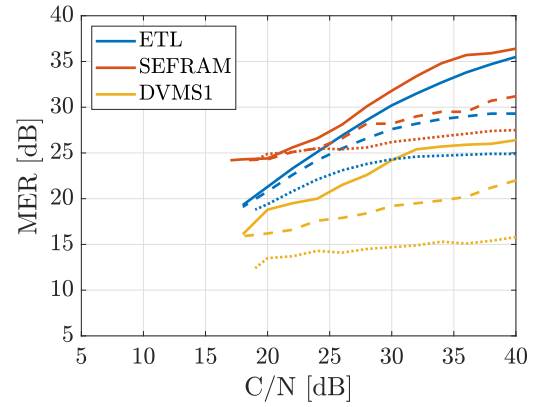
(a) BER vs  $C/N$  ( $C/N$  decreases on both generators)



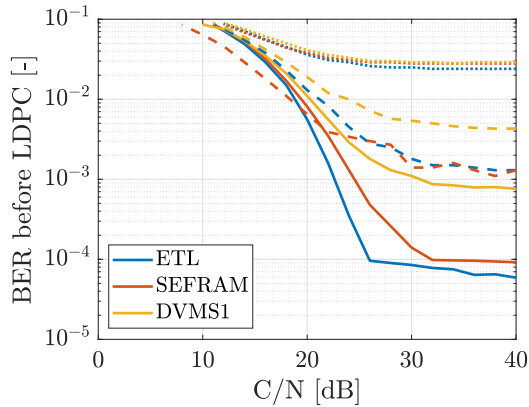
(b) MER vs  $C/N$  ( $C/N$  decreases on both generators)



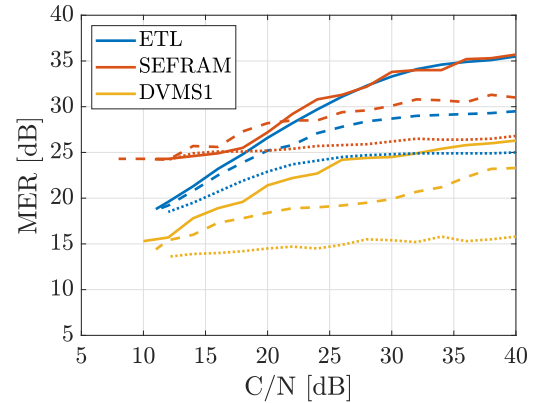
(c) BER vs  $C/N$  ( $C/N$  decreases on SFE)



(d) MER vs  $C/N$  ( $C/N$  decreases on SFE)



(e) BER vs  $C/N$  ( $C/N$  decreases on SFU)



(f) MER vs  $C/N$  ( $C/N$  decreases on SFU)

Fig. 5.11: DVB-T2 MISO TV signal: **RL20 channel**, power imbalance = 5 dB (SFE: -35 dBm, SFU: -30 dBm) – solid lines: no  $I/Q$ -errors, dashed lines:  $AI = 10\%$ , dotted lines:  $AI = 10\%$  and  $PI = 10^\circ$

Tab. 5.2: Required  $C/N$  in unit of dB for QEF reception in **AWGN** channel without power imbalance

$I/Q$ -errors	Changing of $C/N$	STB			Measurement Equipment		
		Thomson	Sencor	STC	ETL	Sefram	DVMS1
no $I/Q$ -errors	Both TXs	19	19	18	18	18	19
	SFE (TX2)	19	19	19	19	19	19
	SFU (TX1)	21	20	20	20	20	20
AI = 10%	Both TXs	19	19	19	19	19	19
	SFE (TX2)	16	16	16	16	16	16
	SFU (TX1)	17	17	16	16	16	16
AI = 10% and PI = 10°	Both TXs	29	30	–	23	27	–
	SFE (TX2)	27	27	–	20	24	–
	SFU (TX1)	25	27	–	20	23	–

Tab. 5.3: Required  $C/N$  in unit of dB for QEF reception in **AWGN** channel with power imbalance of 5 dB (SFU = -35 dBm, SFE = -30 dBm)

$I/Q$ -errors	Changing of $C/N$	STB			Measurement Equipment		
		Thomson	Sencor	STC	ETL	Sefram	DVMS1
no $I/Q$ -errors	Both TXs	19	19	18	19	18	19
	SFE (TX2)	18	18	17	17	17	17
	SFU (TX1)	13	13	12	12	12	12
AI = 10%	Both TXs	20	20	19	19	19	19
	SFE (TX2)	18	18	18	18	18	18
	SFU (TX1)	12	13	11	11	12	11
AI = 10% and PI = 10°	Both TXs	21	20	20	20	20	20
	SFE (TX2)	19	19	19	19	19	19
	SFU (TX1)	14	14	14	14	14	14

Tab. 5.4: Required  $C/N$  in unit of dB for QEF reception in **AWGN** channel with power imbalance of 5 dB (SFU = -30 dBm, SFE = -35 dBm)

$I/Q$ -errors	Changing of $C/N$	STB			Measurement Equipment		
		Thomson	Sencor	STC	ETL	Sefram	DVMS1
no $I/Q$ -errors	Both TXs	19	19	18	19	18	19
	SFE (TX2)	18	18	17	17	17	17
	SFU (TX1)	13	13	12	12	12	12
AI = 10%	Both TXs	19	19	18	19	19	19
	SFE (TX2)	14	13	13	13	13	13
	SFU (TX1)	18	18	18	18	18	18
AI = 10% and PI = 10°	Both TXs	–	–	–	–	–	–
	SFE (TX2)	–	–	–	–	–	–
	SFU (TX1)	–	–	–	–	–	–

Tab. 5.5: Required  $C/N$  in unit of dB for QEF reception in **RC20** channel without power imbalance

$I/Q$ -errors	Changing of $C/N$	STB			Measurement Equipment		
		Thomson	Sencor	STC	ETL	Sefram	DVMS1
no $I/Q$ -errors	Both TXs	19	19	19	19	19	19
	SFE (TX2)	18	18	17	17	17	17
	SFU (TX1)	12	12	12	12	12	12
AI = 10%	Both TXs	19	19	19	19	19	19
	SFE (TX2)	18	18	18	18	18	18
	SFU (TX1)	12	13	12	12	12	12
AI = 10% and PI = 10°	Both TXs	21	21	20	20	20	20
	SFE (TX2)	20	20	19	19	19	19
	SFU (TX1)	14	14	13	13	13	12

Tab. 5.6: Required  $C/N$  in unit of dB for QEF reception in **RC20** channel with power imbalance of 5 dB (SFU = -35 dBm, SFE = -30 dBm)

$I/Q$ -errors	Changing of $C/N$	STB			Measurement Equipment		
		Thomson	Sencor	STC	ETL	Sefram	DVMS1
no $I/Q$ -errors	Both TXs	19	19	18	18	18	18
	SFE (TX2)	18	18	18	18	18	18
	SFU (TX1)	6	6	5	6	5	6
AI = 10%	Both TXs	19	19	19	19	19	18
	SFE (TX2)	18	18	18	18	18	18
	SFU (TX1)	6	6	5	5	6	5
AI = 10% and PI = 10°	Both TXs	19	20	19	19	19	19
	SFE (TX2)	19	19	19	19	19	19
	SFU (TX1)	6	7	6	6	6	6

Tab. 5.7: Required  $C/N$  in unit of dB for QEF reception in **RC20** channel with power imbalance of 5 dB (SFU = -30 dBm, SFE = -35 dBm)

$I/Q$ -errors	Changing of $C/N$	STB			Measurement Equipment		
		Thomson	Sencor	STC	ETL	Sefram	DVMS1
no $I/Q$ -errors	Both TXs	19	19	19	19	19	19
	SFE (TX2)	18	18	17	18	17	18
	SFU (TX1)	12	12	11	12	9	12
AI = 10%	Both TXs	19	20	19	19	19	19
	SFE (TX2)	18	18	18	18	18	18
	SFU (TX1)	10	11	10	10	11	10
AI = 10% and PI = 10°	Both TXs	20	21	20	20	21	20
	SFE (TX2)	20	20	19	19	20	19
	SFU (TX1)	14	14	13	13	13	13



Tab. 5.8: Required  $C/N$  in unit of dB for QEF reception in **RL20** channel without power imbalance

$I/Q$ -errors	Changing of $C/N$	STB			Measurement Equipment		
		Thomson	Sencor	STC	ETL	Sefram	DVMS1
no $I/Q$ -errors	Both TXs	19	19	19	19	19	19
	SFE (TX2)	18	18	17	18	17	18
	SFU (TX1)	11	11	10	10	12	10
AI = 10%	Both TXs	20	19	19	19	19	19
	SFE (TX2)	18	18	18	18	18	18
	SFU (TX1)	13	13	11	11	12	11
AI = 10% and PI = 10°	Both TXs	22	22	21	21	21	20
	SFE (TX2)	20	20	20	19	19	20
	SFU (TX1)	14	14	13	13	13	13

Tab. 5.9: Required  $C/N$  in unit of dB for QEF reception in **RL20** channel with power imbalance of 5 dB (SFU = -35 dBm, SFE = -30 dBm)

$I/Q$ -errors	Changing of $C/N$	STB			Measurement Equipment		
		Thomson	Sencor	STC	ETL	Sefram	DVMS1
no $I/Q$ -errors	Both TXs	19	19	18	18	18	18
	SFE (TX2)	18	18	18	18	18	18
	SFU (TX1)	6	6	5	4	6	4
AI = 10%	Both TXs	19	19	19	19	18	18
	SFE (TX2)	18	18	18	18	18	18
	SFU (TX1)	6	6	6	5	4	5
AI = 10% and PI = 10°	Both TXs	19	19	19	19	19	19
	SFE (TX2)	19	20	19	19	18	19
	SFU (TX1)	6	6	5	6	5	6

Tab. 5.10: Required  $C/N$  in unit of dB for QEF reception in **RL20** channel with power imbalance of 5 dB (SFU = -30 dBm, SFE = -35 dBm)

$I/Q$ -errors	Changing of $C/N$	STB			Measurement Equipment		
		Thomson	Sencor	STC	ETL	Sefram	DVMS1
no $I/Q$ -errors	Both TXs	19	19	19	19	19	19
	SFE (TX2)	18	18	17	18	17	18
	SFU (TX1)	12	12	11	11	11	11
AI = 10%	Both TXs	20	20	19	19	19	19
	SFE (TX2)	18	18	18	18	18	18
	SFU (TX1)	12	12	11	11	10	11
AI = 10% and PI = 10°	Both TXs	21	21	20	20	20	20
	SFE (TX2)	19	19	19	19	19	19
	SFU (TX1)	13	13	12	12	12	12

## 6 Measurement of the DVB-T2 MISO TV signal in portable and mobile channels

This chapter describes the measurement and analysis of the DVB-T2 MISO-based TV signal under different mobile and portable laboratory conditions, considering the influence of  $I/Q$ -errors and power imbalance between TXs. The measurement setup and laboratory workplace remain the same as in the previous measurement scenario (DVB-T2 MISO fixed reception). However, the signal configuration of the DVB-T2 MISO signal is adjusted to be more appropriate to scenarios in mobile and portable fading channels, specifically: PI, PO, TU6 and RA6.

### 6.1 DVB-T2 MISO portable and mobile signal configuration

In the DVB-T2 MISO system configuration, the video transport stream (TS) is generated within the broadcast multiplexer (BMUX) block of the SFU signal generator [11]. Two slightly different types of signal configuration were used in this measurement according to [10]. The first one is for a MISO-based portable reception and was used to explore the performance of the DVB-T2 MISO signal in PI and PO fading channels. The second configuration differs only in a few adjustable parameters of the DVB-T2 system, specifically CR, FFT mode and PP. This configuration is used for TU6 and RA6 fading channels. The complete signal configuration for both mobile and portable scenarios is summarized Table 6.1. The measurement procedure remains the same as described for fixed reception.

Bandwidth	8 MHz
FFT mode	16K extended
Guard interval	1/8
Code rate	1/2
Pilot pattern	PP1
Transmission technique	MISO
Modulation	16-QAM
Rotation of constellation	ON

(a) Portable scenario

Bandwidth	8 MHz
FFT mode	4K normal
Guard interval	1/8
Code rate	2/3
Pilot pattern	PP2
Transmission technique	SISO
Modulation	QPSK
Rotation of constellation	ON

(b) Mobile scenario

Tab. 6.1: DVB-T2 MISO-based signal configuration for portable and mobile reception

For a more comprehensive analysis, three different measurement equipment were

used, as well as three different STBs. All the devices were compared with each other in terms of QEF reception. The measurement was carried in three cycles: without power imbalance between TXs and with a power imbalance of 5 dB for each TX, as in the previous chapter. MER and BER parameters were used to describe the performance of the DVB-T2 MISO system.

## 6.2 Results

In this chapter, the chosen results for each measurements scenarios are analyzed and concluded (see figures from Fig. 6.1 to Fig. 6.12). Once again, the graphical results and tables of C/N values needed for QEF reception for each measuring device and STB are summarized (see tables from Table 5.2 to Table 6.13).

The performance of the DVB-T2 MISO-based signal was evaluated under PI and PO portable scenarios, as well as TU6 and RA6 mobile scenarios, taking into consideration  $I/Q$ -errors in one TX and power imbalance of 5 dB between TXs (in one TX and subsequently in the other one). BER before LDPC and MER parameters were measured as a dependence on the C/N ratio of both TXs, as well as for each TX individually, while the other TX maintained the maximum defined value of C/N ratio (in this case:  $C/N = 40 \text{ dB}$ ), consistent with previous measurements.

### 6.2.1 Results for portable scenarios (PI, PO)

The obtained results for PI and PO channels are plotted from Fig. 6.1 to Fig. 6.6 and display similar trends. The more robust configuration, ensured by  $CR = 1/2$  and QPSK modulation, used for portable transmission provides significant protection of the transmitted signal data even for  $I/Q$ -error of  $AI = 10\%$ . However, there is monitored significant degradation in the signal quality, indicated by the objective parameters, in the worst-case scenario,  $AI = 10\%$  and  $PI = 10^\circ$ , when TX1 has the same or higher power level. When TX2 has a higher power level the impact of  $I/Q$ -errors is less significant. It is visible that the TX1 (SFU) affected by PI-based fading has a less significant impact on the overall transmission. When its C/N decreasing, it does not influence the overall performance of the DVB-T2 MISO system in terms of BER before LDPC and MER parameters as much as the decreasing C/N ratio of TX2 (SFE – interference-free TX) or both C/N ratios simultaneously.

There are visible differences between the measuring equipment in MER measurement. While Sefram and ETL measurement devices provide very similar results for each case of measurement, DVMS1 seems to be more affected by the fading in the channel path when TX1 has the same or higher power level.

In the case of interference-free TX2, has a higher power level, the obtained results shows more similarity between each measuring device.

In terms of QEF reception tables, see in Table 6.2 – Table 6.7, we can see that there are no C/N values for QEF reception when the C/N ratio of TX1 (signal path from SFE is affected by fading channel model and  $I/Q$ -errors) is decreasing. The received signal shows no signs of erroneous reception. This only confirms that the performance of the DVB-T2 MISO system is highly dependent on the interference-free transmitter (TX2, SFU).

## 6.2.2 Mobile channel results (TU6, RA6)

Results from the measurement of the DVB-T2 MISO signal, influenced by different  $I/Q$ -errors under mobile fading channels are plotted from Fig. 6.7 to Fig. 6.12.

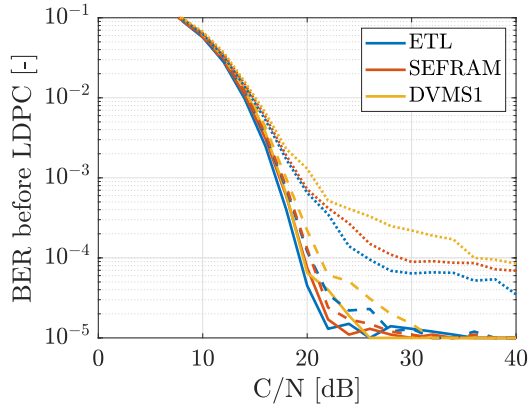
Results obtained for the TU6 channel model display significant difference compared to the results obtained for the RA6 channel model. In the case of the TU6 channel scenario, see Fig. 6.7 – Fig. 6.9, there is a noteworthy impact of  $I/Q$ -errors when the TXs maintain the same power level or when TX1 (SFU, with  $I/Q$ -errors) has a higher power level. However, when TX2 (SFE, the interference-free transmitter) has a higher power level, the impact of  $I/Q$ -errors is significantly mitigated.

Regarding the differences between measurement devices, it is clearly observable that the TU6-based channel fading significantly affects the measured MER and BER before LDPC values of DVMS1 and Sefram, while ETL is equipped with mobile measurement mode, which is more suitable for monitoring parameters under mobile channel conditions.

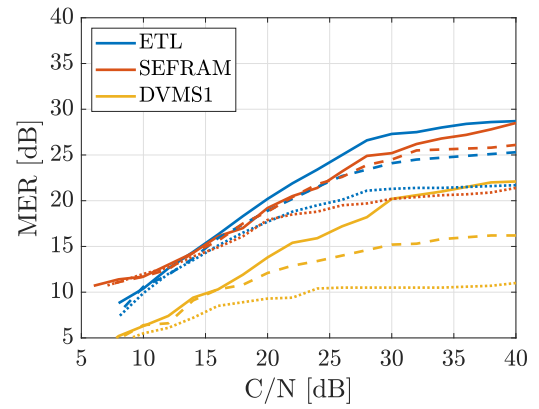
However, the obtained values of  $C/N$ , see Table 6.8 – Table 6.10, needed for QEF reception for each measuring device and STB do not show any noteworthy differences despite the variations in the measured objective parameters. When TX2 (SFE signal generator) has a higher power level, the measured DVB-T2 MISO system remains fully usable even when the  $C/N$  ratio of TX1 (SFU) goes to zero.

In case of RA6 fading channel model, the results (see Fig. 6.10 – Fig. 6.12) exhibit noticeable differences compared to the results obtained for channel model TU6. The overall behaviour of the system is similar to the TU6, but in this case, the RA6 channel represent a more significant challenge for the measuring equipment, especially for Sefram and DVMS1. The ETL TV analyzer, which possesses a mobile measurement mode suited to mobile scenarios, shows slightly weaker reception at low  $C/N$  value (see Table 6.8 – Table 6.13). The influence of  $I/Q$ -errors is not as strong as in the previous cases. Only in the worst case we can see some noteworthy differences in BER before LDPC and MER values.

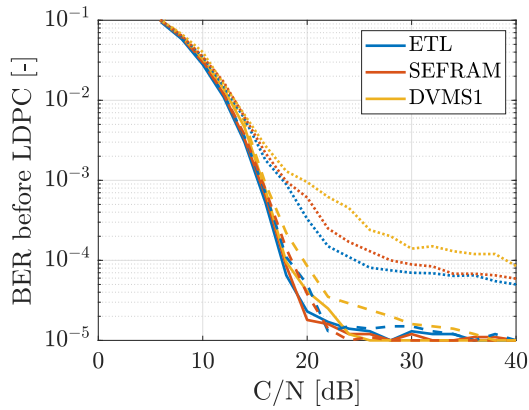
The QEF values for each measurement scenario are clearly shown in Table 6.11 – Table 6.13 and confirm the effect of RA6 fading channel on TX1 (SFU), while the other transmitter, TX2, can maintain the quality of transmission of the MISO technique. In terms of comparison between measuring equipment and STBs, there is no a significant difference. However, some devices measure better  $C/N$  values for QEF reception throughout all the measurement, within a range of 1 to 2 dB.



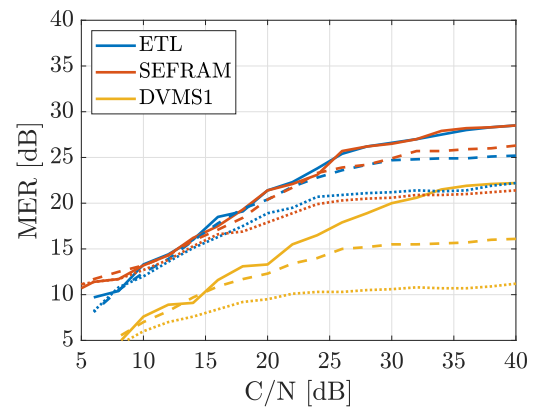
(a) BER vs  $C/N$  ( $C/N$  decreases on both generators)



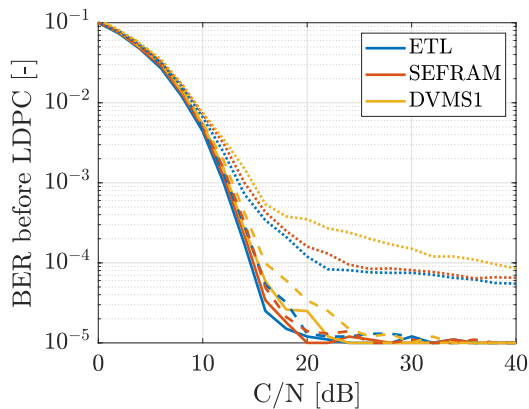
(b) MER vs  $C/N$  ( $C/N$  decreases on both generators)



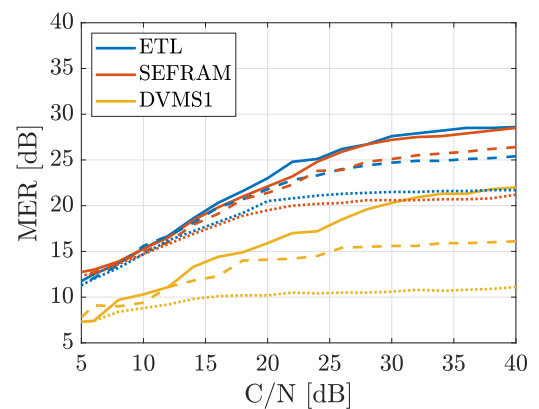
(c) BER vs  $C/N$  ( $C/N$  decreases on SFE)



(d) MER vs  $C/N$  ( $C/N$  decreases on SFE)

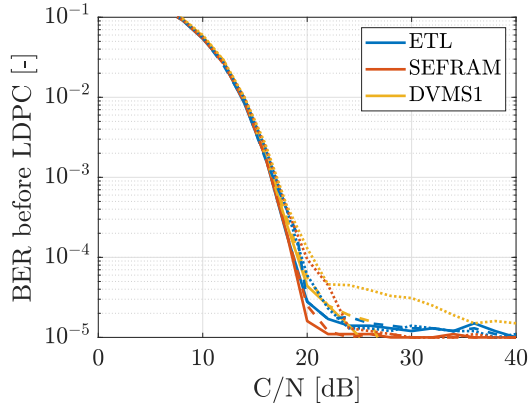


(e) BER vs  $C/N$  ( $C/N$  decreases on SFU)

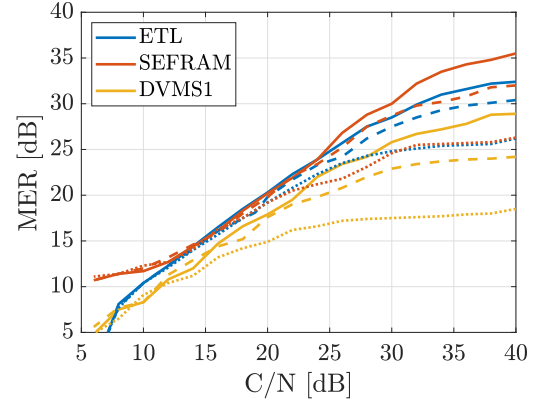


(f) MER vs  $C/N$  ( $C/N$  decreases on SFU)

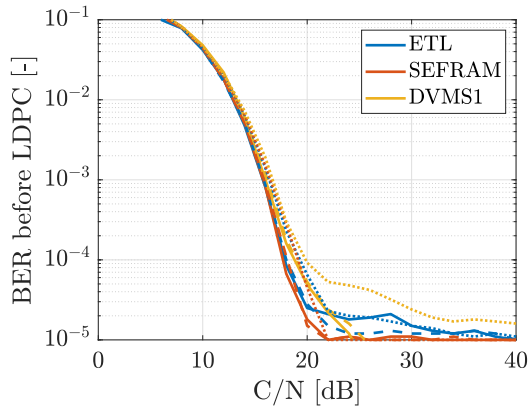
Fig. 6.1: DVB-T2 MISO TV signal: **PI** – solid lines: no  $I/Q$ -errors, dashed lines:  $AI = 10\%$ , dotted lines:  $AI = 10\%$  and  $PI = 10^\circ$



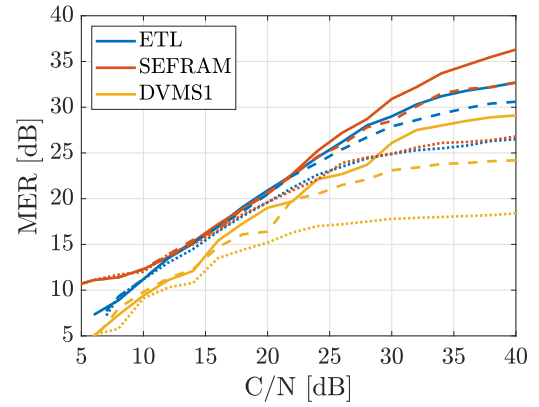
(a) BER vs  $C/N$  ( $C/N$  decreases on both generators)



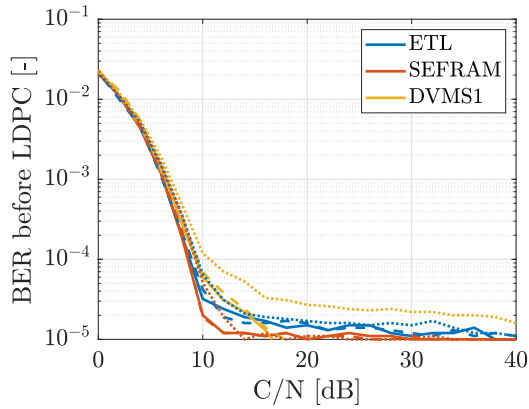
(b) MER vs  $C/N$  ( $C/N$  decreases on both generators)



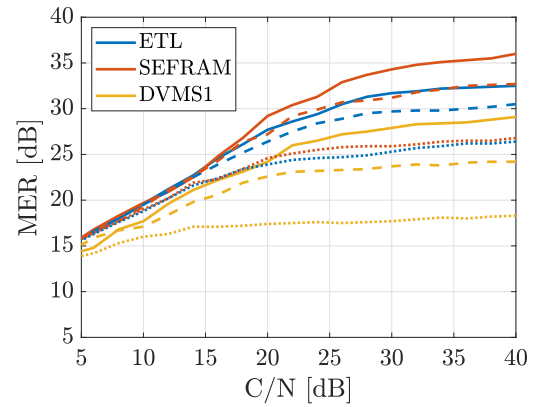
(c) BER vs  $C/N$  ( $C/N$  decreases on SFE)



(d) MER vs  $C/N$  ( $C/N$  decreases on SFE)

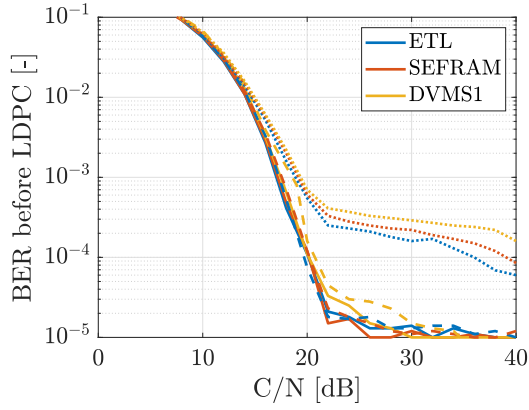


(e) BER vs  $C/N$  ( $C/N$  decreases on SFU)

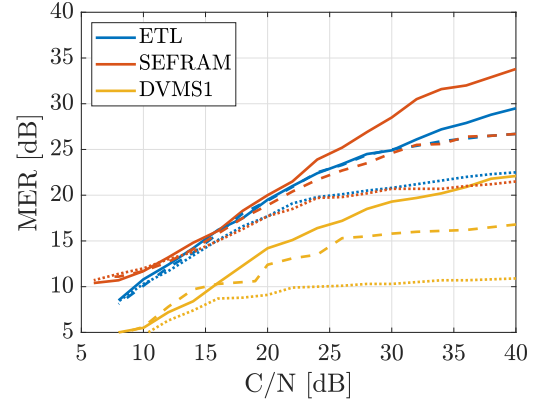


(f) MER vs  $C/N$  ( $C/N$  decreases on SFU)

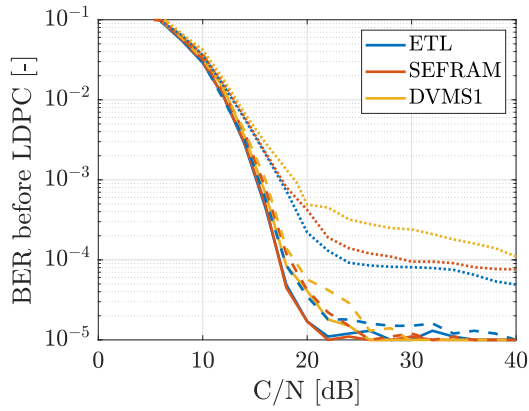
Fig. 6.2: DVB-T2 MISO TV signal: **PI**, power imbalance = 5 dB (SFE: -30 dBm, SFU: -35 dBm) – solid lines: no  $I/Q$ -errors, dashed lines:  $AI = 10\%$ , dotted lines:  $AI = 10\%$  and  $PI = 10^\circ$



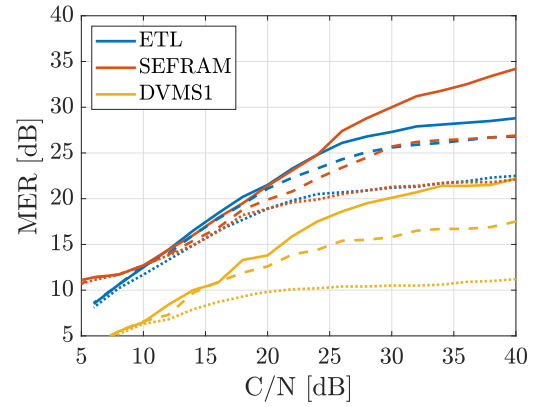
(a) BER vs  $C/N$  ( $C/N$  decreases on both generators)



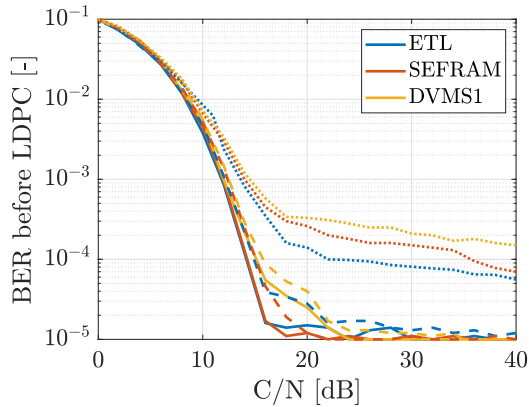
(b) MER vs  $C/N$  ( $C/N$  decreases on both generators)



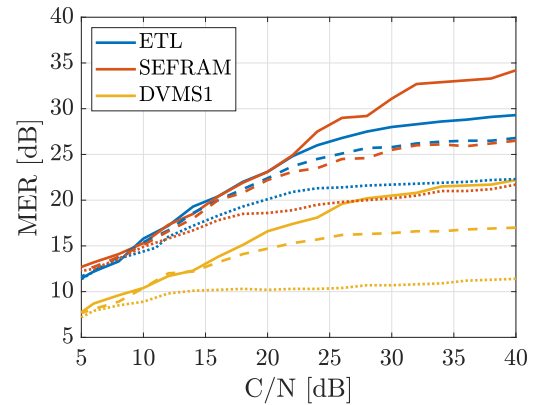
(c) BER vs  $C/N$  ( $C/N$  decreases on SFE)



(d) MER vs  $C/N$  ( $C/N$  decreases on SFE)



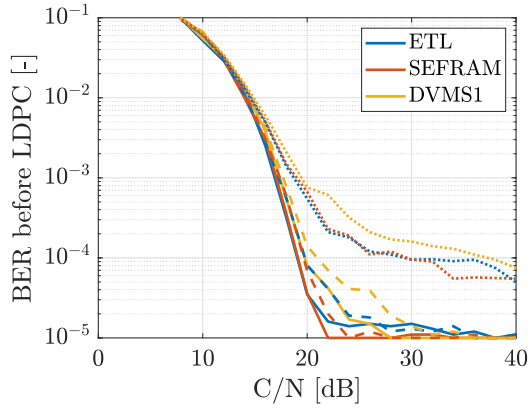
(e) BER vs  $C/N$  ( $C/N$  decreases on SFU)



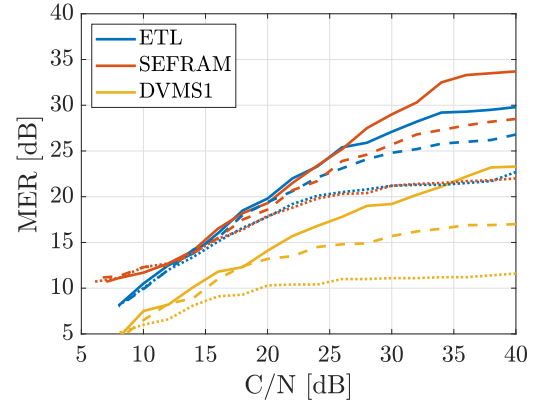
(f) MER vs  $C/N$  ( $C/N$  decreases on SFU)

Fig. 6.3: DVB-T2 MISO TV signal: **PI**, power imbalance = 5 dB (SFE: -35 dBm, SFU: -30 dBm) – solid lines: no  $I/Q$ -errors, dashed lines:  $AI = 10\%$ , dotted lines:  $AI = 10\%$  and  $PI = 10^\circ$

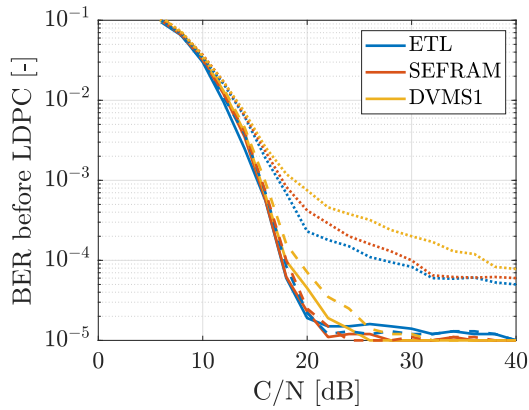




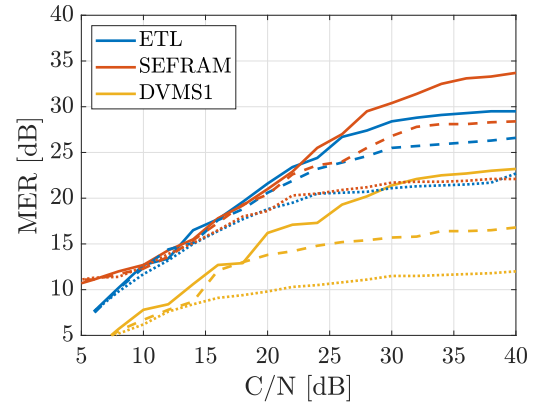
(a) BER vs  $C/N$  ( $C/N$  decreases on both generators)



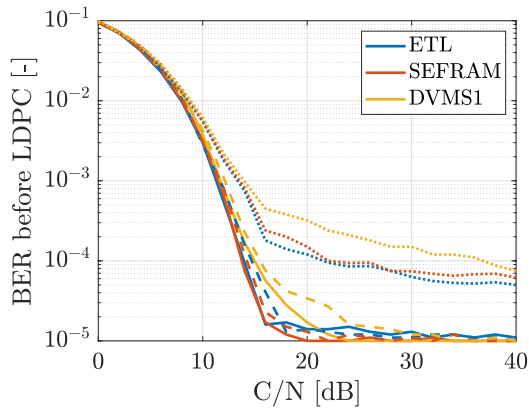
(b) MER vs  $C/N$  ( $C/N$  decreases on both generators)



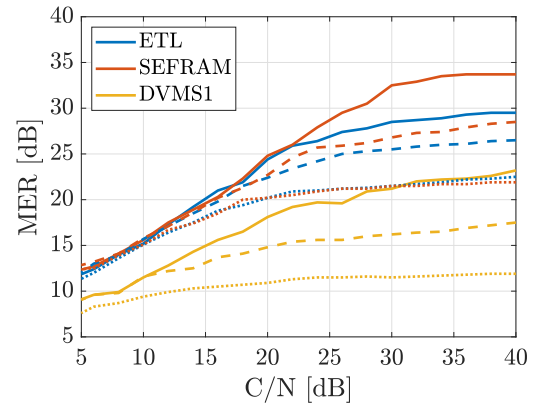
(c) BER vs  $C/N$  ( $C/N$  decreases on SFE)



(d) MER vs  $C/N$  ( $C/N$  decreases on SFE)

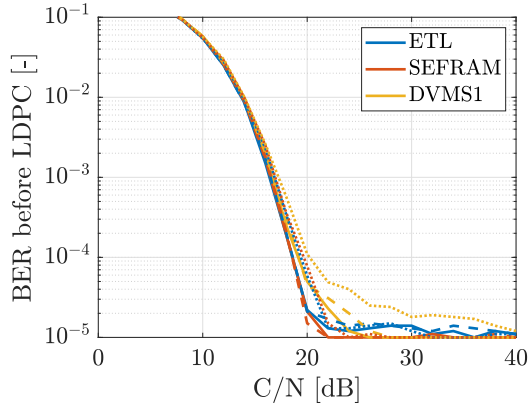


(e) BER vs  $C/N$  ( $C/N$  decreases on SFU)

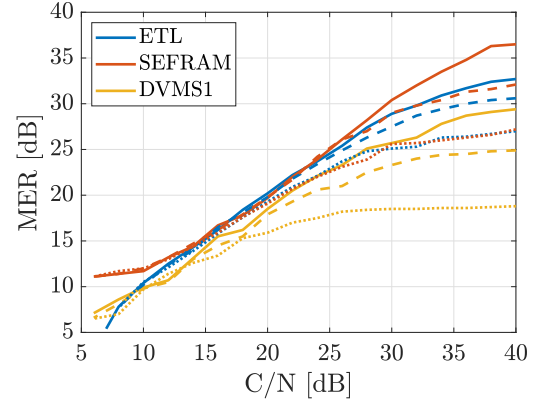


(f) MER vs  $C/N$  ( $C/N$  decreases on SFU)

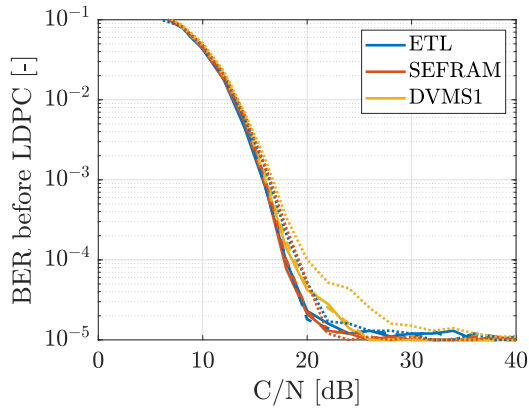
Fig. 6.4: DVB-T2 MISO TV signal: **PO** – solid lines: no  $I/Q$ -errors, dashed lines:  $AI = 10\%$ , dotted lines:  $AI = 10\%$  and  $PI = 10^\circ$



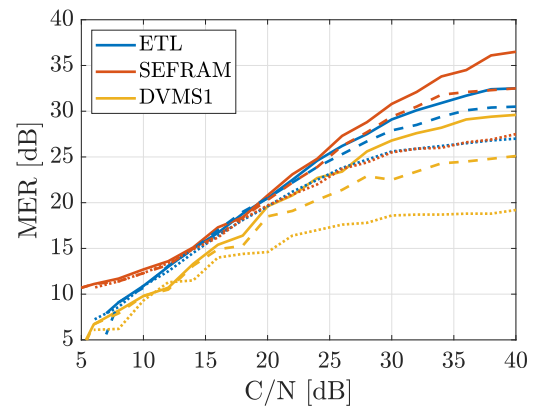
(a) BER vs  $C/N$  ( $C/N$  decreases on both generators)



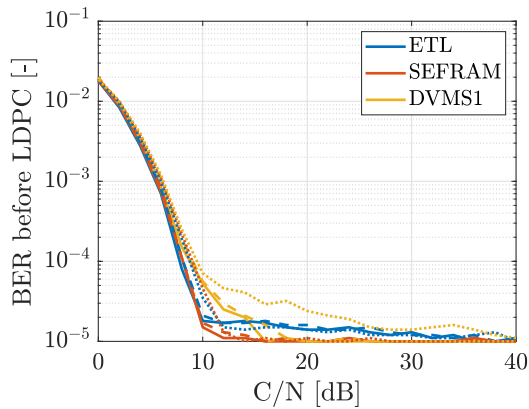
(b) MER vs  $C/N$  ( $C/N$  decreases on both generators)



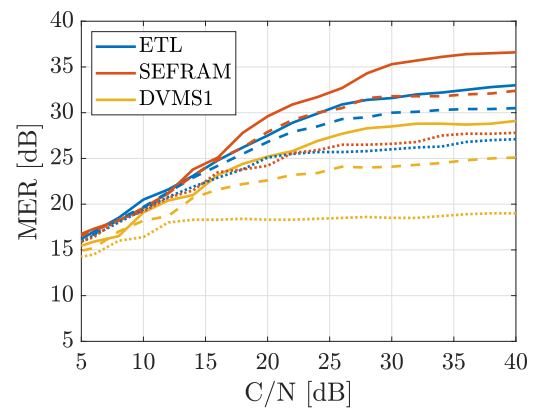
(c) BER vs  $C/N$  ( $C/N$  decreases on SFE)



(d) MER vs  $C/N$  ( $C/N$  decreases on SFE)

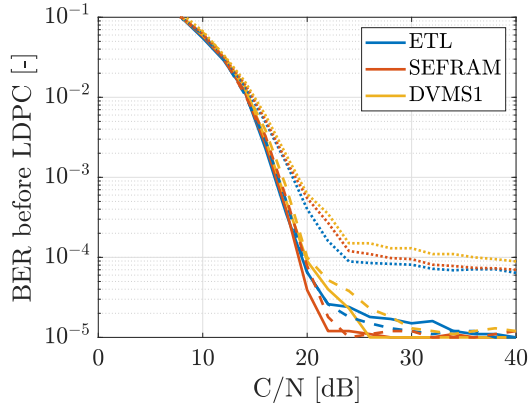


(e) BER vs  $C/N$  ( $C/N$  decreases on SFU)

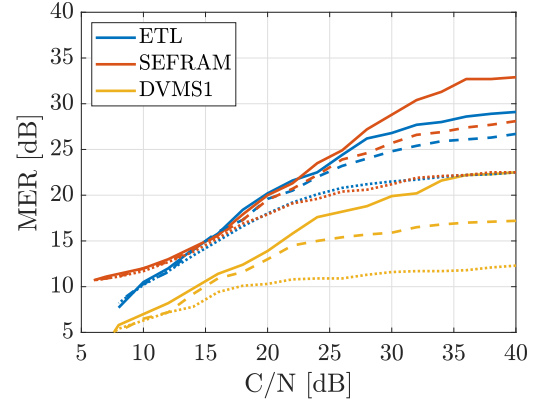


(f) MER vs  $C/N$  ( $C/N$  decreases on SFU)

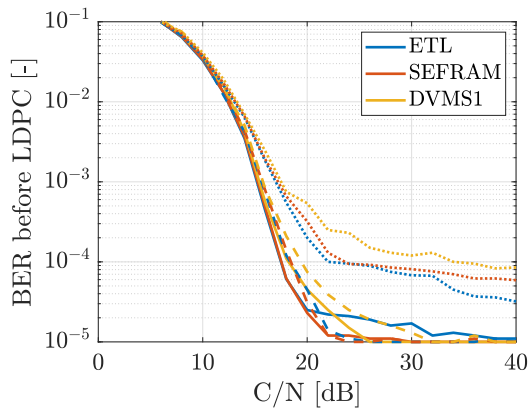
Fig. 6.5: DVB-T2 MISO TV signal: **PO**, power imbalance = 5 dB (SFE: -30 dBm, SFU: -35 dBm) – solid lines: no  $I/Q$ -errors, dashed lines:  $AI = 10\%$ , dotted lines:  $AI = 10\%$  and  $PI = 10^\circ$



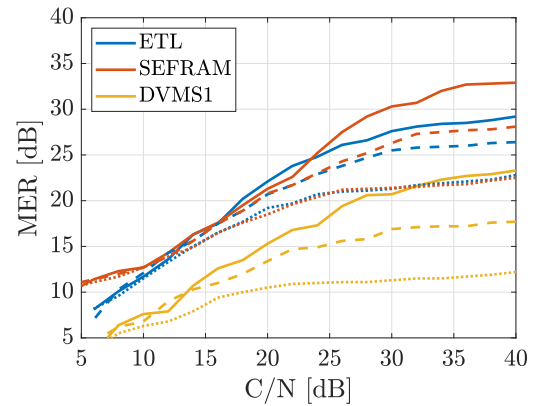
(a) BER vs  $C/N$  ( $C/N$  decreases on both generators)



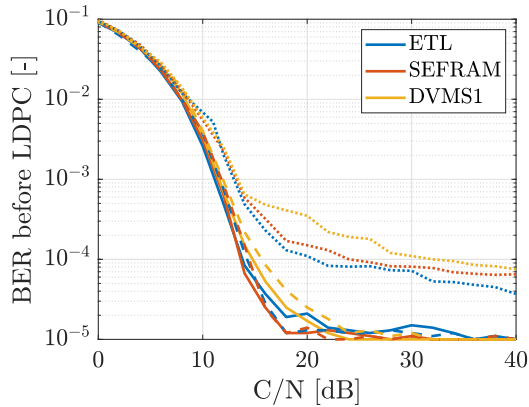
(b) MER vs  $C/N$  ( $C/N$  decreases on both generators)



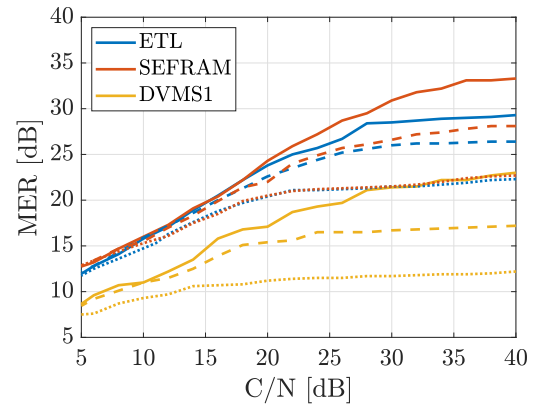
(c) BER vs  $C/N$  ( $C/N$  decreases on SFE)



(d) MER vs  $C/N$  ( $C/N$  decreases on SFE)

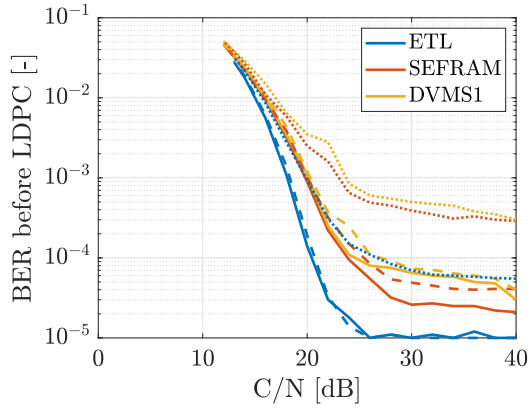


(e) BER vs  $C/N$  ( $C/N$  decreases on SFU)

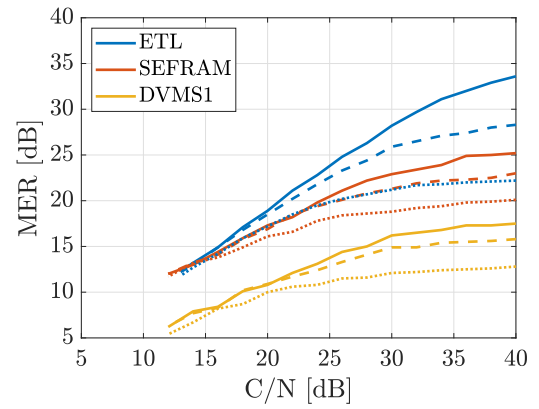


(f) MER vs  $C/N$  ( $C/N$  decreases on SFU)

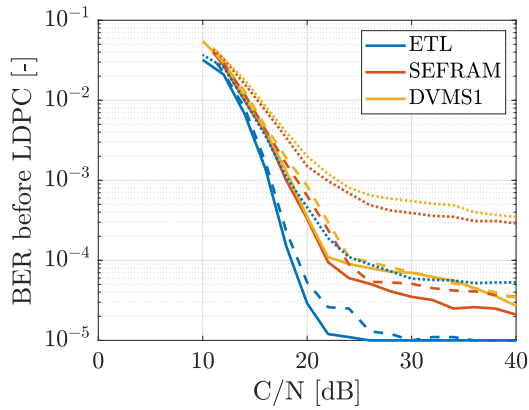
Fig. 6.6: DVB-T2 MISO TV signal: **PO**, power imbalance = 5 dB (SFE: -35 dBm, SFU: -30 dBm) – solid lines: no  $I/Q$ -errors, dashed lines:  $AI = 10\%$ , dotted lines:  $AI = 10\%$  and  $PI = 10^\circ$



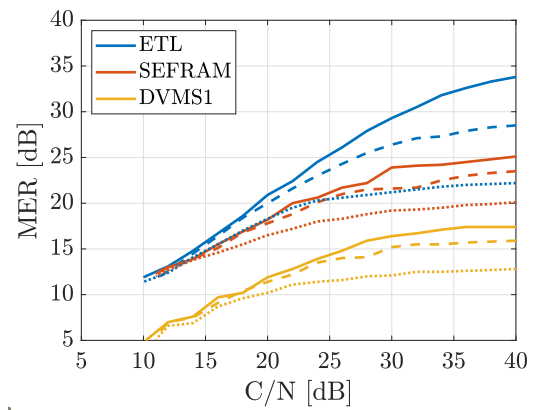
(a) BER vs  $C/N$  ( $C/N$  decreases on both generators)



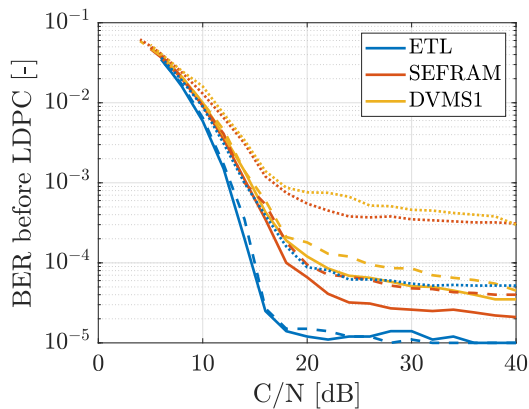
(b) MER vs  $C/N$  ( $C/N$  decreases on both generators)



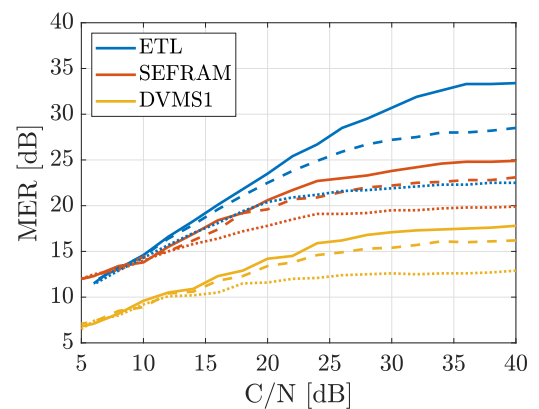
(c) BER vs  $C/N$  ( $C/N$  decreases on SFE)



(d) MER vs  $C/N$  ( $C/N$  decreases on SFE)

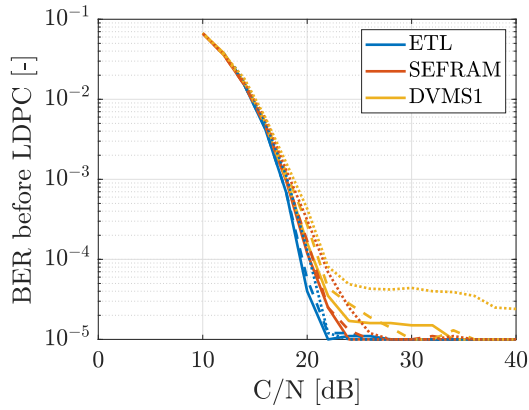


(e) BER vs  $C/N$  ( $C/N$  decreases on SFU)

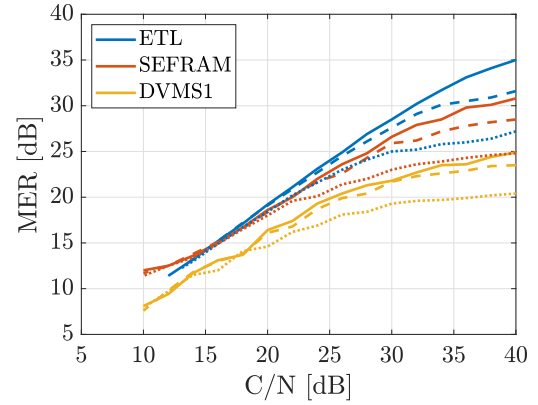


(f) MER vs  $C/N$  ( $C/N$  decreases on SFU)

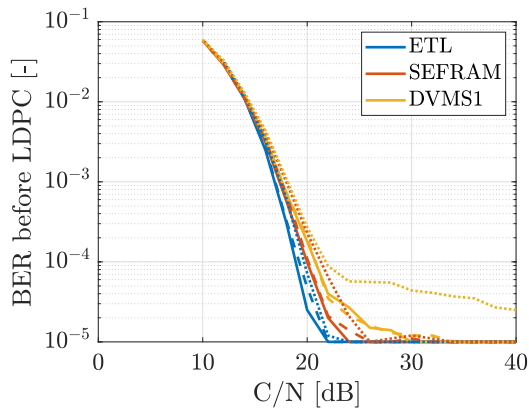
Fig. 6.7: DVB-T2 MISO TV signal: **TU6** – solid lines: no  $I/Q$ -errors, dashed lines:  $AI = 10\%$ , dotted lines:  $AI = 10\%$  and  $PI = 10^\circ$



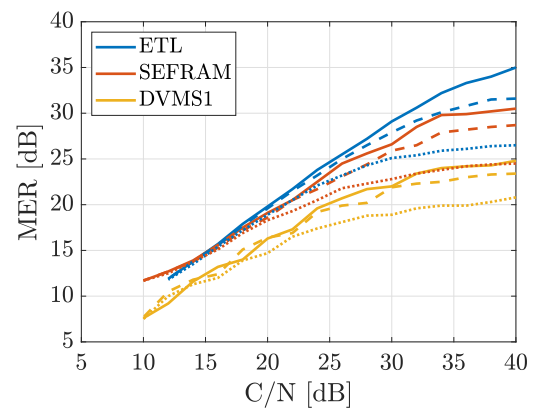
(a) BER vs  $C/N$  ( $C/N$  decreases on both generators)



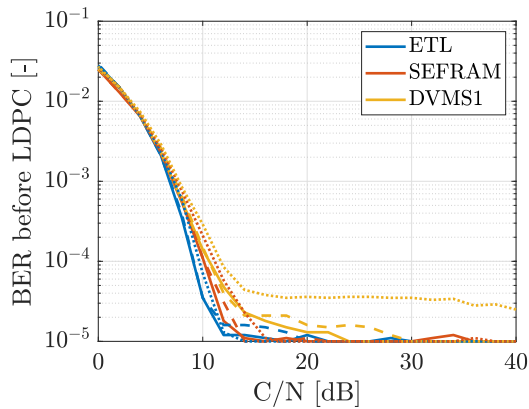
(b) MER vs  $C/N$  ( $C/N$  decreases on both generators)



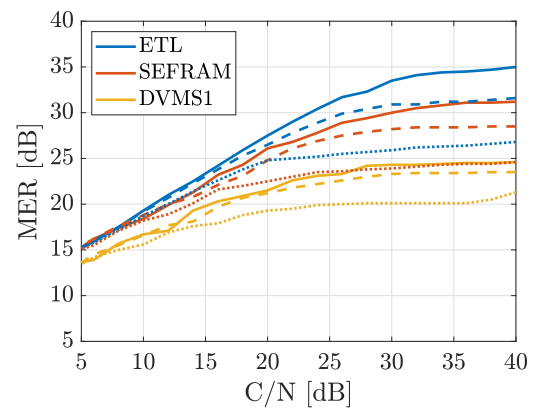
(c) BER vs  $C/N$  ( $C/N$  decreases on SFE)



(d) MER vs  $C/N$  ( $C/N$  decreases on SFE)

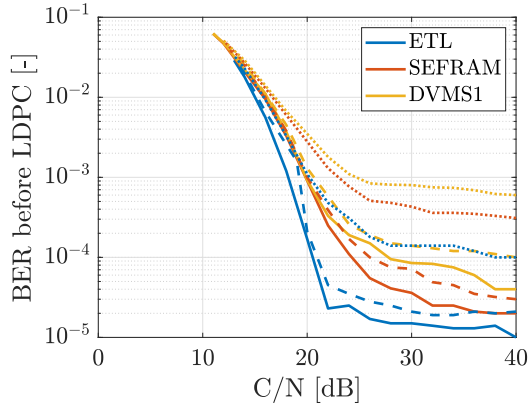


(e) BER vs  $C/N$  ( $C/N$  decreases on SFU)

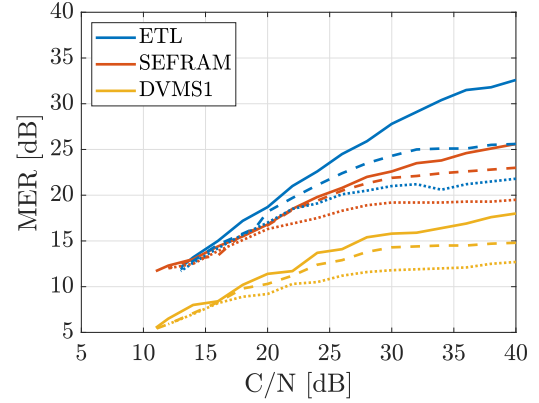


(f) MER vs  $C/N$  ( $C/N$  decreases on SFU)

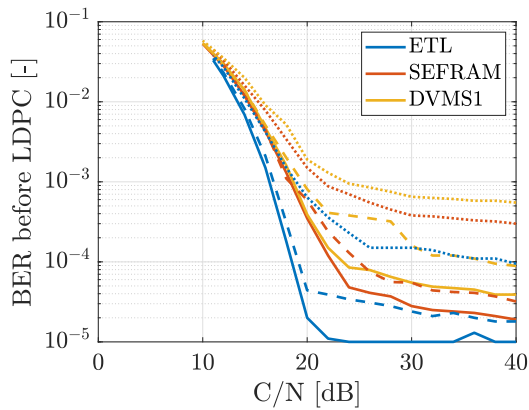
Fig. 6.8: DVB-T2 MISO TV signal: **TU6**, power imbalance = 5 dB (SFE: -30 dBm, SFU: -35 dBm) – solid lines: no  $I/Q$ -errors, dashed lines:  $AI = 10\%$ , dotted lines:  $AI = 10\%$  and  $PI = 10^\circ$



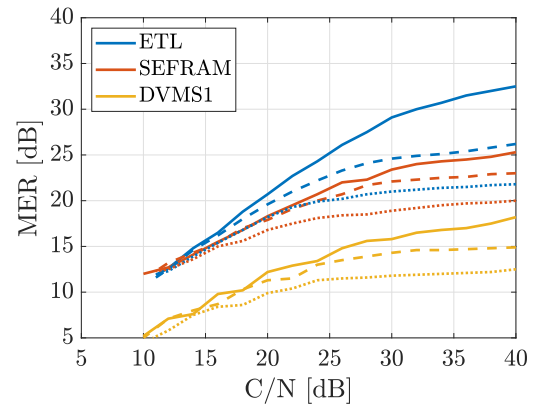
(a) BER vs  $C/N$  ( $C/N$  decreases on both generators)



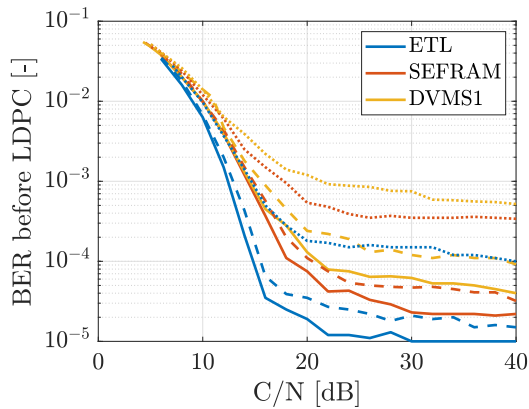
(b) MER vs  $C/N$  ( $C/N$  decreases on both generators)



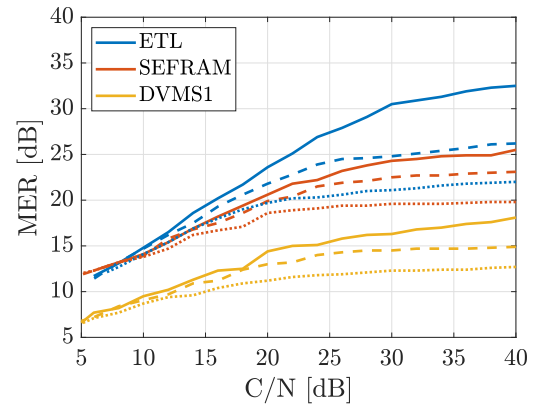
(c) BER vs  $C/N$  ( $C/N$  decreases on SFE)



(d) MER vs  $C/N$  ( $C/N$  decreases on SFE)

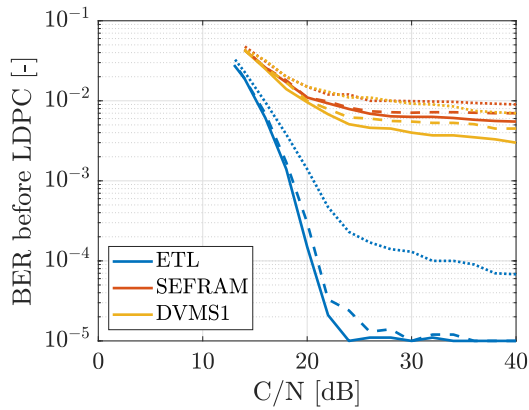


(e) BER vs  $C/N$  ( $C/N$  decreases on SFU)

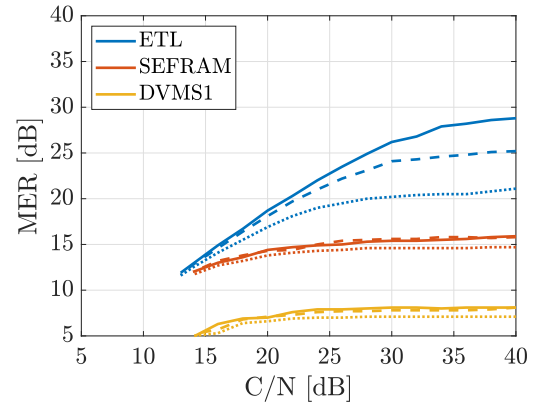


(f) MER vs  $C/N$  ( $C/N$  decreases on SFU)

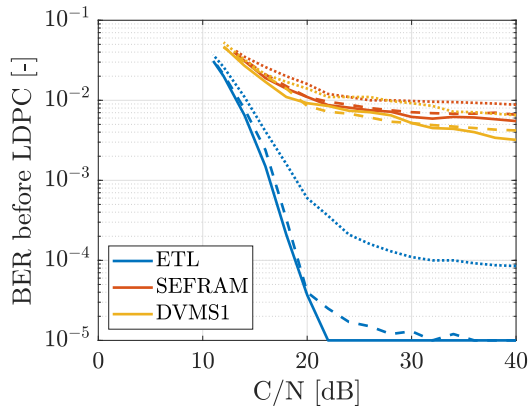
Fig. 6.9: DVB-T2 MISO TV signal: **TU6**, power imbalance = 5 dB (SFE: -35 dBm, SFU: -30 dBm) – solid lines: no  $I/Q$ -errors, dashed lines:  $AI = 10\%$ , dotted lines:  $AI = 10\%$  and  $PI = 10^\circ$



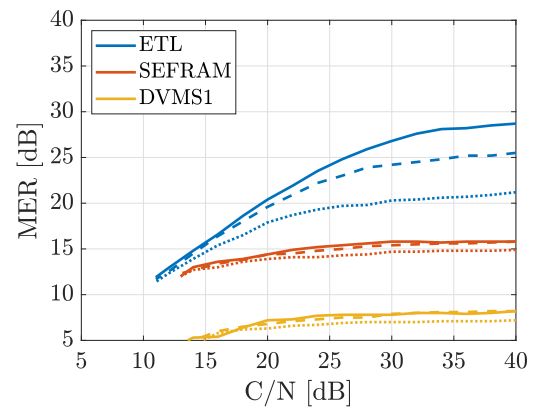
(a) BER vs  $C/N$  ( $C/N$  decreases on both generators)



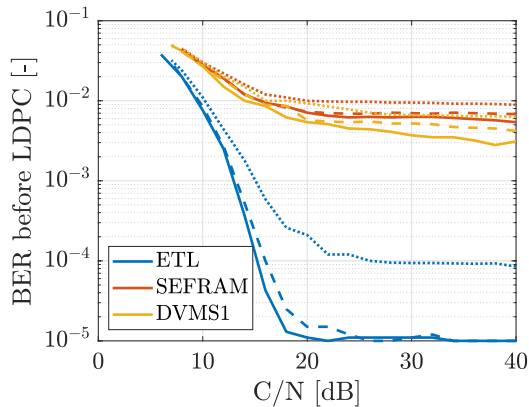
(b) MER vs  $C/N$  ( $C/N$  decreases on both generators)



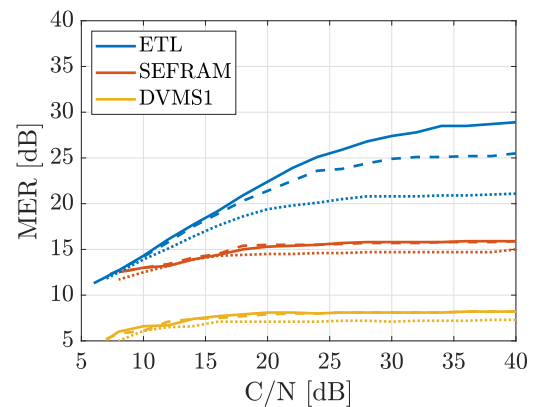
(c) BER vs  $C/N$  ( $C/N$  decreases on SFE)



(d) MER vs  $C/N$  ( $C/N$  decreases on SFE)

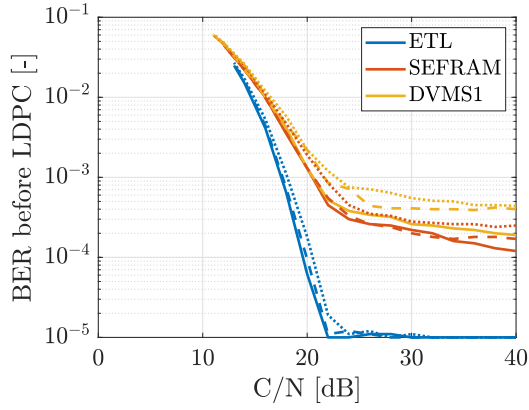


(e) BER vs  $C/N$  ( $C/N$  decreases on SFU)

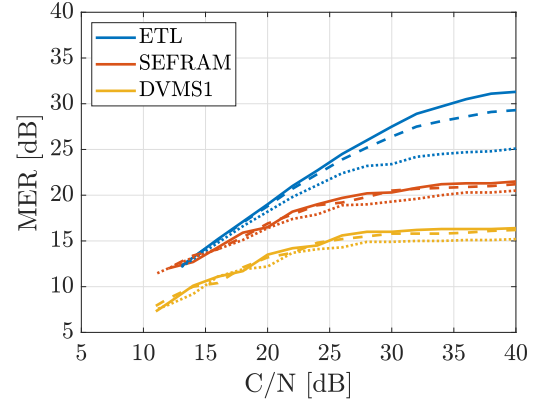


(f) MER vs  $C/N$  ( $C/N$  decreases on SFU)

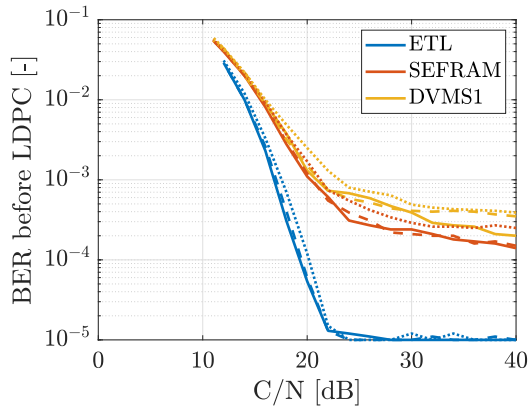
Fig. 6.10: DVB-T2 MISO TV signal: **RA6** – solid lines: no  $I/Q$ -errors, dashed lines:  $AI = 10\%$ , dotted lines:  $AI = 10\%$  and  $PI = 10^\circ$



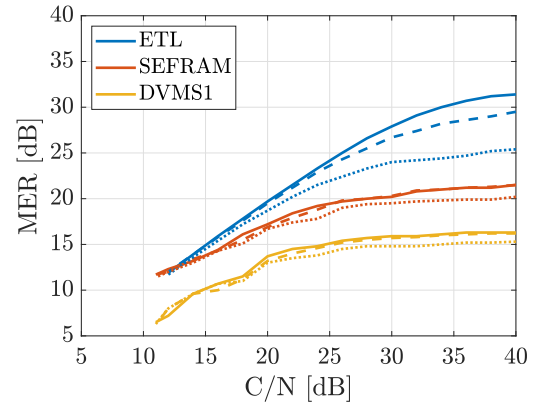
(a) BER vs  $C/N$  ( $C/N$  decreases on both generators)



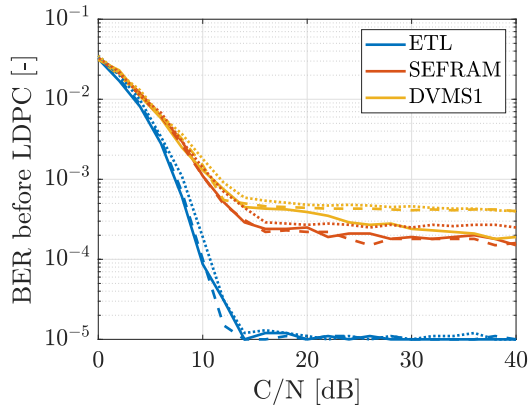
(b) MER vs  $C/N$  ( $C/N$  decreases on both generators)



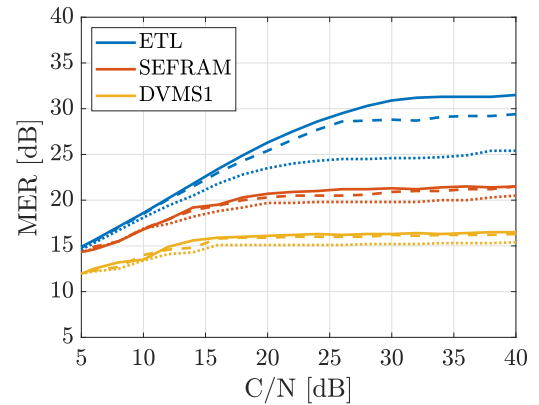
(c) BER vs  $C/N$  ( $C/N$  decreases on SFE)



(d) MER vs  $C/N$  ( $C/N$  decreases on SFE)



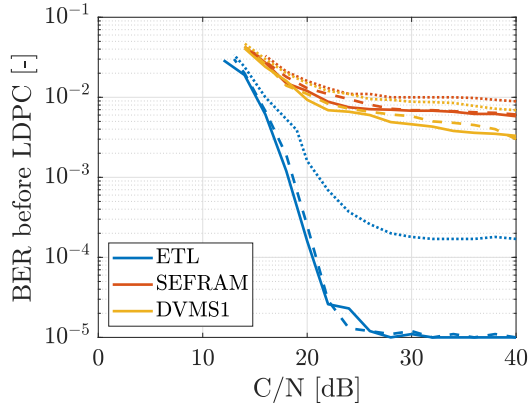
(e) BER vs  $C/N$  ( $C/N$  decreases on SFU)



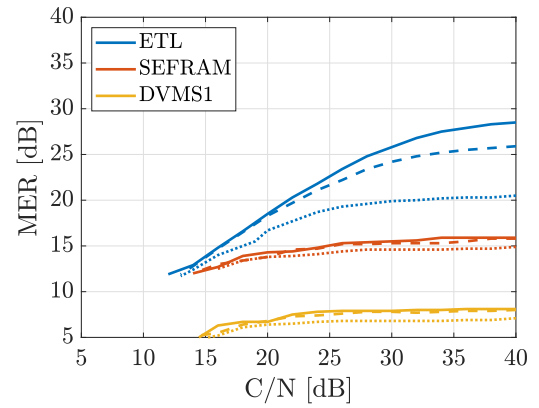
(f) MER vs  $C/N$  ( $C/N$  decreases on SFU)

Fig. 6.11: DVB-T2 MISO TV signal: **RA6**, power imbalance = 5 dB (SFE: -30 dBm, SFU: -35 dBm) – solid lines: no  $I/Q$ -errors, dashed lines:  $AI = 10\%$ , dotted lines:  $AI = 10\%$  and  $PI = 10^\circ$

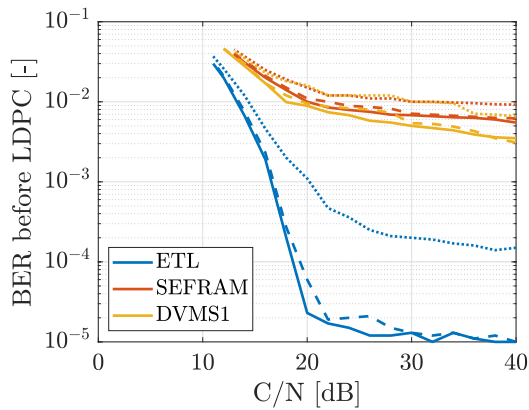




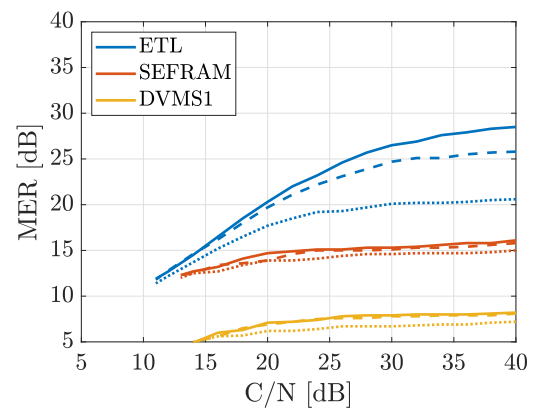
(a) BER vs  $C/N$  ( $C/N$  decreases on both generators)



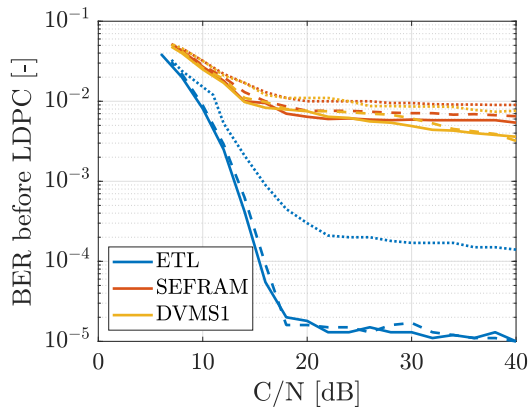
(b) MER vs  $C/N$  ( $C/N$  decreases on both generators)



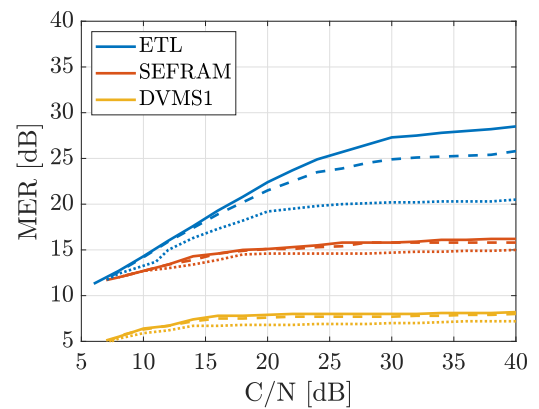
(c) BER vs  $C/N$  ( $C/N$  decreases on SFE)



(d) MER vs  $C/N$  ( $C/N$  decreases on SFE)



(e) BER vs  $C/N$  ( $C/N$  decreases on SFU)



(f) MER vs  $C/N$  ( $C/N$  decreases on SFU)

Fig. 6.12: DVB-T2 MISO TV signal: **RA6**, power imbalance = 5 dB (SFE: -35 dBm, SFU: -30 dBm) – solid lines: no  $I/Q$ -errors, dashed lines:  $AI = 10\%$ , dotted lines:  $AI = 10\%$  and  $PI = 10^\circ$

Tab. 6.2: Required  $C/N$  in unit of dB for QEF reception in **PI** channel without power imbalance

$I/Q$ -errors	$C/N$ changing	STB			Measurement Equipment		
		Thomson	Sencor	STC	ETL	Sefram	DVMS1
no $I/Q$ -errors	Both TXs	7	7	6	8	6	6
	SFE (TX2)	5	5	5	6	5	5
	SFU (TX1)	–	–	–	–	–	–
AI = 10%	Both TXs	7	7	7	8	7	7
	SFE (TX2)	5	5	4	6	5	4
	SFU (TX1)	–	–	–	–	–	–
AI = 10% and PI = 10°	Both TXs	7	7	6	8	7	6
	SFE (TX2)	5	5	5	6	5	5
	SFU (TX1)	–	–	–	–	–	–

Tab. 6.3: Required  $C/N$  in unit of dB for QEF reception in **PI** channel with power imbalance of 5 dB (SFU = -35 dBm, SFE = -30 dBm)

$I/Q$ -errors	$C/N$ changing	STB			Measurement Equipment		
		Thomson	Sencor	STC	ETL	Sefram	DVMS1
no $I/Q$ -errors	Both TXs	6	6	6	7	6	6
	SFE (TX2)	5	5	5	6	5	5
	SFU (TX1)	–	–	–	–	–	–
AI = 10%	Both TXs	6	6	6	7	6	6
	SFE (TX2)	6	6	5	7	5	5
	SFU (TX1)	–	–	–	–	–	–
AI = 10% and PI = 10°	Both TXs	6	6	6	7	6	6
	SFE (TX2)	5	5	5	7	5	5
	SFU (TX1)	–	–	–	–	–	–

Tab. 6.4: Required  $C/N$  in unit of dB for QEF reception in **PI** channel with power imbalance of 5 dB (SFU = -30 dBm, SFE = -35 dBm)

$I/Q$ -errors	$C/N$ changing	STB			Measurement Equipment		
		Thomson	Sencor	STC	ETL	Sefram	DVMS1
no $I/Q$ -errors	Both TXs	7	7	6	8	6	6
	SFE (TX2)	5	5	4	6	5	4
	SFU (TX1)	–	–	–	–	–	–
AI = 10%	Both TXs	7	7	6	8	7	6
	SFE (TX2)	5	5	5	6	5	5
	SFU (TX1)	–	–	–	–	–	–
AI = 10% and PI = 10°	Both TXs	7	7	6	8	7	6
	SFE (TX2)	5	5	4	6	5	4
	SFU (TX1)	–	–	–	–	–	–

Tab. 6.5: Required  $C/N$  in unit of dB for QEF reception in **PO** channel without power imbalance

$I/Q$ -errors	$C/N$ changing	STB			Measurement Equipment		
		Thomson	Sencor	STC	ETL	Sefram	DVMS1
no $I/Q$ -errors	Both TXs	7	7	6	8	6	6
	SFE (TX2)	5	5	5	6	5	5
	SFU (TX1)	–	–	–	–	–	–
AI = 10%	Both TXs	6	7	6	8	7	6
	SFE (TX2)	5	5	5	6	5	5
	SFU (TX1)	–	–	–	–	–	–
AI = 10% and PI = 10°	Both TXs	7	7	7	8	7	6
	SFE (TX2)	5	5	5	6	5	5
	SFU (TX1)	–	–	–	–	–	–

Tab. 6.6: Required  $C/N$  in unit of dB for QEF reception in **PO** channel with power imbalance of 5 dB (SFU = -35 dBm, SFE = -30 dBm)

$I/Q$ -errors	$C/N$ changing	STB			Measurement Equipment		
		Thomson	Sencor	STC	ETL	Sefram	DVMS1
no $I/Q$ -errors	Both TXs	6	6	6	7	6	6
	SFE (TX2)	6	6	5	7	5	5
	SFU (TX1)	–	–	–	–	–	–
AI = 10%	Both TXs	6	6	5	8	6	6
	SFE (TX2)	6	6	5	7	5	6
	SFU (TX1)	–	–	–	–	–	–
AI = 10% and PI = 10°	Both TXs	6	6	6	8	6	6
	SFE (TX2)	6	6	6	7	6	6
	SFU (TX1)	–	–	–	–	–	–

Tab. 6.7: Required  $C/N$  in unit of dB for QEF reception in **PO** channel with power imbalance of 5 dB (SFU = -30 dBm, SFE = -35 dBm)

$I/Q$ -errors	$C/N$ changing	STB			Measurement Equipment		
		Thomson	Sencor	STC	ETL	Sefram	DVMS1
no $I/Q$ -errors	Both TXs	7	7	6	8	6	7
	SFE (TX2)	5	5	5	6	5	5
	SFU (TX1)	–	–	–	–	–	–
AI = 10%	Both TXs	6	6	6	8	6	6
	SFE (TX2)	5	5	5	6	5	5
	SFU (TX1)	–	–	–	–	–	–
AI = 10% and PI = 10°	Both TXs	6	6	6	8	6	6
	SFE (TX2)	5	5	5	6	5	5
	SFU (TX1)	–	–	–	–	–	–

Tab. 6.8: Required  $C/N$  in unit of dB for QEF reception in **TU6** channel without power imbalance

$I/Q$ -errors	$C/N$ changing	STB			Measurement Equipment		
		Thomson	Sencor	STC	ETL	Sefram	DVMS1
no $I/Q$ -errors	Both TXs	12	13	12	13	12	12
	SFE (TX2)	11	11	10	10	11	10
	SFU (TX1)	5	6	5	6	5	5
AI = 10%	Both TXs	12	13	12	13	12	12
	SFE (TX2)	11	11	11	11	11	11
	SFU (TX1)	5	5	5	6	5	4
AI = 10% and PI = 10°	Both TXs	12	13	12	13	12	12
	SFE (TX2)	11	11	11	10	11	11
	SFU (TX1)	5	5	5	6	5	5

Tab. 6.9: Required  $C/N$  in unit of dB for QEF reception in **TU6** channel with power imbalance of 5 dB (SFU = -35 dBm, SFE = -30 dBm)

$I/Q$ -errors	$C/N$ changing	STB			Measurement Equipment		
		Thomson	Sencor	STC	ETL	Sefram	DVMS1
no $I/Q$ -errors	Both TXs	11	11	10	12	10	10
	SFE (TX2)	10	10	10	12	10	10
	SFU (TX1)	-	-	-	-	-	-
AI = 10%	Both TXs	11	11	10	13	10	10
	SFE (TX2)	10	10	10	12	10	10
	SFU (TX1)	-	-	-	-	-	-
AI = 10% and PI = 10°	Both TXs	11	11	10	13	10	10
	SFE (TX2)	10	10	10	12	10	10
	SFU (TX1)	-	-	-	-	-	-

Tab. 6.10: Required  $C/N$  in unit of dB for QEF reception in **TU6** channel with power imbalance of 5 dB (SFU = -30 dBm, SFE = -35 dBm)

$I/Q$ -errors	$C/N$ changing	STB			Measurement Equipment		
		Thomson	Sencor	STC	ETL	Sefram	DVMS1
no $I/Q$ -errors	Both TXs	12	12	11	13	11	11
	SFE (TX2)	11	11	10	11	10	10
	SFU (TX1)	5	6	5	6	6	5
AI = 10%	Both TXs	12	12	11	13	12	11
	SFE (TX2)	11	11	10	11	11	10
	SFU (TX1)	5	5	4	6	4	4
AI = 10% and PI = 10°	Both TXs	6	6	6	8	6	6
	SFE (TX2)	5	5	5	6	5	5
	SFU (TX1)	5	6	5	7	5	5

Tab. 6.11: Required  $C/N$  in unit of dB for QEF reception in **RA6** channel without power imbalance

$I/Q$ -errors	$C/N$ changing	STB			Measurement Equipment		
		Thomson	Sencor	STC	ETL	Sefram	DVMS1
no $I/Q$ -errors	Both TXs	14	14	14	13	14	14
	SFE (TX2)	12	12	12	11	13	12
	SFU (TX1)	7	7	7	6	8	7
AI = 10%	Both TXs	14	14	14	13	14	14
	SFE (TX2)	12	12	12	11	13	12
	SFU (TX1)	8	8	7	7	8	7
AI = 10% and PI = 10°	Both TXs	14	14	14	13	14	14
	SFE (TX2)	13	13	13	11	13	12
	SFU (TX1)	8	8	8	7	8	8

Tab. 6.12: Required  $C/N$  in unit of dB for QEF reception in **RA6** channel with power imbalance of 5 dB (SFU = -35 dBm, SFE = -30 dBm)

$I/Q$ -errors	$C/N$ changing	STB			Measurement Equipment		
		Thomson	Sencor	STC	ETL	Sefram	DVMS1
no $I/Q$ -errors	Both TXs	12	12	11	13	12	11
	SFE (TX2)	12	12	11	12	11	11
	SFU (TX1)	-	-	-	-	-	-
AI = 10%	Both TXs	12	12	11	13	12	11
	SFE (TX2)	12	12	11	12	11	11
	SFU (TX1)	-	-	-	-	-	-
AI = 10% and PI = 10°	Both TXs	12	12	12	13	11	11
	SFE (TX2)	12	12	11	12	11	12
	SFU (TX1)	-	-	-	-	-	-

Tab. 6.13: Required  $C/N$  in unit of dB for QEF reception in **RA6** channel with power imbalance of 5 dB (SFU = -30 dBm, SFE = -35 dBm)

$I/Q$ -errors	$C/N$ changing	STB			Measurement Equipment		
		Thomson	Sencor	STC	ETL	Sefram	DVMS1
no $I/Q$ -errors	Both TXs	14	14	13	12	14	14
	SFE (TX2)	12	12	11	11	13	12
	SFU (TX1)	7	7	6	6	7	7
AI = 10%	Both TXs	14	14	13	13	14	14
	SFE (TX2)	13	13	12	11	13	12
	SFU (TX1)	8	8	7	7	8	7
AI = 10% and PI = 10°	Both TXs	14	15	14	13	16	14
	SFE (TX2)	13	13	12	11	13	13
	SFU (TX1)	8	8	8	7	8	7

# Conclusion

This bachelor thesis examines the performance of the DVB-T2 system under various transmission conditions, with a particular focus on DVB-T2 MISO transmission. For this purpose, a universal and versatile laboratory measurement workplace was realized to measure real DVB-T2 SISO TV signals and DVB-T2 MISO TV signals generated under laboratory conditions. The realized concept allows to measure and evaluate the measured DVB-T2 signal from the perspective of the measurement equipment and STBs used.

The laboratory measurements were divided into two parts. In the first part, a real DVB-T2 SISO signal for different MUXs was measured. The results revealed differences among the four MUXs in terms of the measured objective parameters. Notably, MUX21 exhibits the highest BER before LDPC and the lowest MER values, even without any attenuation. The other MUXs show relatively minor differences in results. Additionally, the study establishes that STBs can still demodulate signals with higher attenuation values compared to the measuring equipment used.

The second part of the measurement focused on the measurement of the DVB-T2 MISO-based signal, which is significantly influenced by various types of I/Q-errors, power imbalances between transmitters, and channel conditions for fixed, portable, and mobile reception. The results clearly indicate that PI and especially the combination of PI and AI in the OFDM modulator have the most significant impact on the performance of the measured DVB-T2 MISO signal.

For fixed reception scenario, the fading channels RC20 and RL20 do not significantly affect the overall system performance, but the effect of I/Q errors is clearly observable in each scenario. This phenomenon is confirmed by the C/N values for QEF reception for each STB and measuring equipment.

In the case of mobile and portable reception, emulated by different fading channel models, the effect of fading in transmission path appears much stronger than in previous cases. The employment of RA6 fading channel especially affects the measured values of the Sefram and DVMS1 measuring devices. Added I/Q errors do not significantly degrade performance. Their influence is most visible when TX1 (SFU with I/Q-errors) has a higher power value. However, in the opposite case, the effect of I/Q-errors is clearly mitigated. More robust configurations for mobile and portable transmission provide high-quality protection for the transmitted signal, as evidenced by the QEF reception values. Next, there is a notable difference between the objective results obtained from the three types of measuring equipment for each scenario.

A part of this bachelor thesis was successfully presented at the student conference Student EEICT 2024 <https://www.eeict.cz/download>.

# Bibliography

- [1] FISCHER, Walter. *Digital video and audio broadcasting technology: a practical engineering guide*. 3rd ed. Berlin: Springer, 2010. ISBN 978-3-642-11611-7.
- [2] ETSI 2023, EUROPEAN BROADCASTING UNION 2023. *ETSI TS 102 755 V1.1.1 (2023-02) Digital Video Broadcasting (DVB); Frame structure channel coding and modulation for a second generation digital terrestrial television broadcasting system (DVB-T2)*. 2023.
- [3] DVB. *DVB Coding-Transport* [online]. [cit. 2023-12-22]. Available from: <https://dvb.org/solutions/coding-transport/> 2023.
- [4] DVB. *1. DTT deployment data* [online]. [cit. 2023-12-22]. Available from: <https://dvb.org/solutions/dtt-deployment-data/>
- [5] BEUTLER, Roland. *The Digital Dividend of Terrestrial Broadcasting*. New York: Springer. ISBN 978-1-4614-1568-8.
- [6] EUROPEAN TELECOMMUNICATIONS STANDARDS INSTITUTE 1998. *Generic coding of moving pictures and associated audio information [ITU-T Recommendations H.262 (1995) and H.222.0 (1995)]*. 1991.
- [7] EUROPEAN TELECOMMUNICATIONS STANDARDS INSTITUTE 2011. *Digital Video Broadcasting (DVB); Generic Stream Encapsulation (GSE) implementation guidelines*. 2011.
- [8] EIZMENDI, Inaki, et al. *DVB-T2: The second generation of terrestrial digital video broadcasting system*. *IEEE transactions on broadcasting*, 2014. 60.2: 258-271.
- [9] YOUSSEFOVÁ, Kristina. *Měření a analýza TV signálu v systému DVBT2*. 2019.. Bachelor's thesis. Brno university of technology, Faculty of electrical engineering and communication, Department of radio electronics. Supervisor Ladislav Polák.
- [10] SERIES, B. T. *Frequency and network planning aspects of DVB-T2*. 2012.
- [11] POLAK, Ladislav, et al. In *On the Performance of DVB-T2 MISO System: Special Fixed Transmission Scenarios*. In: 2021 31st International Conference Radioelektronika. IEEE, 2021. p. 1-4.
- [12] Rep. ITU-R BT.2254-2. *Frequency and network planning aspects of DVB-T2*. Report ITU-R BT.2254-2 (11/2014).

- [13] ETSI, T. R. 101 290 V1. 2.1, Digital Video Broadcasting (DVB); Measurement guidelines for DVB system. *European Broadcasting Union, Geneva*, 2001.
- [14] HUTTL, Ondrej; KRATOCHVIL, Tomas. DVB-H and DVB-SH digital TV broadcasting and its transmission channel environments. In: *2009 19th International Conference Radioelektronika*. IEEE, 2009. p. 341-344.
- [15] FAILLI, M. Digital land mobile radio communications-COST 207: final report. *Luxembourg: Commission of European Communities*, 1989.
- [16] CHIARAVIGLIO, Luca, et al. 5G in rural and low-income areas: Are we ready?. In: *2016 ITU Kaleidoscope: ICTs for a Sustainable World (ITU WT)*. IEEE, 2016. p. 1-8.
- [17] ETSI, T. R. 102 377: Digital Video Broadcasting (DVB); Implementation Guidelines for DVB Handheld Services (DVB-H). 2009.
- [18] POLAK, L., KRATOCHVIL, T. Simulation and Measurement of the Transmission Distortions of the Digital Television DVB-T/H Part 3: Transmission in Fading Channels, *Radioengineering*, Dec. 2010, vol. 19, no. 4, p. 703-711.
- [19] ETSI 2020, EUROPEAN BROADCASTING UNION 2020. *Digital Video Broadcasting (DVB); Measurement guidelines for DVB systems DVB Measurement Guidelines*. 2020.
- [20] ČTÚ *Vyhodnocení Přechodu na DVB-T2* [online]. Available from: <https://www.ctu.cz/sites/default/files/obsah/vyhodnoceni-prechodu-dvbt2.pdf>
- [21] ČTÚ *Kapacita datových toků. Český telekomunikační úřad* [online]. Available from: <https://www.ctu.cz/kapacita-datovych-toku> 24 October 2023.
- [22] ČTÚ *Přehled platných individuálních oprávnění – Televizní Vysílače*. [online]. Available from: <https://www.ctu.cz/vyhledavaci-databaze/prehled-televiznich-vysilacu/>
- [23] ČTÚ *Pokrytí: Zemské digitální televizní a Rozhlasové Vysílání v ČR*. [online]. [cit. 2023-12-22]. Available from: <https://digi.ctu.cz/dtv/>
- [24] PROAKIS, John G. *Digital communications*. 5th ed. Boston: McGraw-Hill, 2008. ISBN 978-0-07-295716-7.



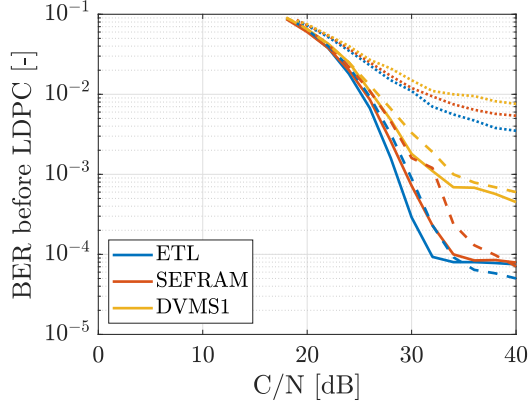
- [25] GBADAMASSI, Abdoul-Warris, et al. Co-located and distributed MISO techniques in DVB-T2 Single Frequency Networks. In: *2021 4th International Conference on Advanced Communication Technologies and Networking (Comm-Net)*. IEEE, 2021. p. 1-9.
- [26] GHAYYIB, Hamzah Sabr; MOHAMMED, Samir Jasim. Performance improvement of DVB-T2 SFNS by using MISO transmission scheme. In: *AIP Conference Proceedings*. AIP Publishing, 2022.
- [27] POLAK, Ladislav, et al. Single Frequency Networks for DVB-T2: Analysis of Real Case Scenarios in Czech Republic. In: *2023 33rd International Conference Radioelektronika*. IEEE, 2023. p. 1-6.

# List of appendices

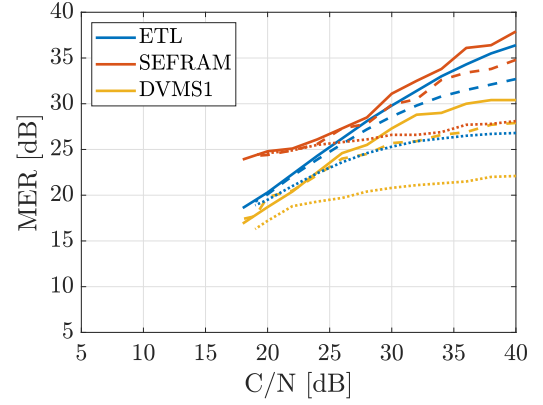
A Results of MISO measurement

79

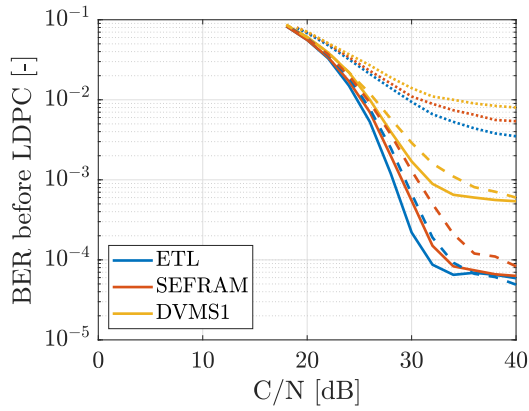
## **A Results of MISO measurement**



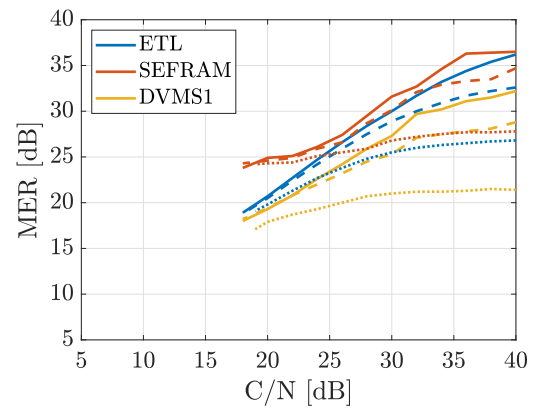
(a) BER vs  $C/N$  ( $C/N$  decreases on both generators)



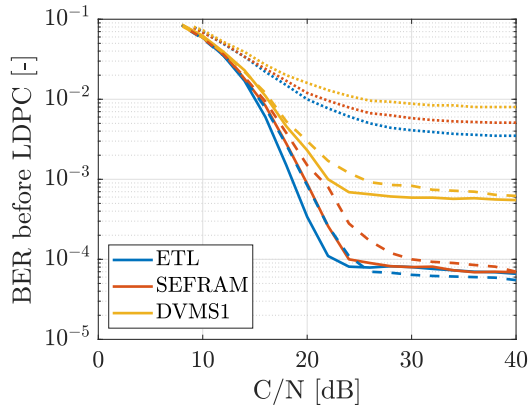
(b) MER vs  $C/N$  ( $C/N$  decreases on both generators)



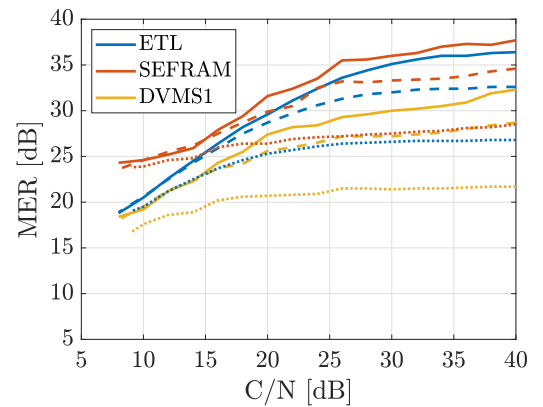
(c) BER vs  $C/N$  ( $C/N$  decreases on SFE)



(d) MER vs  $C/N$  ( $C/N$  decreases on SFE)

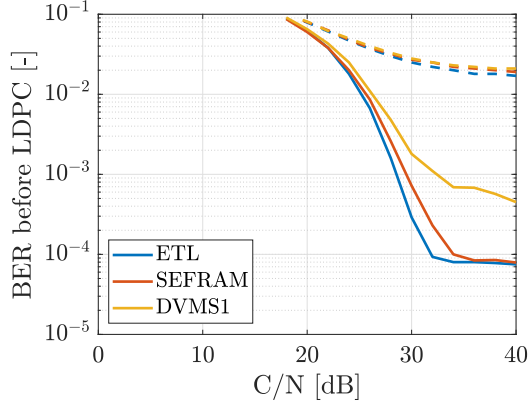


(e) BER vs  $C/N$  ( $C/N$  decreases on SFU)

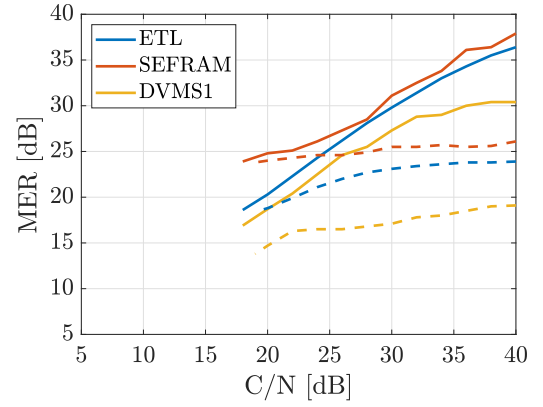


(f) MER vs  $C/N$  ( $C/N$  decreases on SFU)

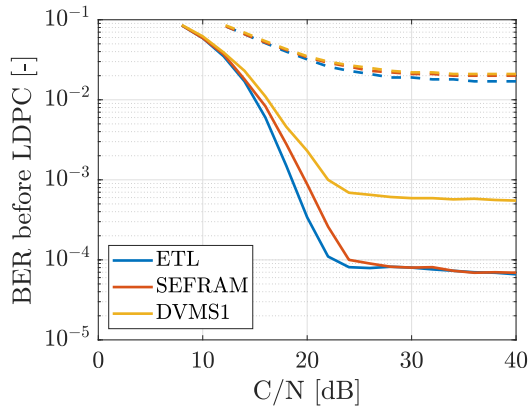
Fig. A.1: DVB-T2 MISO TV signal: **AWGN**, power imbalance = 10 dB (SFE: -25 dBm, SFU: -35 dBm) – solid lines: no  $I/Q$ -errors, dashed lines:  $AI = 10\%$ , dotted lines:  $AI = 10\%$  and  $PI = 10^\circ$



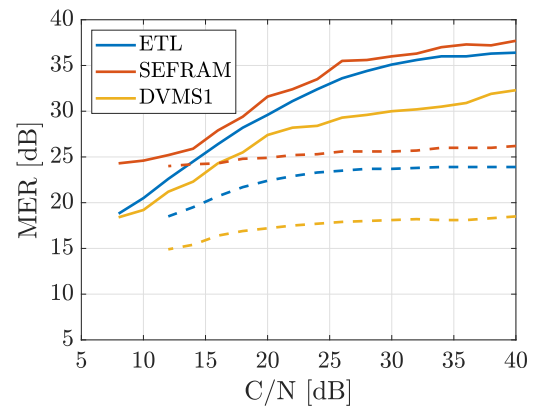
(a) BER vs  $C/N$  ( $C/N$  decreases on both generators)



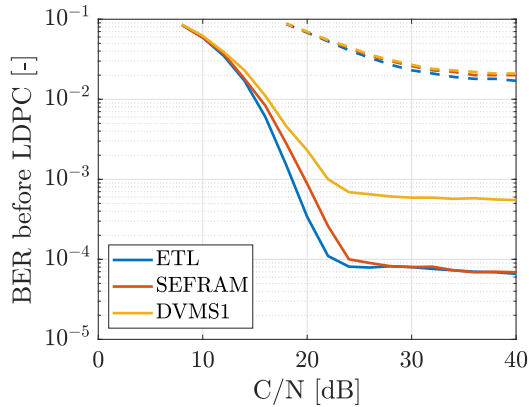
(b) MER vs  $C/N$  ( $C/N$  decreases on both generators)



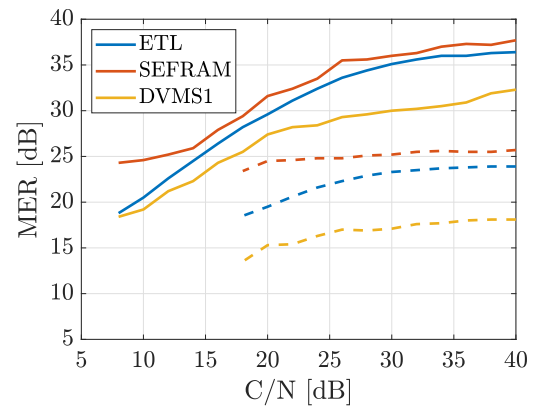
(c) BER vs  $C/N$  ( $C/N$  decreases on SFE)



(d) MER vs  $C/N$  ( $C/N$  decreases on SFE)

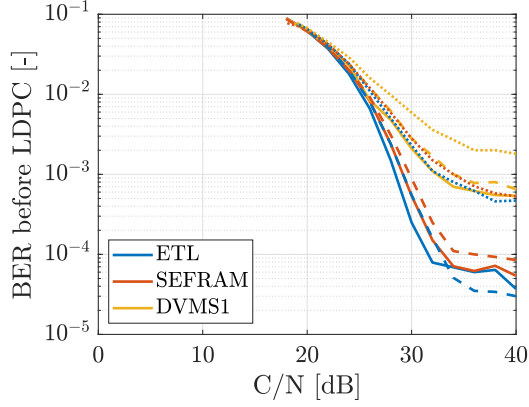


(e) BER vs  $C/N$  ( $C/N$  decreases on SFU)

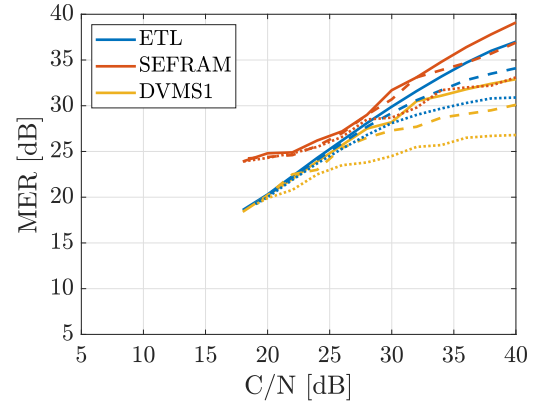


(f) MER vs  $C/N$  ( $C/N$  decreases on SFU)

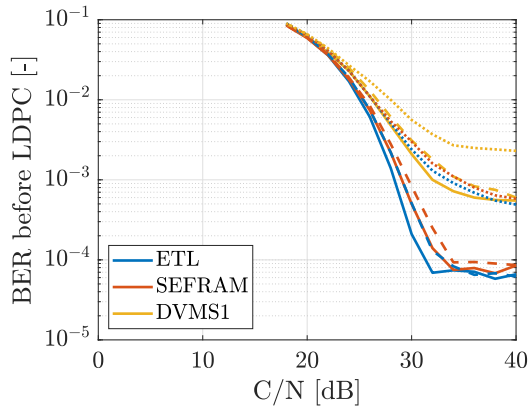
Fig. A.2: DVB-T2 MISO TV signal: **AWGN**, power imbalance = 10 dB (SFE: -35 dBm, SFU: -25 dBm) – solid lines: no  $I/Q$ -errors, dashed lines:  $AI = 10\%$ , dotted lines:  $AI = 10\%$  and  $PI = 10^\circ$



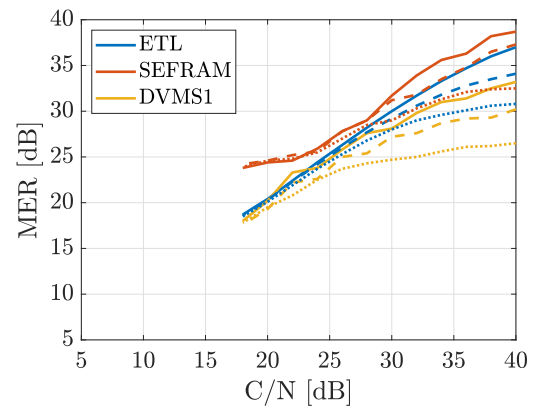
(a) BER vs  $C/N$  ( $C/N$  decreases on both generators)



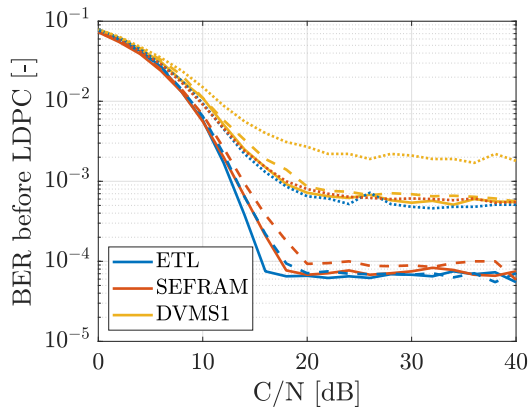
(b) MER vs  $C/N$  ( $C/N$  decreases on both generators)



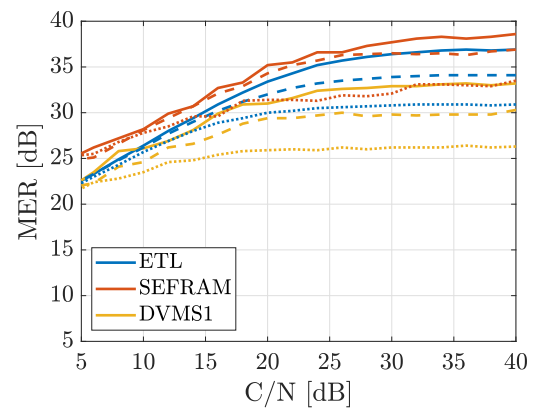
(c) BER vs  $C/N$  ( $C/N$  decreases on SFE)



(d) MER vs  $C/N$  ( $C/N$  decreases on SFE)

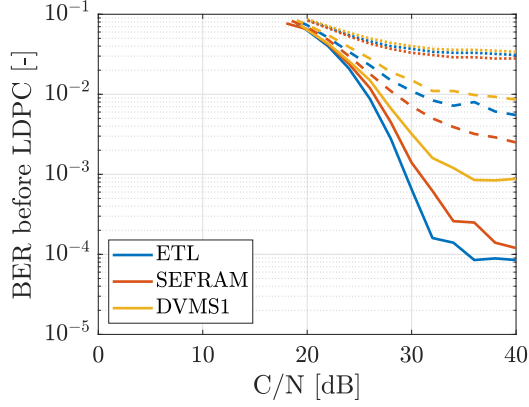


(e) BER vs  $C/N$  ( $C/N$  decreases on SFU)

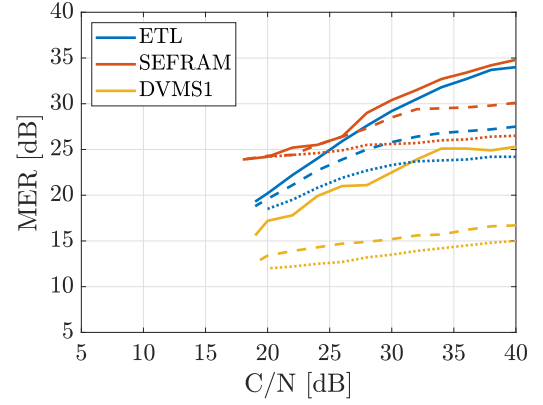


(f) MER vs  $C/N$  ( $C/N$  decreases on SFU)

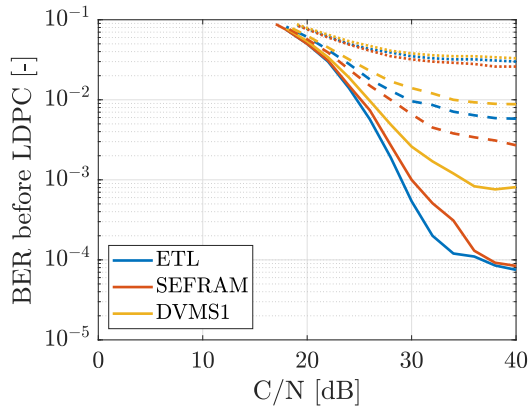
Fig. A.3: DVB-T2 MISO TV signal: **RC20**, power imbalance = 10 dB (SFE: -25 dBm, SFU: -35 dBm) – solid lines: no  $I/Q$ -errors, dashed lines:  $AI = 10\%$ , dotted lines:  $AI = 10\%$  and  $PI = 10^\circ$



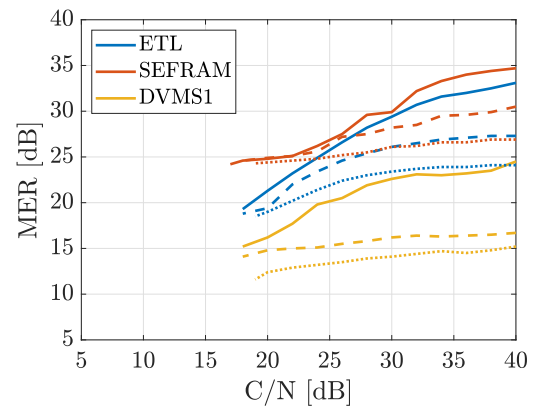
(a) BER vs  $C/N$  ( $C/N$  decreases on both generators)



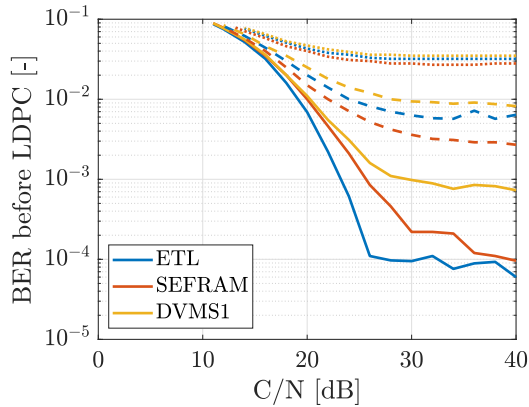
(b) MER vs  $C/N$  ( $C/N$  decreases on both generators)



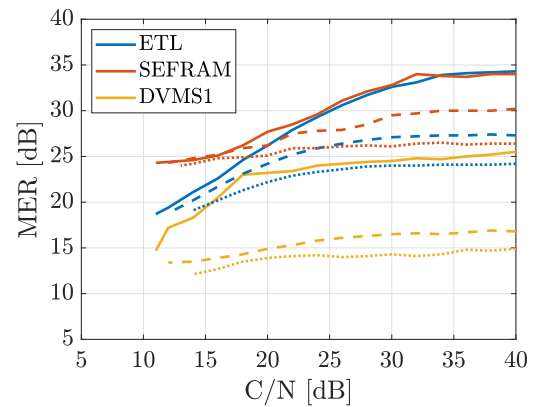
(c) BER vs  $C/N$  ( $C/N$  decreases on SFE)



(d) MER vs  $C/N$  ( $C/N$  decreases on SFE)

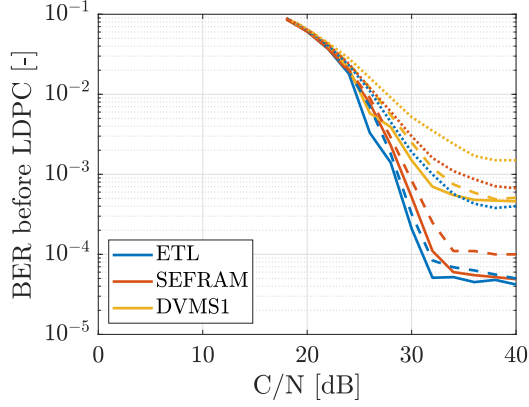


(e) BER vs  $C/N$  ( $C/N$  decreases on SFU)

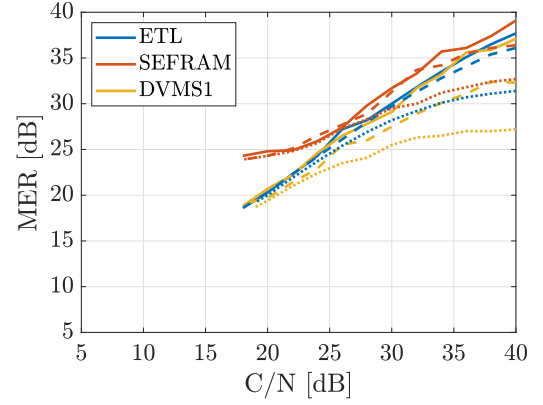


(f) MER vs  $C/N$  ( $C/N$  decreases on SFU)

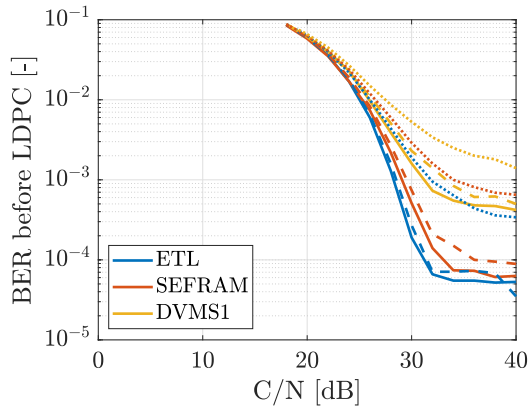
Fig. A.4: DVB-T2 MISO TV signal: **RC20**, power imbalance = 10 dB (SFE: -35 dBm, SFU: -25 dBm) – solid lines: no  $I/Q$ -errors, dashed lines:  $AI = 10\%$ , dotted lines:  $AI = 10\%$  and  $PI = 10^\circ$



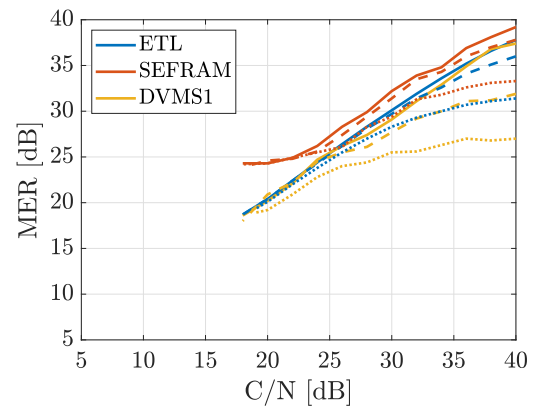
(a) BER vs  $C/N$  ( $C/N$  decreases on both generators)



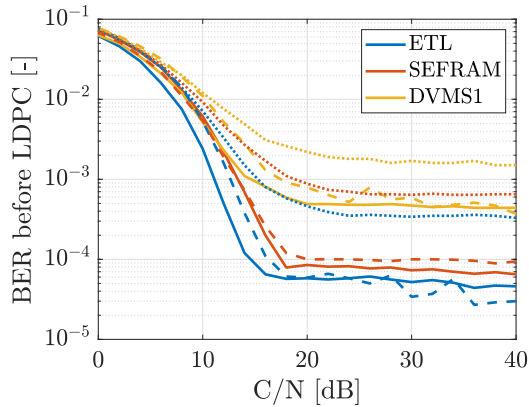
(b) MER vs  $C/N$  ( $C/N$  decreases on both generators)



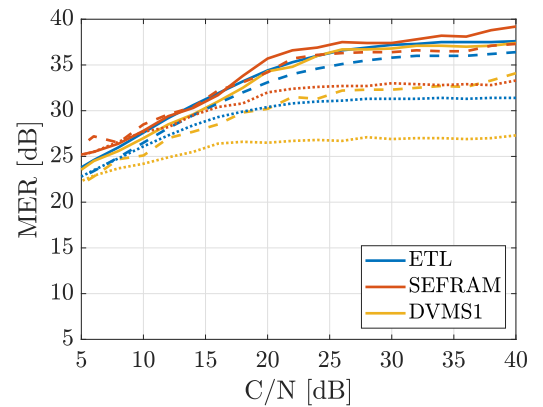
(c) BER vs  $C/N$  ( $C/N$  decreases on SFE)



(d) MER vs  $C/N$  ( $C/N$  decreases on SFE)



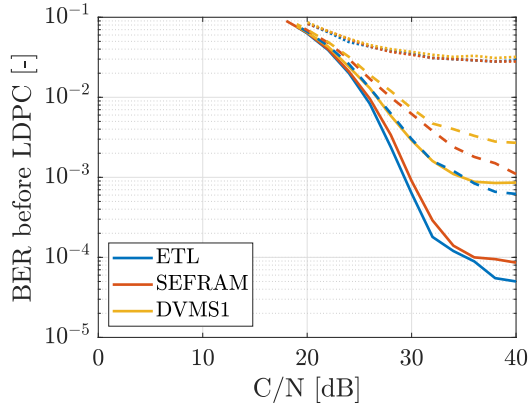
(e) BER vs  $C/N$  ( $C/N$  decreases on SFU)



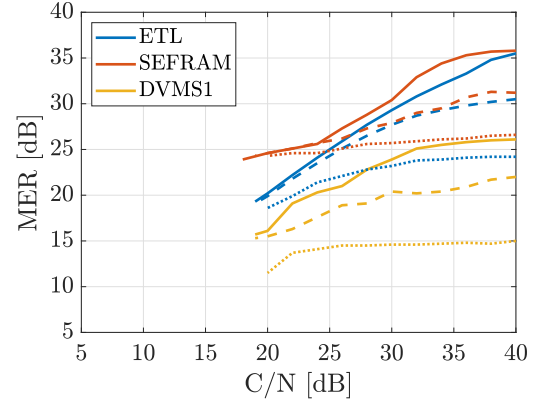
(f) MER vs  $C/N$  ( $C/N$  decreases on SFU)

Fig. A.5: DVB-T2 MISO TV signal: **RL20**, power imbalance = 10 dB (SFE: -25 dBm, SFU: -35 dBm) – solid lines: no  $I/Q$ -errors, dashed lines:  $AI = 10\%$ , dotted lines:  $AI = 10\%$  and  $PI = 10^\circ$

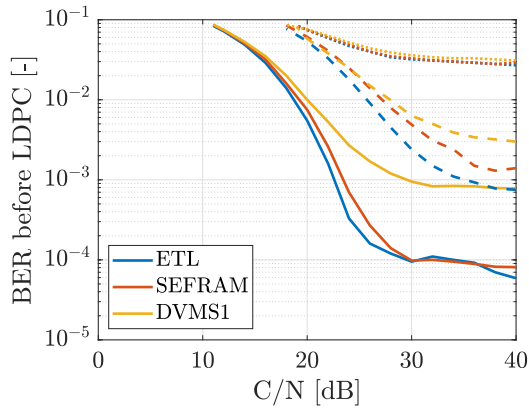




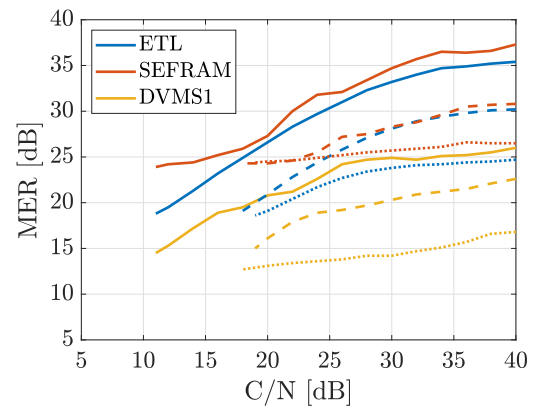
(a) BER vs  $C/N$  ( $C/N$  decreases on both generators)



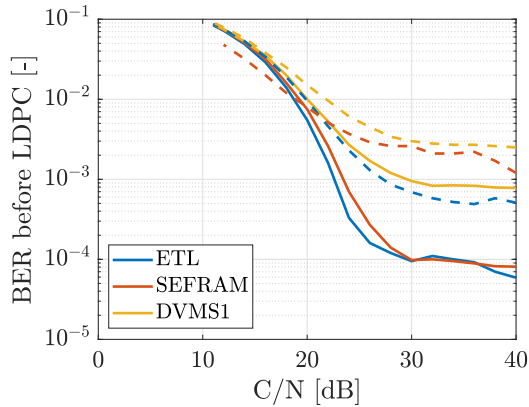
(b) MER vs  $C/N$  ( $C/N$  decreases on both generators)



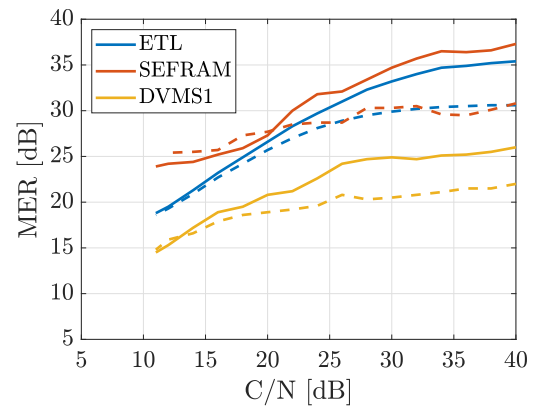
(c) BER vs  $C/N$  ( $C/N$  decreases on SFE)



(d) MER vs  $C/N$  ( $C/N$  decreases on SFE)



(e) BER vs  $C/N$  ( $C/N$  decreases on SFU)



(f) MER vs  $C/N$  ( $C/N$  decreases on SFU)

Fig. A.6: DVB-T2 MISO TV signal: **RL20**, power imbalance = 10 dB (SFE: -35 dBm, SFU: -25 dBm) – solid lines: no  $I/Q$ -errors, dashed lines:  $AI = 10\%$ , dotted lines:  $AI = 10\%$  and  $PI = 10^\circ$